Cruising Control of Electric Vehicle Using Situation Transition Based Driving Assistant

August 2017

ROUZIER, Baptiste Michel

A Thesis for the Degree of Ph.D. in Engineering

Cruising Control of Electric Vehicle Using Situation Transition Based Driving Assistant

August 2017

Graduate School of Science and Technology
Keio University

ROUZIER, Baptiste Michel

Acknowledgments

This thesis gathers the results of my research work during my PhD Degree in Keio University. This experience was the occasion for me to deepen my knowledge in fields that passionate me. Moreover, it also gave me the chance to meet, discuss and exchange ideas with different professors, researchers and other great people.

First of all, my thanks go to my advisor and supervisor Prof. Toshiyuki Murakami whose help was crucial to the conduction of my work. I greatly appreciated his support and guidance and most of all his kindness. It was a real honor and pleasure for me to work during the last five years in his laboratory.

I would like to express my appreciation to the members of committee that examined my thesis. Prof. Kouhei Ohnishi, Prof. Hiroaki Nishi and Prof. Takahiro Yakoh. Their help and contribution to this thesis were greatly appreciated.

I am also grateful toward the other SUM professors and members, whose advice and comments guided me trough my research work.

I would also like to express my deepest gratitude to the Fujiwara Scholarship, without which it would not have been possible to prolong my Master Degree to a PhD degree.

It was a great pleasure to work with the other members of the Murakami laboratory and especially with Mehdi Hazaz, Florent Hoareau and Yukihiro Okumura who especially helped me in the conduction of my research work.

Finally, I would like to thank my parents, my family and Yoko Iizuka, for their support and encouragements, and dedicate this thesis to my grandfather.

<div align="right">

August 2017,
Baptiste ROUZIER

</div>

Abstract

The drastic increase of the number of cars registered around the world, as well as the central role personal vehicles have in the daily life of many persons, created several problems such as environment concerns or road traffic deaths. This thesis aims at proposing solutions to the road fatalities, and more generally to the road accidents, by using active driving assistance and remote control of road vehicles. Those two concepts can separately have a positive impact on the safety of the cruising task, the active driving assistant by offering an automated support to the human driver through torques on the pedal and steering wheel of the controlled vehicle. Indeed, a great number of incidents on the road are caused by human driver behavior. The driving task being extremely demanding, the driver has to stay completely focused and has to react quickly and efficiently to every dangerous evolution of the environment of the vehicle. The driving assistant thus has a better reaction time compared to its human user and is not subject to focus loss. On the other hand, the application of remote control enables, especially in fret applications, to shorten the duration of continuous driving sessions, and by then to reduce the exhaustion of the driver, lowering the accident probability. However, remote control implies a communication time delay that can be a source of accident as the remote driver can become unable to react quickly enough to a hazard when this delay becomes too important. This is the reason why this thesis proposes a combination of remote control and active driving assistant, that can react to the evolution of the controlled vehicle's surrounding without time delay.

This thesis describes the methods used to analyze the car's environment to detect and locate possible threats to the safety of the car's users or object to avoid on the road. Several types of objects, i.e. other vehicles, pedestrians or road lines, are detected through the use of a stereo camera system and a combination of different computer vision processes. To be able to be operated while cruising, this detection should be performed in real time. Methods to reach that status are described. Moreover, to complete the partial information acquired from the camera, an information sharing protocol is also introduced.

Then the methods used to compute the assisting torques based on the representation of the detected dangers by virtual potentials is explained. Those potentials have to be carefully defined and shaped in order to offer the proper reaction from the driving assistant to a given situation. From the very implementation of the driving support, a control sharing is created between the human driver and the automated support, as the two have an impact on the trajectory and speed choices of the car. In order to improve the efficiency of the proposed method, the effect of both the human and algorithm on the control of the car should be modulated depending of the situation. If the situation is safe the driver should let be free, but when, by instance, this one lost his focus, the driving assistant should prevail over him. This modulation is performed thanks to a fuzzy logic engine able to take into account non Boolean values with a behavior closest to the human evaluation process.

To evaluate the efficiency of the proposed assistant test systems had to be designed. In order to be as close as possible of the condition that would be obtained in a real cruising situations, a one seated electric vehicle was modified to enable the application of both driving assistant and remote control. This vehicle was used to test the behavior of the driving support in case of line crossing. However it would be dangerous to test collision avoidance using a vehicle of this size and mass. That is why a 1/10th scale car was used to conduct those tests, once modified with the addition of a computer vision module.

Finally the results of the conducted experiments are analyzed in order to verify if the proposed driving assistant offer the desired behavior. Moreover, as the driving task is a complicated one, it is difficult to choose evaluation criteria able to sort different propositions of driving assistants in function of their efficiency. This is why a method is proposed to realize such evaluation depending of the desired goal of the driving assistant.

Contents

List of Figures

List of Tables

Chapter 1

Introduction

1.1 Background

1.1.1 Traffic Accidents in the World

Automobiles rapidly became a crucial element in the quotidian lives of numerous persons through the world. Even if the first designs of steam powered cars can be traced back to the late 18th century, and if the first oil powered cars appeared in the 19th century, the mass production of such vehicles started in the early years of the 20th century. One century later, 67 millions newly produced cars were released on the road for the sole 2014 year[2]. This spreading is not limited to high incomes countries, as the increase of the number of registered vehicle was observed more strongly in low and middle income countries. Several backlashes were caused by this surge. In spite of the undeniable negative impact on the environment of the multiplication of oil powered cars, leading for a crucial need of a technological shift to eco-friendly motorization, the number of deaths caused by traffic accidents is one sever concern. According to the World Health Organization 1.25 millions road traffic deaths occur every year[1]. It corresponds to the first cause of death among the persons aged between 15 and 29 years, with more than 300 000 deceases in 2012, before suicides, HIV/AIDS and homicides in 2nd, 3rd and 4th positions.

As shown in Fig.1-1 there are inequalities in the distribution of those deaths around the world. Indeed the death rates are higher in low-income countries compared to high-income countries. This can be explained by better legislation in the late ones but also by
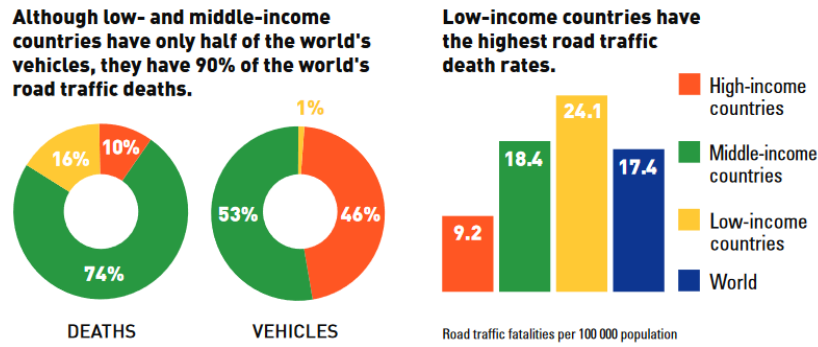
Fig. 1-1: Ratio of deaths and vehicles in the world[1].
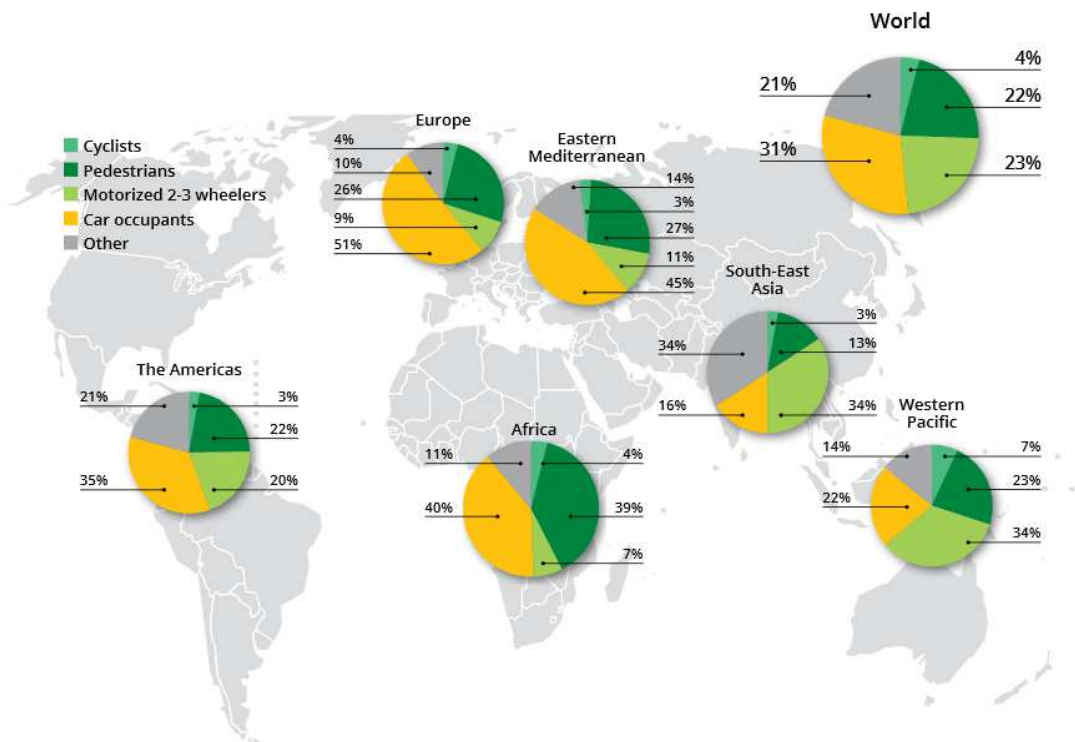
Fig. 1-2: Road traffic deaths by type of road user, by WHO region[2].

the fact that increased quality and safety of cars go with higher prices.

Fig.1-2 demonstrates the impact on the different types of road users of the road incidents. As it can be observed car users are not the only victims and it can be seen that several categories of road users, the ones whose protections are the weakest, are the first victims of traffic accidents. This is why the improvements in term of safety in the 4 wheels vehicles domain should not be only focused on the security of its users. The decrease of

the road mortality also passes through the ability of cars to protect all of the road users.

1.1.2 Automated Driving

The first cause of road accident is not failures of vehicles but the behaviors of the drivers. Indeed the driving task is complicated and implies to take simultaneously into account a huge quantity of parameters, including the speed of the cars, the direction of the wheels, the shape of the road, the meteorological situation, the presence or not of obstacles on the road and the behavior of the other road users. This accumulation of factors makes driving a very tiring activity that requires a continuous focus from the driver. Thus every external factors that could reduce this focus potentially increase the hazard of a driving situation. Those factors include, but are not limited to, sleepiness and alcohol. Even if measures are taken by numerous countries to handle those issues, it seems clear that every technology able to help the driver should be considered. Automation technology especially seems to be fitted to assist to the driving task. Indeed automation process are able to react quickly to any situation and are not subject to focus loss. This is why the autonomous vehicle technology raises so much interest as it is both able to nullify the focus loss of the driver and to take into account the surrounding of the controlled car in order to protect all of the road users. A lot a researches[9][10] were conducted based on this idea of a car able to drive itself and this concept is well known of the public. It even manages to raise enthusiasm to the point were contests are organized[11] and discussions are conducted on its impact in the future. Based on the supposition that this technology would present no failure and would reach a market share of 90%, it is expected to notably reduce the mortality rate on the road[12]. However a completely autonomous technology faces several difficulties. In that situation, no human driver is involved in the driving task but human remains involved in potential accident. Because of the difficulty to foresee all of the reactions of a control algorithm in every possible situations, it is almost impossible to guarantee that no failure will ever happen. Then this kind of vehicle requires special authorizations in order to be used on the road. Fig.1-3 shows by instance the current situation for the authorization of autonomous cars in the United States.

Moreover drivers could be reluctant to let the car choose its direction and speed by
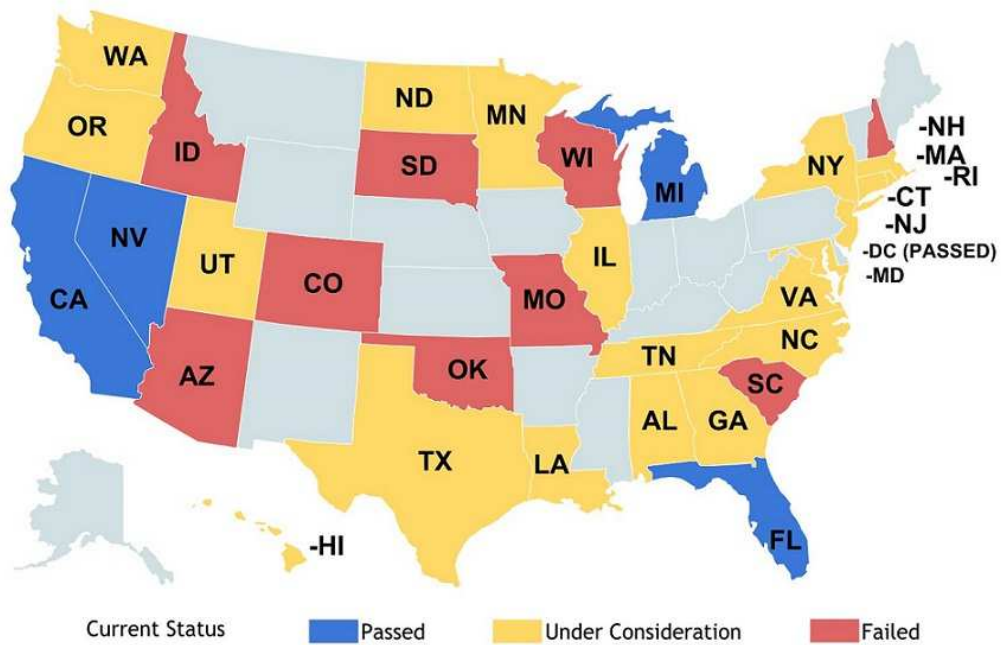
Fig. 1-3: Autonomous cars legislatures in the U.S.[3].

Table 1.1: Impact of sleep on crash risk[6].

Diminution of sleep time compared to usual time	Multiplication of crash risk
1-2 hours	1.3
2-3 hours	3.0
3-4 hours	2.1
4 or more hours	10.2

lack of confidence toward automation. This could then slow down the spreading of this technology, reducing its efficiency. This is why an other approach, were the automation would not lead to autonomous vehicles can be considered as interesting, this approach being the active driving assistant.

1.1.3 Remote Controlled Cruising

Table.1.1 demonstrates the impact of drowsiness on crash risks. It can be observed that the more the driver is drowsy, corresponding to increasing diminutions of sleep time,

the more crashes happen. As driving a car is a very demanding activity in term of focus, it leads to an increased drowsiness of the drivers, especially in long sessions. This kind of session can be observed with persons whose occupations are related to driving, like fret transporter or taxi driver. One possible method to reduce the duration of certain driving sessions would be the use of remote controlled vehicles. Indeed in case of remote driving, it is possible to change the driver when this one shows signs of sleepiness. This scenario is not applicable to every driving case, as in most cases peoples use vehicles to go from one place to an other. Remote control of vehicles is mainly interesting in case of fret transportation or public transportation. However this is not the only application of remote control. More specific scenarios can be imagined, like for examples, short duration remote assists if a vehicle's driver requires it, or even remote control to help to park vehicles from an external point of view. Usually remote control of robots or mobile objects is used to explore or access places that are not reachable by humans or which environment are dangerous for peoples. Remote controlled robots can be used to explore disaster area[13] or to inspect power plant walls[14] for examples. Nevertheless there is a major constraint to the application of remote control to cruising vehicles. By its very nature, remote control implies a time delay between the command signal emission and the execution of the orders, caused by the communication delay. If this delay is not constraining for low speed vehicles, it becomes a major concern in the case of remotely controlled cars. Indeed, in cruising situations, the environment of a car is evolving extremely rapidly and the reaction of the driver is required to be fast enough to ensure a safe driving. Moreover any incident of an exploration robot, even if annoying, does not involve the safety and lives of humans. This is why a mere remote control would be dangerous to apply on a car. However if combining that control method with an automation method it should be possible to counter the effects of the communication time delay when this one tends to become too dangerous. The proposed method is to combine the remote control with an active driving assistant.

1.2 Active Driving Assistance

1.2.1 Principle

Active driving assistant can be seen as a compromise between a control based on human instructions only, as in nowadays cars, and completely autonomous vehicles. The purpose of the driving assistant is to offer to the human user an active support while letting him keep the control of the car. The assistance is considered as active because the assistant has a direct impact on the direction of the car and on its speed. It is not a mere warning system that would buzz in hazardous situations. The driving support is based on the analysis of the car's environment to locate potential dangers, estimate their degree of hazard, and finally offer to the driver some help to control the trajectory of the car as well as its velocity. This support is given through torques applied on the steering wheel and pedal of the controlled car. Conversely to the driver it helps, the driving assistant is not subject to loss of focus, can handle a high number of parameters simultaneously and does not become tired after long driving sessions. However the assist offered to the human is not the only element determining the behavior of the controlled vehicle, as the driver himself also controls the vehicle. Indeed even if quick to react, the driving support could offer unforeseen reactions to very specific and unexpected situations as it seems very unlikely that the programming of such assistants would be able to take into account every possible scenarios encountered by millions of users driving on a daily basis. Thus, keeping the ability of humans to react to unforeseen dangers and their experiments in driving, contributes to improve the safety of the whole system. Moreover as expressed before, the efficiency of a technology to reduce the casualties on the roads is also dependent of its wide acceptation by users. Even the perfect system would be useless if the drivers did not want to use it. From that point of view active assistant could be more easily accepted by car's operators as there is already a great variety of assistant inside of a car, by instance ABS, sleepiness sensors or cruise control. For that acceptance to be the highest as possible it is required that the support does not enter constantly in conflict with the driver. For that purpose, the effect of the driving assistant should be adjusted depending of the situation. In case of imminent hazard, the influence of the support should be strong enough to avoid the danger, while letting the driver free in other scenarios. That kind of active assistant

is also a way to compensate for the communication time delay. Indeed the negative effect of this one implies that the driver is delayed in his reaction to a problem, and that this reaction itself is delayed in its application. However the driving assistant, being able to be embarked in the controlled vehicle, can react to any hazard without the influence of the communication tome delay, preventing the collision or the road exit by instances.

1.2.2 Expected Behavior

In order to evaluate the efficiency of the proposed method, it is necessary to state what is expected of it. The main focus of a driving assistant is to keep the occupants of the car, and the other users of the road, safe. It is crucial to ensure that the collisions are avoided and that other hazardous situations can be prevented. From the same point of view, the safety offered by the driving assistant ca be evaluated by it capacity to suppress the effects of the communication time delay. It is expected from the car to keep the safest trajectory possible. It is also expected that the car is able to avoid involuntary lane changing and road exit. It should also be able to stop before a collision with an obstacle or to modify the path of the car to avoid that collision. The driving assistant should also be comfortable to use for the human drivers. That means that the variation of speed and trajectory should not be too sudden, that the offered torques should not be oscillating too much and that the reaction of the driving assistant should be close to what a human driver would do in the same situation. Finally the conflicts between the driver and the driving assistant should be evaluated. The driving support should be able to regulate its effect depending of its surrounding, the state of the driver, and the quality of the communication between the driving station and the controlled vehicle. The purpose of this modulation is to ease the interactions of the driver with the support, by reducing as much as possible the opposite actions between the two.

1.3 Related Works and Thesis Contribution

1.3.1 Related Works

The driving assistant proposed in this thesis is based on the use of a stereo camera analyzing the environment of the car in order to detect and locate elements that could

Advanced Interfaces for Vehicle
Teleoperation: Collaborative Control, Sensor
Fusion Displays, and Remote Driving Tools,
Fong, Terrence and Thorpe, Charles and Baur,
Charles

A Study on EMG-Based Human
Motion Prediction for Power
Assist Exoskeletons, *K. Kiguchi*

A remote-controlled land and water
traversing vehicle for flood search
operation, *J. L. B. Abesamis and A. M.*
F. Mediodia and C. J. M. Akol and R.
P. M. Quesea and E. Sybingco

Development of a lightweight power-
assist suit using pneumatic artificial
muscles and balloon-amplification
mechanism, *H. Inose and S. Mohri and*
Y. Yamada and T. Nakamura and K.
Yokoyama and I. Kikutani

Remote
Control

Power
Assist

Human
Assist

Environment
Recognition

A Study on EMG-Based Human
Motion Prediction for Power Assist
Exoskeletons, *K. Kiguchi*

A remote-controlled land and water
traversing vehicle for flood search
operation, *J. L. B. Abesamis and A.*
M. F. Mediodia and C. J. M. Akol and
R. P. M. Quesea and E. Sybingco

Compliant velocity based force
coordinate transformation control for gait
rehabilitation, *M. Sasayama and T.*
Murakami,

A novel lane detection based on geometrical model and
Gabor filter, *S. Zhou and Y. Jiang and J. Xi and J. Gong*
and G. Xiong and H. Chen

Fig. 1-4: Key concepts of the thesis.

be dangerous or be endangered by the car. Those objects are then represented by virtual potential fields from which a local path planning is conducted to offer a proper assistance to the human driver through torques applied on the steering wheel and pedal of the controlled vehicle. This support can also be applied to cars that would be remotely controlled. By its approach, the proposed work shares some characteristics with other fields of research, and can be seen as the convergence of several concepts, as shown in Fig1-4. As its main purpose is to help a human driver to perform safe driving, the driving assistant is part of the Human Assist research field. Human Assist researches aim at helping the human to conduct a specific activity, either for rehabilitation purpose, when a human cannot perform a task anymore[15], or to improve his ability to conduct that activity beyond what could normally be possible, by instance using exoskeletons[16][17][18] to increase the strength of its wearer or with the presented driving support to increase

the rapidity of the human reactions. This domain is contiguous with the power assist technology which consist in assisting to a task by giving extra power to the user. The way this extra power is received can vary, from assisting suits[19] [16] to torques in steering wheel and pedal as proposed in this thesis. As explained before the driving assistant system proposed here is also applied to reduce the impact of the communication time delay while remote controlling the car. As stated before remote control of robots is mainly applied to small and low speed vehicles in a high variety of situations[20] and especially to explore disaster area[21]. Finally, a very impacting factor on the efficiency of the proposed system is the ability of the assistant to analyze correctly the surrounding of the car. This part is relevant of the Environment Recognition concept that aims to find specific objects in the environment of the controlled robot and to estimate their locations. The detected objects can be, for examples, road marks[22] or humans[21].

1.3.2 Contribution

This thesis is intended to bring some answers to the issues raised by the remote control of vehicles on the road and more generally by the will to enhance the safety of every road user in order to help to reduce the casualties caused by the traffic accidents. Even if some of the previously described issues are not new and were the subjects of several research works, the fact that the controlled vehicle is designed to cruise on populated roads raises new requirements including high frequency computations. Some methods are then detailed to solve these problems and the main contributions of the thesis can be summarized as follows.

- A computer vision algorithm performing detection and location estimation of hazards by using with profits the specificity of the used material to enable real time computation on a portable hardware.

- A method to modulate the control sharing between the driver and the assistant depending of the status of the driver, the state of the communication between the driving station and the controlled car and of the state of that car.

- A method to apply the assisting torques depending of the results of the environment analysis whether using remote control or not.

- A method to estimate the efficiency of the proposed driving assistant in different scenarios.

1.4   Thesis Outline

The following chapters of that thesis are organized as shown in Fig.1-5. Chapter 2 will describe the environment analysis conducted by the driving assistant. It will underline how the detection of hazards was made as complete and fast as possible by combining the results of different image processes and by optimizing the computations.

Chapter 3 is focused on the methods used to modelize different kinds of dangers in order to obtain the expected behavior from the driving assistant, and how this one is applied to the controlled vehicle. It also describes the way the control is shared between the driving support and the driver depending on a modulation based on a fuzzy logic engine.

Then Chapter 4 will depict the experimental systems used to test the driving assistant, including the way they was designed, the constraints they have to fulfill and the followed experimental procedures.

Chapter 5 is focused on the analysis of experimental results. It will describe a method that aims to estimate the efficiency of such assistants and compare the obtained results with what is expected of a driving support.

Finally the Chapter 7 will be the occasion to summarize the content of the thesis and to offer perspectives to future works in order to improve the proposed system.

```
┌─────────────────────┐
│     Chapter 1:      │
│    Introduction     │
└─────────────────────┘

┌─────────────────────┐      ┌─────────────────────────┐
│     Chapter 2:      │      │       Chapter 3:        │
│ Environment Awareness│      │ Environment Modelization│
└─────────────────────┘      └─────────────────────────┘

        ┌─────────────────────┐
        │     Chapter 4:      │
        │ Experimental Systems│
        └─────────────────────┘

        ┌─────────────────────┐
        │     Chapter 5:      │
        │   Results Analyses  │
        └─────────────────────┘

        ┌─────────────────────┐
        │     Chapter 6:      │
        │     Conclusion      │
        └─────────────────────┘
```
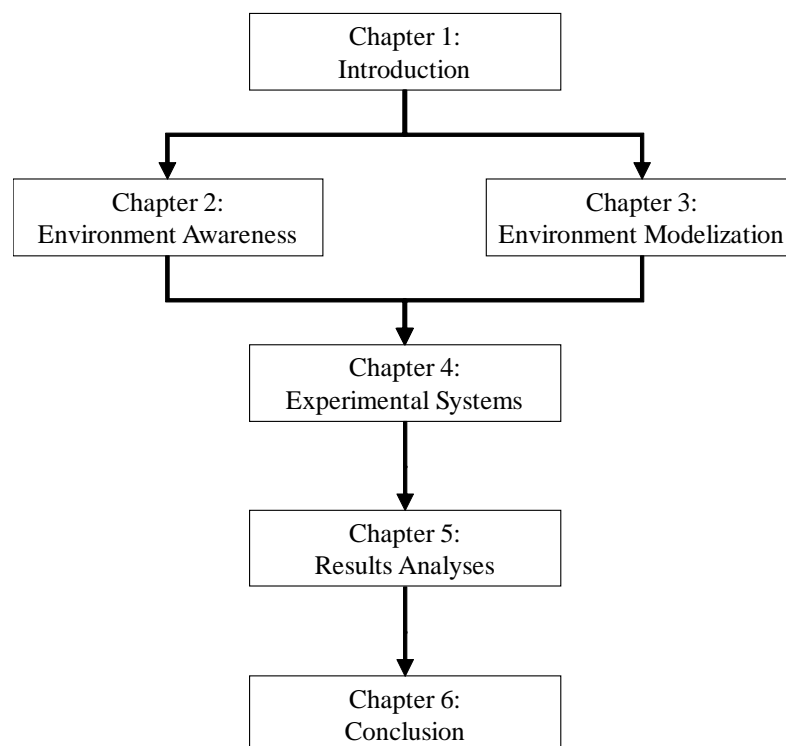
Fig. 1-5: Chapters organization.

Chapter 2

Environment Awareness

2.1 Interest of Environment Awareness

In order to propose an active driving assistant able to reduce the number of accidents on the road, and by then the number of traffic deaths, the Environment Awareness of this one has to be considered. The Environment Awareness is the ability of the driving assistant to examine its surrounding to recognize information useful to perform safe cruising. This ability is not restrained to the driving support field. Indeed the environment awareness is also crucial for the human drivers. This is why a great number of indications are offered to them, either road markings, to give information about the shape of the road, or road signs, to obtain recommendations about speed or warning about specific dangers. In the case of the driving support, the environment awareness includes methods to find specific objects in the proximity of the controlled vehicle, by instance other vehicles, to locate them in that environment, that means translating the results obtained trough sensors to coordinates in the 3D space of the car, and to estimate the evolution of the controlled car in that same space. The main concerns raised by those methods are the following. The detection should be as complete as possible. That means that no important or dangerous object should remain undetected. Moreover the location estimation that follows this detection should return results accurate enough to allow an efficient computation of the active support. It is also necessary that the acquired data should be frequently updated. This frequency should be high enough to correspond to the evolution of the situations

encountered while driving, where the speed of the evolving objects is high. Finally it can be stated that an increased environment awareness, obtained through accurate and fast detection of potential hazards, leads to increased safety and pertinence of the support offered by the active driving assistant.

2.2 Cinematic Model

As stated in the previous section, in order to know its environment, it is required from the controlled car that it is able to estimate its position inside of this one. Indeed when a danger is detected by the sensors of the car, its position is only known in the referential $\Re$ of the car, $(G, \vec{x}, \vec{y})$ in Fig.2-1. In order to compute the position of that danger in the experiment referential $\Re_0$ $(O, \vec{x_o}, \vec{y_0})$, the orientation, ω, and the position of the center, G, of the car should be known. This simple transformation is described by the following equation.

$$\vec{X_{\Re_0}} = R_{\Re/\Re_0}\vec{X_{\Re}} + \vec{OG} \tag{2.1}$$

Where $\vec{X_{\Re_0}}$ is the position of an object in $\Re_0$, $\vec{X_{\Re}}$ its position in the car referential $\Re$ and $R_{\Re/\Re_0}$ the rotation matrix between $\Re$ and $\Re_0$ expressed as follows.

$$R_{\Re/\Re_0} = \begin{bmatrix} \cos(\omega) & -\sin(\omega) & 0 \\ \sin(\omega) & \cos(\omega & 0 \\ 0 & 0 & 1 \end{bmatrix} \tag{2.2}$$

Moreover, it is important, to estimate the assistance to offer to the driver, to know the position and orientation of the car in $\Re_0$. Indeed if some danger is not detected by the car sensors, either for a period of time or because this information was acquired otherwise, this experiment referential become the only mean to know the position of a danger, being the only absolute and shared referential.

The cinematic model used to estimate the orientation of the car and the position of its center is presented in Fig.2-1. It is a very simple model based on a two wheel simplification of the behavior of the car. It was chosen based on several statements. Firstly, one of the system used to test the driving assistant is limiting the data that can be acquired. Indeed
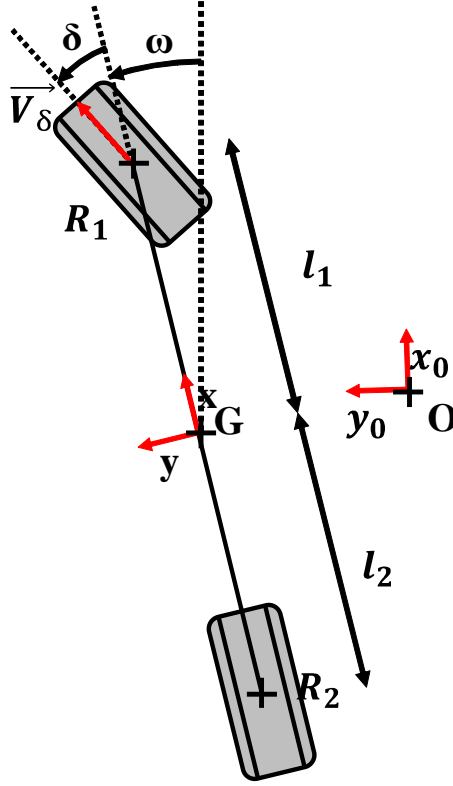
Fig. 2-1: Used cinematic model.

this system is a modified commercial electric vehicle which implies a limited number of possible sensors. It is possible to measure the rotation speed of the front wheels and the angular positions of the steering wheel, steering shaft and pedal. Using a model requiring a high number of parameters is then impossible. Moreover the situations studied in this thesis are quite simple and the involved steering angles are quite small. This is why the accuracy of that model is sufficient. To propose a more sophisticated model, it would be necessary to add extra sensors on the previously described vehicle, by instance inertial measurement units. This model is described by the following equations:

$$\dot{\omega} = \frac{V_\delta \sin \delta}{l_1 + l_2} \tag{2.3}$$

$$\overrightarrow{V_G} = V_\delta \cos \delta \, \overrightarrow{x} + l_2 \frac{V_\delta \sin \delta}{l_1 + l_2} \overrightarrow{y} \tag{2.4}$$

Where ω is the orientation of the car in $\Re_0$, $\vec{V_G}$ the speed of the car center in $\Re_0$, V_δ

the speed of the front wheels, δ the orientation of the fronts wheels and l_1 and l_2 the longitudinal dimensions of the controlled car.

The orientation of the car and the position of G in $\Re_0$ are then obtained by integration and with the following conversion derived from $R_{\Re/\Re_0}$

$$\overrightarrow{x} = \cos\omega\overrightarrow{x_0} + \sin\omega\overrightarrow{y_0} \tag{2.5}$$

$$\overrightarrow{y} = -\sin\omega\overrightarrow{x_0} + \cos\omega\overrightarrow{y_0} \tag{2.6}$$

2.3 Detection using Artificial Vision

2.3.1 System Presentation

In this thesis the main method used to analyze the environment of the controlled vehicle is based on a computer vision algorithm that uses a stereo camera system. The purpose of this algorithm is to detect and locate several types of potential hazards. The location of objects is estimated thanks to the stereo camera system. This one returns two simultaneous images, in a very eyes fashioned way. It is then possible to determine the location of a object in the camera space by comparing the positions of that object on the obtained two images. The selected stereo system is a PlayStation® camera, described in Appendix A. This choice was motivated by the relative inexpensiveness of the camera compared to other stereo camera systems. It is also able to be effective at short range, around 40 centimeters, conversely to most of wider stereo devices. The artificial vision algorithm was designed to detect other vehicles cruising on the road with the controlled car, to detect pedestrians but also to detect the road lines. All of these processes will be described in the next subsections and are represented in Fig.2-2.

The first step of the algorithm is an initialization phase in which the data needed for the rest of the processing are loaded. Then at each images acquisition, where two images are acquired simultaneously, corresponding to the right and left channels cameras of the stereo camera system, the images are remapped to correct their distortions, and are both used to reconstruct the environment in three dimensions and to detect the previously listed objects. Finally, combining the reprojection and detection, the locations of the detected
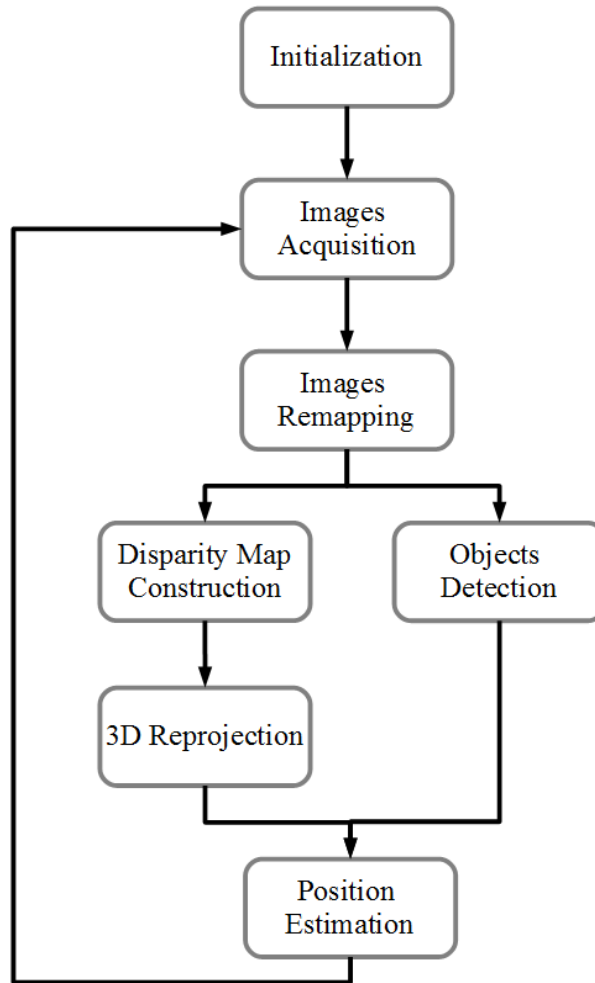
Fig. 2-2: Architecture of the algorithm used to find the space position of objects.

objects are estimated. This computer vision program is running on Jetson development kit, described in AppendixB. This kits, using GPU processing can be used to perform efficient portable computing[23] [24] [25].

2.3.2 3D Reconstruction of the Environment

A major step in the computer vision algorithm is the 3D reconstruction of the environment. The purpose is to determine for each pixel of one of the image, the position of that point in the camera space. This computation is based on the use of a stereo camera as shown in Fig.2-3. In this figure the two cameras of a stereo system are oriented toward two objects, located at different positions, the red sphere being closer of the cameras that
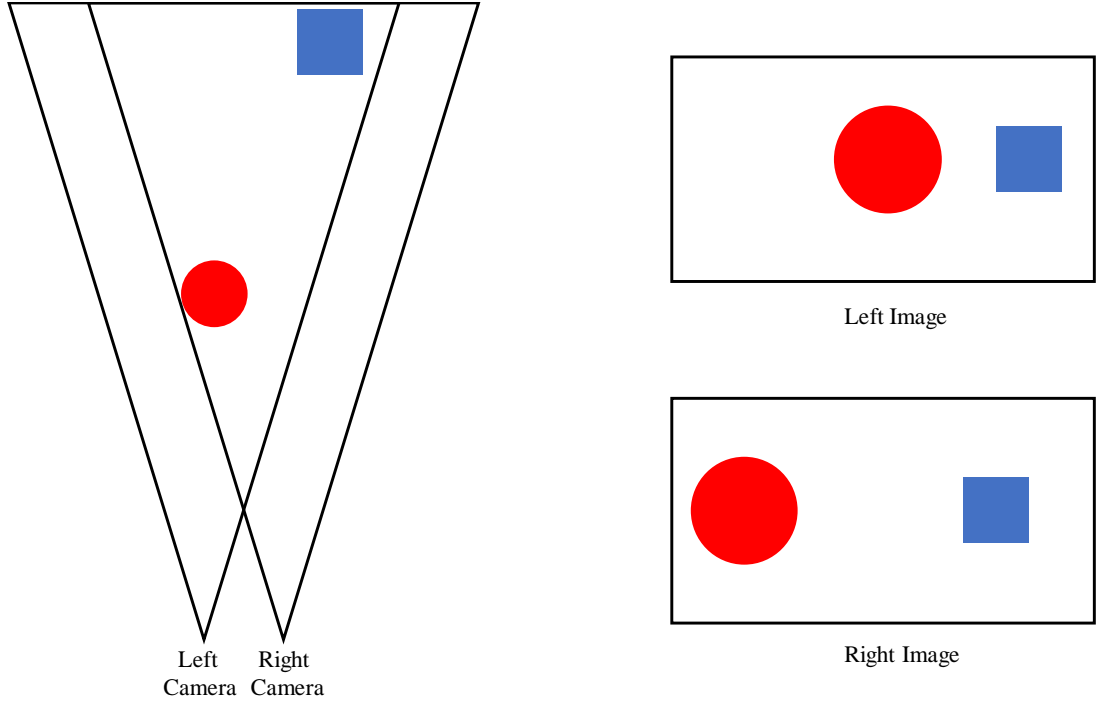
Fig. 2-3: Principle of stereo camera system.

the blue square. The images obtained by those cameras demonstrate the principle used by a stereo system to determine the location of objects. The closer an object is to the cameras, the bigger its location will vary between the left and right images. This principle is the same that is used by the human brain by using the information obtained from the left and right eyes, and is used in numerous research works[26] [27] [28].

In order to perform that reprojection, several image processing should be conducted. Indeed in order to obtain a correct result, the twos cameras of the system should be calibrated to correct the distortions of the images through a remapping process. The calibration process is crucial to any use of a camera and was thus the subject of numerous considerations[26] [27]. The radial distortion, caused by the barrel effect can be compensated with the following equations, where (x, y) are the coordinates of a pixel in the image and $(x_{corrected}, y_{corrected})$ the coordinate of the same pixel in the remapped image

$$x_{corrected} = x \left(1 + k_1 r^2 + k_2 r^4 + k_3 r^6\right) \tag{2.7}$$

$$y_{corrected} = y \left(1 + k_1 r^2 + k_2 r^4 + k_3 r^6\right) \tag{2.8}$$
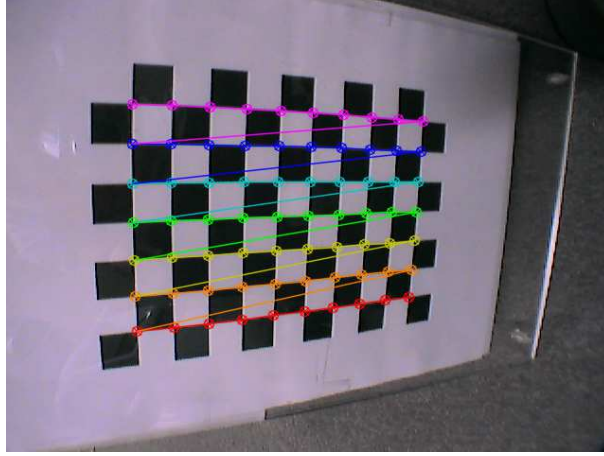
Fig. 2-4: Example of chessboard detection.

Then, the tangential distortion, caused by imperfections in the parallelism of the lenses, can be compensated with the following equations.

$$x_{corrected} = x + \left(2p_1 xy + p_2 \left(r^2 + 2x^2 \right) \right) \tag{2.9}$$

$$y_{corrected} = y + \left(p_1 \left(r^2 + 2y^2 \right) + 2p_2 xy \right) \tag{2.10}$$

To compute a correspondence between the distance in the real world and the pixels of the camera the following conversion is operated.

$$\begin{bmatrix} x \\ y \\ w \end{bmatrix} = \begin{bmatrix} f_x & 0 & c_x \\ 0 & f_Y & c_y \\ 0 & 0 & 1 \end{bmatrix} \begin{bmatrix} X \\ Y \\ Z \end{bmatrix} \tag{2.11}$$

Where X, Y and Z represent the real space, f_x and f_y the camera focal lengths and c_x and c_y the pixel coordinates of the optical center. The calibration of each camera is done by determining the coefficients k_1, k_2, k_3,p_1, p_2, f_x, f_y, c_x and c_y.

After the calibration of the cameras, the stereo system itself should be calibrated by determining the translation and rotation matrices between the two cameras.

Those calibrations are conducted once, outside of this computer vision program by using chessboards images taken from both of the camera as in Fig.2-4. Knowing the size of the squares of the chessboard and by using several images it is possible to construct

Fig. 2-5: Original Left channel image used for the disparity computation.

a system of equations allowing to determine all of the previously described parameters. Those parameters are loaded during the initialization step of the program.

In order to proceed to the reprojection, a disparity map has to be created. This map represents the difference of location of an object between the right and left images. This disparity is directly related to the distance between the observed object and the stereo system. The algorithm used to construct the disparity map is based on a block matching algorithm. This one consist in dividing an image into macroblocks and try to find the position of that block in the second image. The value of the difference of positions corresponds to the disparity. The block matching algorithm can also be used in video compression[29] [30] or in motion estimation[31] [32].

Fig.2-5 and Fig.2-6 show an example of disparity map with one of the original image that lead to its creation. In this example the brighter the further. It can be observed that the disparity map become progressively brighter on the walls, reflecting that the objects progressively become further. Some white areas can also be seen in completely uniform areas, like the shirt of the photographed person. This is caused by the difficulty to recognize group of pixels by block matching algorithm in areas where the color is too uniform.

This disparity map is used to construct a representation in the 3D space of the observed scenery according to the followings equations.

$$[X\ Y\ Z\ W]^T = Q * [x\ y\ \texttt{disparity}(x,y)\ 1]^T \tag{2.12}$$
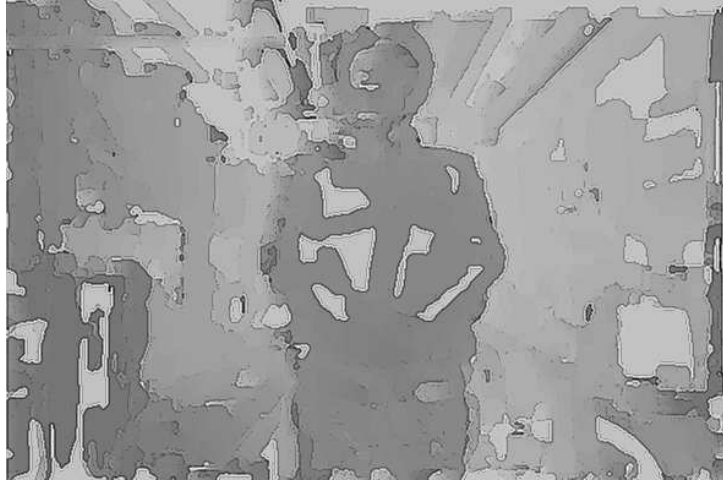
Fig. 2-6: Example of disparity result.
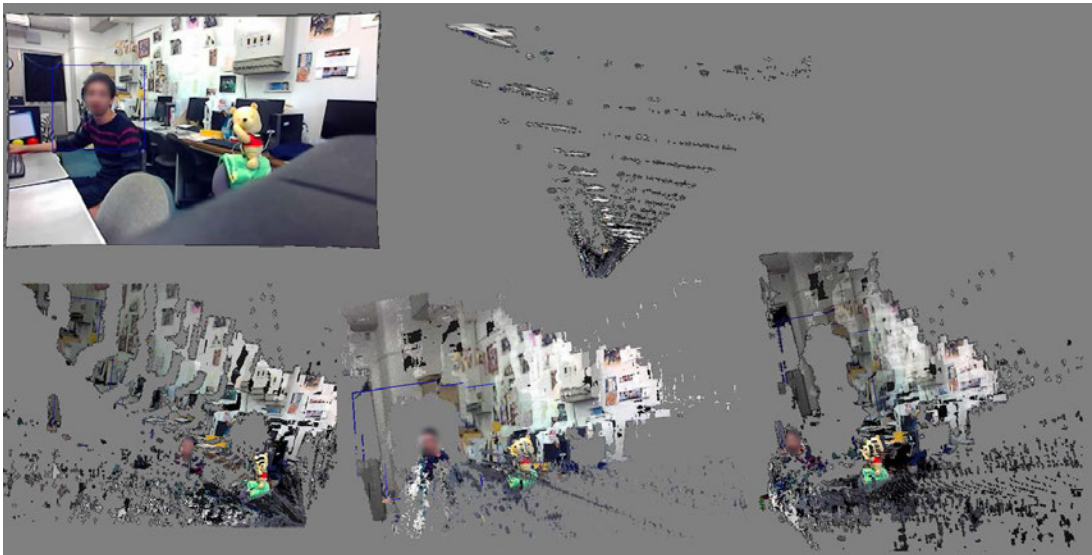
Fig. 2-7: Example of point cloud visualization.

$$\texttt{3dImage}(x, y) = (X/W,\ Y/W,\ Z/W) \tag{2.13}$$

Where Q is a matrix obtained in the calibration process of the stereo system and depending of the geometry of this one. The result of this reprojection is a three channels image, where to each pixel of the original image is associated its coordinates in the 3d space of the stereo system. The result can be transformed in a point cloud in order to be visualized as in Fig.2-7. It can be observed that the relative positions of the different objects are respected and that the locations are correctly estimated. The top
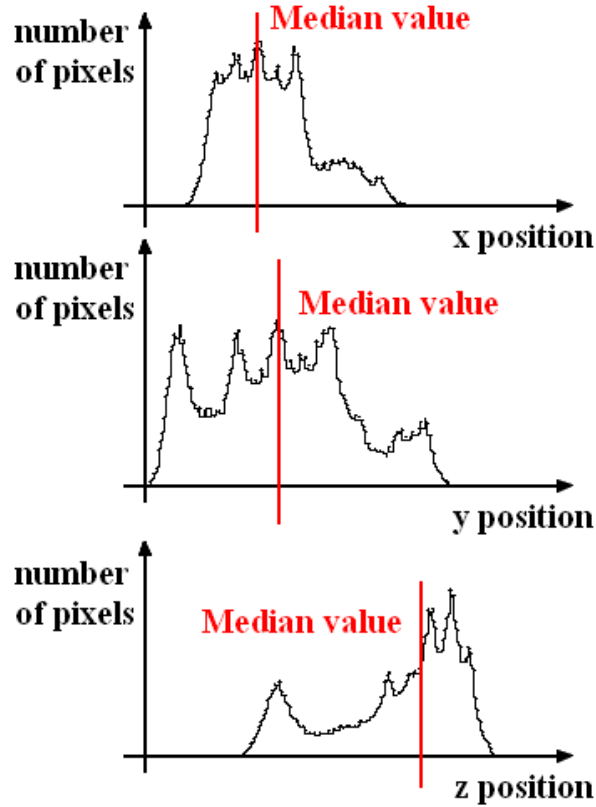
Fig. 2-8: Histograms used for median filtering.

view shows that the points are grouped in several plans. Indeed the deepness values are not continuous. This is caused by the method used to perform this 3d re projection. The disparity obtained by comparing the position of the images being given in pixels, the possible disparity values are then discontinuous.

Once this reprojection is performed, it is possible to estimate the location of some objects or of some parts of objects. As it can be observed in the previous pictures, the 3D reprojection can be noisy and present some irregularities. This is why it is not recommended to use the value of only one pixel in the reprojected image. The used method was based on a median filtering applied on a small area around the pixel of interest. For that purpose histograms are created from the reprojected image.

Histograms are often used on color image as a way to analyze the color composition of an image and can be used as a comparison tool[33]. For each channel of an image, usually

a color channel like the red channel for example, an histogram is constructed by counting the number of pixels that correspond to the same value on the channel. By instance a red channel histogram is created by counting the number of pixel with red values are 0, 1 and so on. In this algorithm the process is the same, except that the channels do not describe colors but positions in the space of the camera. Fig.2-8 is an example of such histograms. It is then possible to compute the median value of each histogram, corresponding to the median values in x, y and z of a sample of the reprojected image. It is then possible to estimate the position in the camera space of a point by determining the median position of a small area surrounding that point.

The accuracy of the proposed method was tested. The error was inferior to 1 cm for an object closer that 75 cm of the stereo system. The error became 3cm at 2 m and 3.5cm at 3m. The error is increasing with the distance because of the block matching error as discussed previously.

2.3.3 Detection of Vehicles and Pedestrians

In order to be efficient, a driving assistant should be able to avoid collisions with the other road users. Those one are mostly inside of other vehicles that are cruising on the same road, by instance in cars, trucks or motorcycles, but can also be pedestrians. To be avoided an object must, first, be detected. In this thesis, the detected road users are the other four wheels vehicles, cars or trucks, as they are the most commonly encountered road users, and the pedestrians, because of their high vulnerability in case of collision.

In parallel of the 3d reconstruction several features are detected using different cascade classifiers. Each cascade is in charge of the detection of a specific feature, in this program, vehicles and pedestrians. The detection of the the front and rear of vehicles is based on the Viola-Jones method[34]. This method is based on Haar features shown on Fig.2-9. Haar features are applied to the different areas of an image at different scales. The average value of the dark region is subtracted to the average value of the light region, the obtained value is then compared to a threshold to determine if the area passed or not. Haar features are weak classifiers, which mean that the answer given by a Haar classifier is a little better than a random guess would have been. Haar cascade classifiers are composed of a
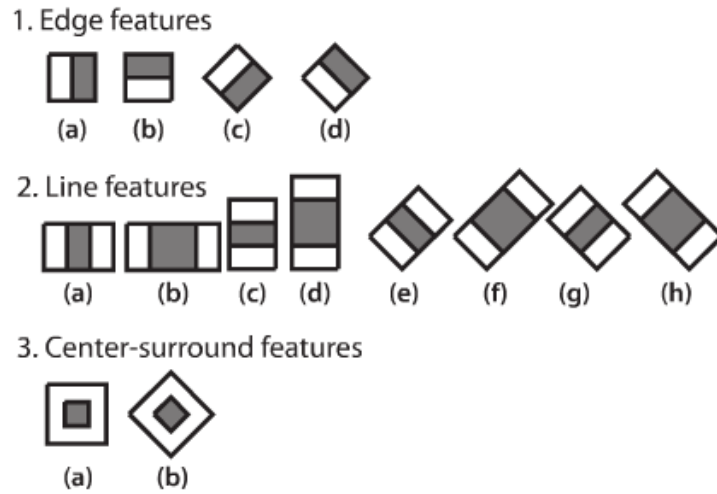
Fig. 2-9: Example of Haar features.
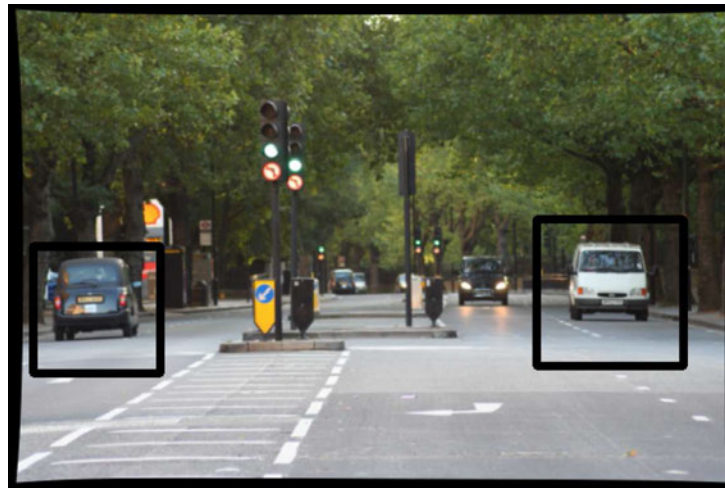
Fig. 2-10: Example of cascaded haar detection.

great number of selected Haar features which order and thresholds have been chosen[35] to detect a particular feature such as a face, an eye or an upper body[36] [37]. Those Haar features are grouped in several filters that are chained. To be detected a feature has to pass every filter conditions. Fig2-10 is an example of such algorithm applied on a road picture.

The pedestrians detection and the detection of the sides of vehicles are realized using Histograms of Oriented gradients[38] [39] [40]. Gradient orientation are computed inside of small pixel agglomerations called cells. Those orientations are used to compute histograms
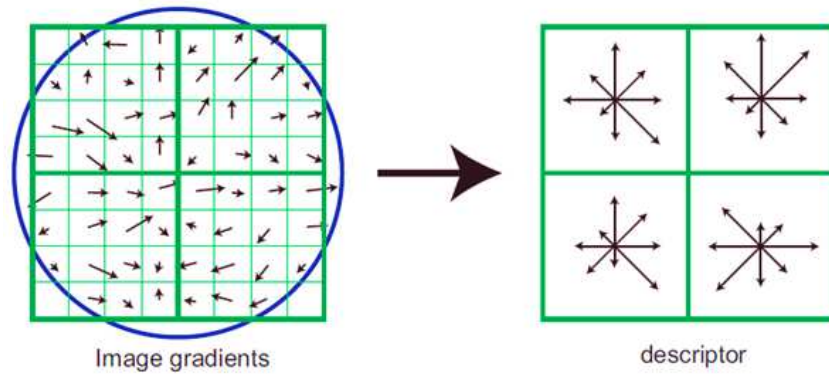
Fig. 2-11: Example of Histogram of Oriented Gradients.
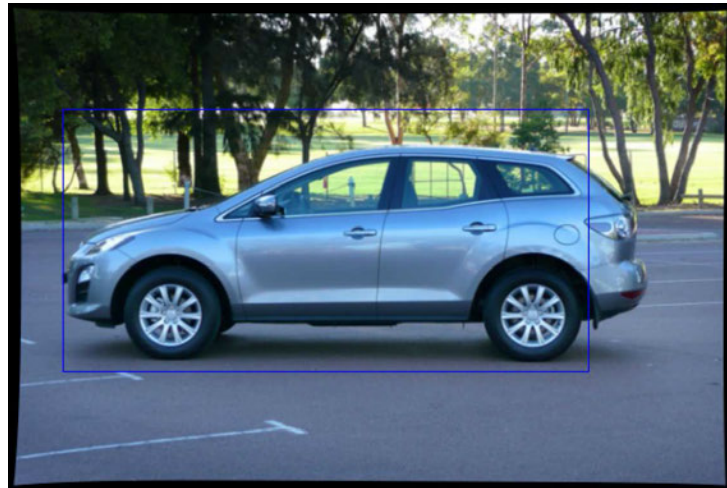
Fig. 2-12: Example of cascaded HOG description.

as shown in Fig.2-11. The histograms calculated for each cell are combined to create a descriptor able to detect the previously defined features, in a similar way to what was explained on the Viola-Jones method. An example of such detection is given in Fig.2-12.

Those detectors are applied on different scale of the same image to detect objects of different size. By then detection of that type are time consuming. In order to increase their speed it is possible to define the scale variation between two detections on the same image, and to resize the dimensions of the studied images. If the late one are reduced the computation time can be greatly increased. The main backlash of this method is that it become difficult to detect small objects. However this also indicates remote objects, especially in this case where no small objects are being detected. As seen before, the

accuracy of long range detection is the weakest so it is interesting to focus on close objects. Moreover as it will be explained in the next chapter, the approach used in this driving assistant is based on local hazards only.

2.3.4 Road Marks Extraction

The analysis of the road marks and especially of the road lines is very important to efficiently avoid numerous hazardous situations including road exits and collisions caused by involuntary lane changes. The knowledge of the lanes segmentation of the road enables a better evaluation of the surrounding environment. For example a detected vehicle getting closer of the controlled car would not be seen as dangerous if located on the reverse direction lane. The problematic of the line detection using cameras was discussed in numerous publications. If different approaches can be considered, the methods often include mathematical models of lines, a restriction method of the image area to study, edges detection and color filtering[41] [42]. This kind of detection algorithms, especially applied to driving assistant, are required to be both quick and efficient. The speed of the detection is crucial in order to perform real time support, as in driving condition the environment is evolving rapidly. The ability of the process to detect all of the desired lines, and only those ones, is also critical to avoid incorrect reactions of the driving assistant. To solve those problems it is required to reduce the area of the image on witch to work, in order to increase the computation speed, and to filter the detected lines according to some models to avoid false detections.

In order to reduce both the computation time and the number of false detections, only the pixels corresponding to the road are kept for further use. That means that in the initial image shown in Fig.2-13, only the pixels whose coordinates in the 3D reprojection are located at the ground level and are laterally not too distant of the car are kept to produce the image shown in Fig.2-14.

Road surface marking are characterized by a uniform color that is very distinct from the asphalt color, typically white or yellow. This choice, made to facilitate the understanding of the road by human drivers, enables the computer vision algorithm to use a color filtering with a satisfying accuracy. Moreover, as only the road part of the image is kept

Fig. 2-13: Example of image on which the line detection is performed.

Fig. 2-14: Restriction of the image to the road area.

from previous filtering, the probability of false detection is reduced. The first step of the line detection is then an extraction of the white part of the image using a color filtering. The result of this filtering is a binary image shown in Fig.2-15.

After that first filter, a median filter is applied to remove the noise from the color extraction, Fig.2-16. The next steps of the algorithm are a Canny Edge detection[43], shown in Fig.2-17, followed by a Probabilistic Hough Line Detection[44]. This algorithm use a polar representation of lines and is used in different applications[45][46][47]. For each element of a subset of all the result pixels of the edge detection, every possible lines going through that pixel are described by a curve in a (θ, r) space, with θ and r the polar model parameters. The intersection of N curves in that space indicates a line crossing those

Fig. 2-15: White color extraction.

Fig. 2-16: Results of median filtering.

N pixels. The result of that detection (Fig2-18) is a list of segments represented by the coordinates of their two extremities in the image.

However, in that state, the result is composed of too many segments describing the same line. This is why they have to be fused. To do so a polar line model represented in Fig2-19, where X_1 and X_2 are the extremities of the segments obtained with the Hough detection, M a point of the line and Y the intersection of the line with the ordinate axis, is used. Each line is represented by a couple (r, θ), where:

$$\theta = \frac{\pi}{2} + \alpha \tag{2.14}$$
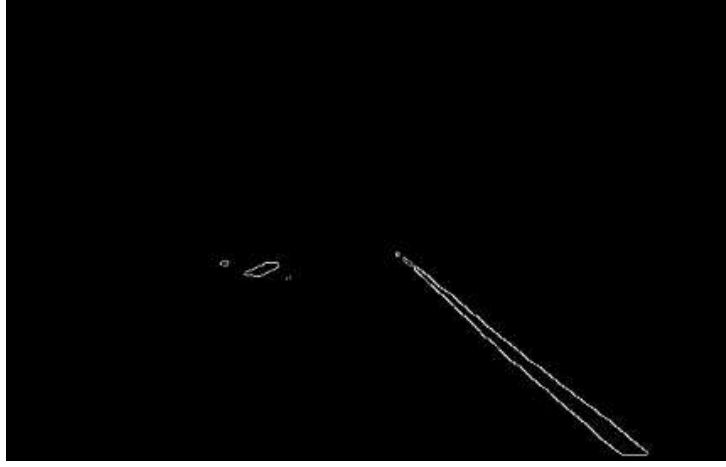
Fig. 2-17: Results of canny edge detection.
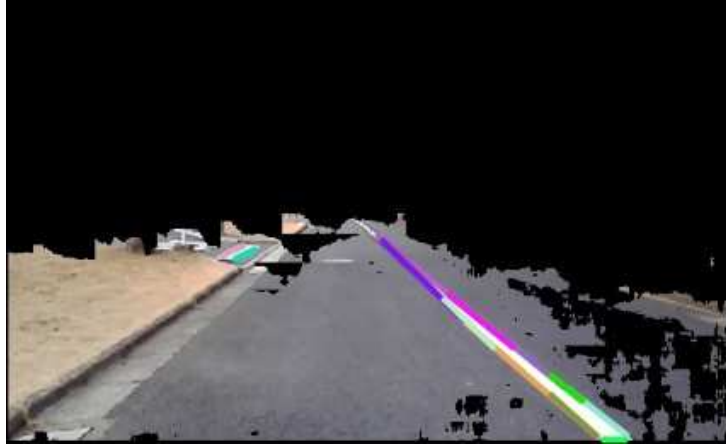
Fig. 2-18: Results of probabilistic hough detection.

$$\alpha = \arctan(\frac{y_2 - y_1}{x_2 - x_1}) \tag{2.15}$$

$$Y = y_1 - x_1 \tan(\alpha) \tag{2.16}$$

$$r = \begin{cases} |x_1 \cos(\theta) + y_1 \sin(\theta)| & \text{if } Y > 0 \\ -|x_1 \cos(\theta) + y_1 \sin(\theta)| & \text{if } Y < 0 \end{cases} \tag{2.17}$$

Before any fusion, the short segments are removed, based on their estimated lengths in the camera space, computed from the 3D reprojection. This enable to remove road line
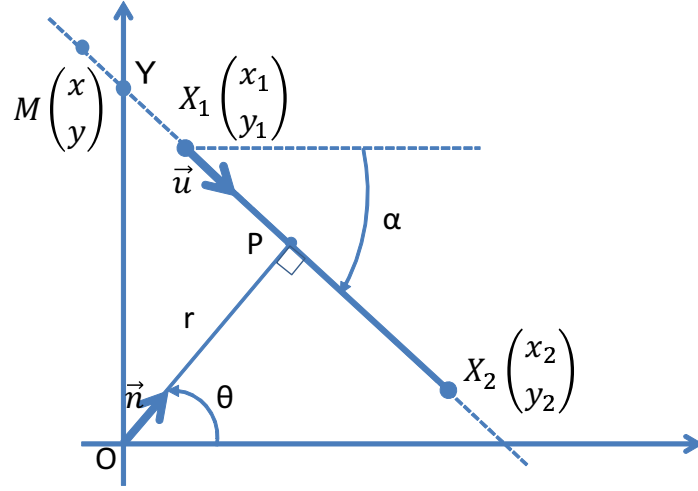
Fig. 2-19: Used polar model.
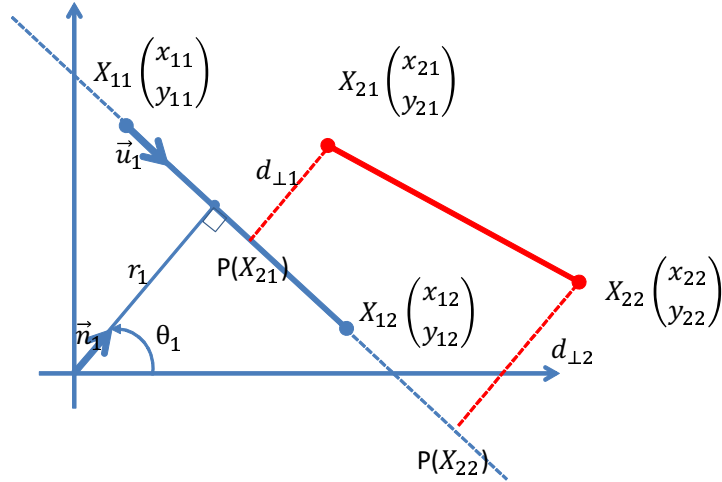
Fig. 2-20: Comparisons of two segments.

extremities for example. Then, a line L1 is fused with an other line L2 if $\theta_1 \approx \theta_2$ and if the orthogonal distances of the extremities of the second segment to the line of the first segment, $d_{\perp 1}$ and $d_{\perp 2}$ (see Fig.2-20) are inferior to a threshold value. $d_{\perp 1}$ and $d_{\perp 2}$ are obtained as follows.

$$d_{\perp 1} = |\overrightarrow{X_{11}X_{12}} \cdot \overrightarrow{n_1}| = |(x_{21} - x_{11})\cos\theta + (y_{21} - y_{11})\sin\theta| \tag{2.18}$$

Then using the projection of the extremities of L2 on L1 it is possible to extend the

Fig. 2-21: Results of segments fusion.

Fig. 2-22: Final result of the line detection.

first line to include the second one. For example $P(X_{21})$ is defined by:

$$\overrightarrow{X_{11}P(X_{21})} = |\overrightarrow{X_{11}X_{12}} \cdot \overrightarrow{u_1}| \cdot \overrightarrow{u_1} = ((x_{21} - x_{11})\sin\theta - (y_{21} - y_{11})\cos\theta) \cdot \overrightarrow{u_1} \qquad (2.19)$$

The result of that fusion process is composed of two parallel lines for each road mark as shown in Fig2-21. Those lines are processed using the coordinates of their extremities in the camera space in order to obtain the final result of the line detection as shown in Fig2-22.

2.4 Computation Acceleration

2.4.1 Acceleration Methods

The main backlash of the previously described methods is that in order to be accurate they are time consuming. However to be efficient, a driving assistant has to be able to react in real time to the evolution of the cruising environment. The meaning of this last sentence is that the computation time of the detection algorithm, and later of the support computing process, should be sufficiently small to take into account the evolution of every possible dangers and that the acquisition of information should not be delayed, especially in remote driving applications. It is difficult to estimate accurately an acceptable threshold for the computation time. Indeed this one can vary in function of the application. In the case of low speed evolving robots, that computation can be quite high. However in the case of a driving support, the speeds of the controlled vehicle and of the moving objects in the surrounding of the car are high. This means that the whole computation loop of the computer vision algorithm should be executed several times per second. It also implies that the processed images should be the more up to date as possible. Finally it is possible to conclude that in case of remote control, the image processing should absolutely be conducted on the controlled vehicle to avoid every time delay caused by the communication between the controller and the controlled object.

They are several methods that can be used to increase the computational speed. First by combining the results of different detections it is possible to increase the rapidity of the next one. For example, the line detection uses the results of the 3d reprojection to reduce the area of the image to take into account. Moreover computer vision algorithms can be accelerated by using parallel computing. Parallel computing is a process by which several computations are conducted simultaneously. It is based on the assertion that large problems can be divided in small and independent ones that can be solved at the same time. This method cannot be applied to every algorithm but can be especially efficient in the case of artificial vision and especially in this case. Indeed a lot of operations in image processing are applied to each pixel and only use local information, i.e. pixel close to the one on which the computation is conducted. By then is possible to perform simultaneously and independently the same operation on each pixel of an image. This is by essence

the idea behind Graphic Processing Unit computation . GPU are processors with low frequencies compared to traditional CPU but with a high number of processing cores, but are a real evolution in parallel computing[48][49][50]. By instance the used Tegra® Jetson TX1 is equipped with a 4 core CPU with a 2GHz frequency, while its GPU posses 256 cores which maximal frequency is 0.8GHz. Moreover CPUs are often able to perform more complicated computations compared to GPUs. This is why the computation are conducted on Jetson development kits, to benefit from both their GPUs and their portability. GPU processing uses specific programming languages, CUDA in the case of the presented algorithm. This one was not directly implemented in CUDA but using OpenCV functions written in CUDA in a C++ code. Finally the different detections can be conducted simultaneously as they are independent. Indeed the results of the line detection are not required to perform any of the obstacle detections that are themselves not related. It is then possible to perform those detection in separated program threads that, instead of using the GPU, use the four cores of the CPU.

2.4.2 Algorithm Structure

Fig.2-23 represents the threads architecture implemented in the previously described program. First a thread was created to specifically handle the image acquisition from the camera. Indeed this process was very slow (up to 40ms)if included in the main thread. The acquisition thread get a new frame at a 60Hz frequency. The acquired images are stored in 2 buffers to ease the exchange between that thread and the main frame and reduce the probability of the two threads trying to access the same buffer at the same time, that would result in a delay of the threads executions. The acquisition thread continuously indicates to the main thread the index of the buffer containing the most up to date frame. The buffer also contain the latest estimated position of the car in the experiment referential $\Re_0$. This position is estimated by the previous cinematic model and is used to calculate the positions of the detected hazards in $\Re_0$. This acquisition thread is also a way to be sure that the image used for the detections are the most up to date as possible, without considering the computation time of the other threads.

The main thread of the algorithm is in charge of the computation that are required by

Main thread
(GPU
Accelerated)

Handles the other threads.

Image remapping,
color change

Disparity Map
Construction

3D Re-projection

Front vehicles detection
(GPU HAAR cascade)

Waits for Detection
Threads

Position Estimation

Lateral
Vehicles
Detection
(HOG
cascade)

Return a list of
detected cars.

Pedestrians
Detection
(HOG
cascade)

Return a list of
detected
pedestrians.

Road Lines
Extraction

Uses the results of the
reprojection. Thus
delayed of one loop.

Return a list of
detected lines.

Images
Acquisition
Thread

Continuously stores
frames in 2 buffers.

Frequency of
acquisition: 60Hz.

Indicates to the
main thread the
buffer index of the
newest frame.

Images
Buffers

Fig. 2-23: Threads architecture of the proposed algorithm.

all the detections. This include the image remapping and the color change that are done using the GPU to increase their speeds. After that point the main threads launches the detection threads, i.e. the detection of sides of vehicles, the detection of pedestrians and the lines detection. It then conducts the 3d reprojection and the detection of fronts and rears of vehicles. Once again all of these processes are conducted on GPU. After those steps the main thread waits for the detection threads to terminate. Indeed the results of all the previously conducted processes are required to perform the location estimations of the detected hazards. Those estimations are also conducted on simultaneous thread. The main thread is the only thread using the GPU as this one cannot be accessed by several threads at the same time. It should then contain the operation that benefit the most of the GPU parallel processing.

The detection threads are merely conducted on the CPU cores as explained in the previous section. The only specificity is the line detection process. Indeed as this one

Table 2.1: Performances by operation.

Jetson Version	TK1		TX1		TX1	
Acqu. frame size	640x400		640x400		1280x800	
Operation	Mean(ms)	SD (ms)	Mean(ms)	SD (ms)	Mean(ms)	SD (ms)
Total Duration	86	15.74	51	11.53	110	14.5
Remap., Color conv.	6	2.41	3	2.69	17	17.02
Block Matching	39	11.11	20	7.81	54	17.55
Reprojection	7	3.46	2	2.0	10	4.00
Haar GPU	28	8.12	22	9.43	19	6.08
Wait CPU	3	7.68	2	4.69	5	8.49
HOG pedestrian	77	18.27	42	6.16	85	14.46
HOG Car	54	15.84	36	7.42	75	11.18
Lines detection	69	18.41	27	3.61	68	15.94

uses the result of the 3D reprojection it needs to wait the results of this process. However performing the road line extraction in the main thread after the reprojection would slow down the whole process. This is why it is executed at the same time as the other detections but using the result of the previous loop of the algorithm.

The obtained performances are discussed in the following subsection.

2.4.3 Performances

Table.2.1 gathers the achieved performances, mean execution durations and standard deviations of that durations, of the computer vision algorithm used to detect and locate hazards as described in the previous section and based on the threads architecture explained before. The measures were conducted on several versions of the Jetson development kit and with different image resolutions. On the TK1 version only the 640x400 resolution was considered as a greater one would imply a computing time not compatible with a driving assistant. In that situation a loop of the algorithm has a mean execution time of 86ms it corresponds to a 11.62Hz frequency. The frequencies reached on the TX1

are 19.6Hz and 9Hz. It can be observed that all of these frequencies are compatible with the real time computation required for the driving assistant. The advantages of a higher resolution are a higher capacity to detect small or far objects and a better accuracy of the reprojection of the farthest points. However they are obtained at the price of a twice lower frequency. A choice has then to be conducted depending of the application and of the desired performances.

It can also be observed that the duration of the computations conducted in the GPU using thread, the block matching, reprojection, and the GPU Haar, is similar to the durations of the detections conducted in parallel in other threads. Then the time spend waiting for the threads convergence is small and is often null.

2.5 Exchange of Hazards Information

A very important factor for the efficiency of the driving assistance is its capacity to detect every danger on the road. If a hazard is ignored, the results returned by the path planning could be wrong. This is why the sole use of a stereo camera system cannot be satisfying. Indeed the detection is limited to the field of vision of the stereo camera system. Moreover even if located in the field of vision of the system an object could remain undetected. If an object is hidden behind a bigger object, it cannot be detected by cameras. This situation is not specific to the camera and can be encountered with other types of sensors. Furthermore a broadcasting of hazards can ensure a quicker propagation of the danger information than a mere detection. To solve this problem a communication system was designed. Its purpose is to share information about hazards between different vehicles or other still transmitters. The principle of this system is shown the Fig. 2-24.

The communication system is based on several emitters sharing their lists of hazards. Each hazard is described by a position and an orientation, a shape detected by a camera or directly set by an operator, a type, a degree of certainty, an identifier and the date of the last update. The type is used to know which virtual potential field, described in the next chapter, is to be used to represent the hazard according to its shape, but also to determine the duration of the validity of the information. This one is much longer for a still obstacle than for a moving car. The level of certainty is used to define a rank of accuracy of
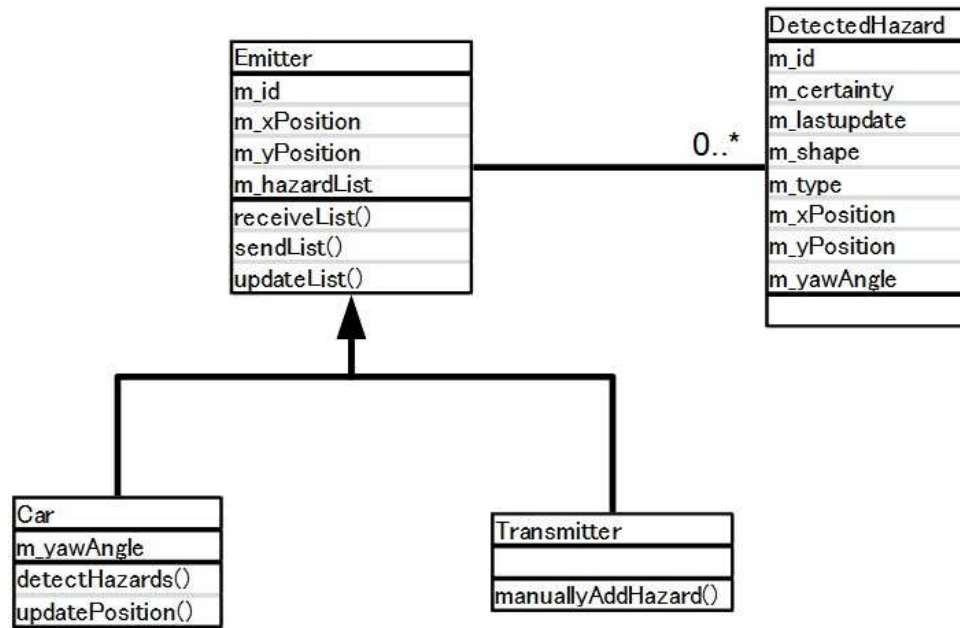
Fig. 2-24: Class diagram of the communication system.

the information. For example, the information concerning the shape of a vehicle can be considered as completely accurate if the vehicle itself send these specifications, compared to the accuracy of a shape obtained through image processing.

The emitters can be separated in two categories, cars or other vehicles using a driving support, and transmitters with a stationary position. The emitters send periodically their lists of hazards to the other emitters. The purpose is to construct in each emitter a list of dangers representing every menaces. When receiving a list, an emitter try to find if the received dangers are already in its hazard list by looking at the identifiers and the positions of the dangers. If two hazards are very close but with two different identifiers they can be considered as the same object depending of their types and the distance between them. If a hazard was not previously contained in the list it is added to this one. In case of a detected correspondence, data is updated taking into account the date of the last updates and the levels of certainties. Hazards whose last updates are too old are cleared from the list periodically to suppress obsolete information.

The specificities of the car are the following. Their hazards lists contain information about themselves that are shared with the other emitters. Their positions are also updated
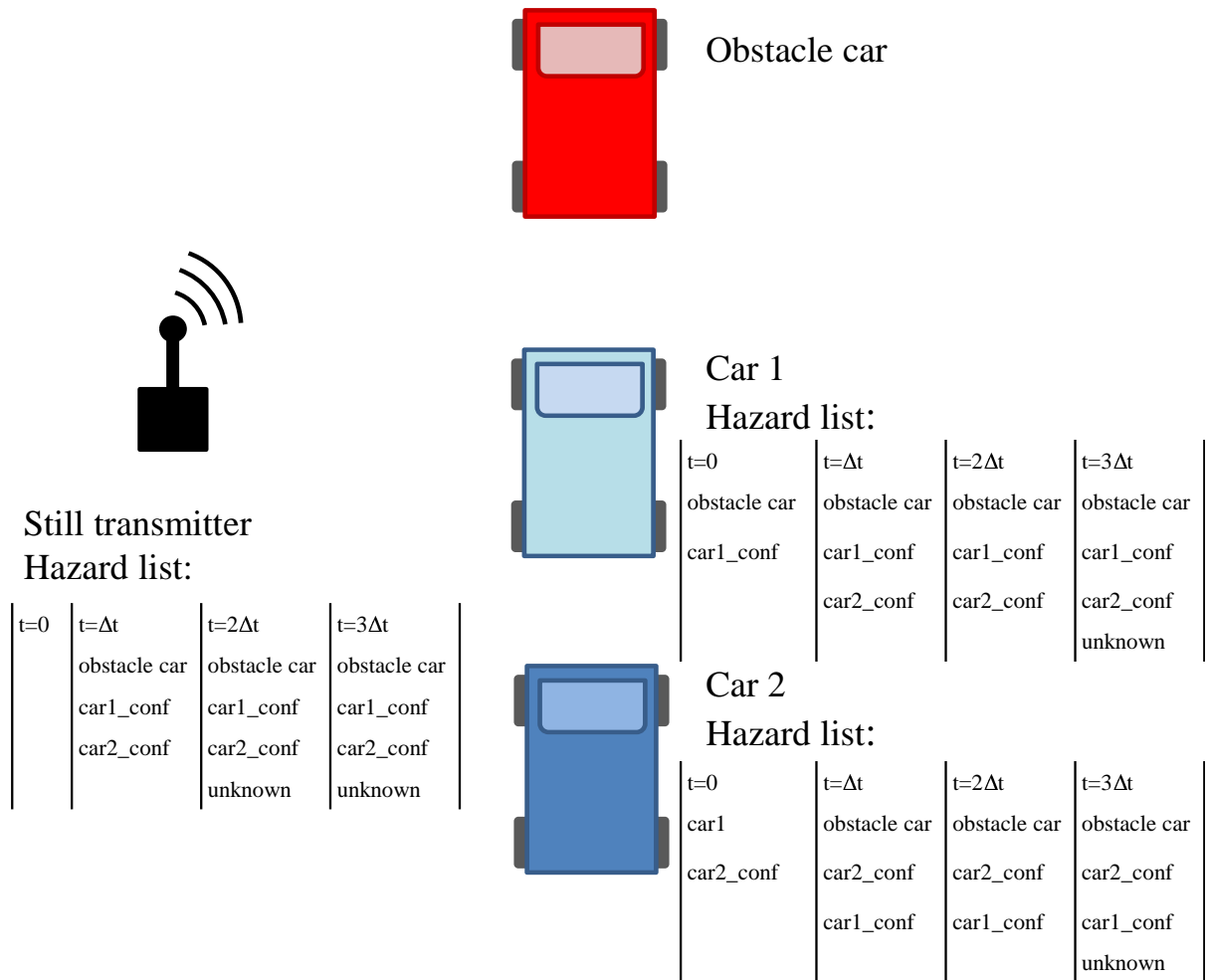
Fig. 2-25: Example of hazard list sharing.

periodically and the hazards considered too far away are removed from the list. Cars also use their detection system to identify dangers to add to their lists.

The purpose of the transmitters is mainly to help the sharing of information as relays. They can also be used to manually declare some hazards with the highest level of certainty or to detect dangers from a different point of view. It could be used in the case of road accidents or roadworks to specify an access restrained area.

Fig.2-25 represents an example of that hazard sharing. In this scenario, two cars, Car 1 and Car 2 are equipped with a driving assistant and a hazard sharing protocol. An other car without assistance is in front of Car 1 and a still transmitter is located in the vicinity. At $t = 0$, it is supposed that no information was transmitted, and that the only

hazards in the lists are the results of the detections and themselves in the cases of Car 1 and 2. Δt corresponds to the time lap between two information transmissions that are supposed to be simultaneous between all of the emitters. The process is the following. At $t = 0$, the still transmitter has detected no hazard, Car 1 detected the obstacle but not Car 2 that is located behind. Car 2 detected Car 1 but not the hidden obstacle car. At $t = \Delta t$, the first transmission is conducted. The still transmitter received the confirmed information about Car 1 and 2 and the detection information about the obstacle car. Car 1 become aware of Car 2 and the late one obtain the information about the obstacle car and is able to get confirmed data about Car 1. At $t = 2\Delta t$, the still transmitter receives data about an unknown hazard, either manually entered or from an external source. This information is received by the cars at At $t = 4\Delta t$.

2.6 Summary

This chapter presented the different methods used to increase the environment awareness of the controlled vehicle. Mostly based on the use of a stereo camera and different artificial vision processes to detect and locate hazards, i.e. other vehicles, pedestrians and road lines, the main contributions of that thesis concerning that aspect of the driving assistant are related to the increases of accuracy and speed of the awareness mechanism. They are achieved through a specific combination of the different computer vision functions, aiming at using the result of a process to speed up the following, but also using as much as possible parallel processing and GPU computing. This aspect is really dependent of the chosen hardware and its possibilities. Finally, in order to improve the completeness of the detection of the environment hazards, a protocol enabling sharing of information concerning that dangers was presented. This protocol can be used to acknowledge dangers outside of the camera field of view an can be used as a base to develop application based on multiple vehicles using driving support in order to study the behavior of such systems.

Chapter 3

Environment Modelization

3.1 Goal and Principle

The modelization of the environment is complementary to the environment awareness obtained through sensors and other methods described in the previous chapter. Indeed the modelization of the environment aims at defining how a detected hazard is included in the driving assistant path planing and what is its impact on the support offered to the driver. However those two processes are independent because one of them can be changed without any impact on the other. It is possible to completely change the detections methods, by instance to use a LADAR system[51] [52] [53] to complete the 3D reconstruction of the car environment or to change the method used to detect a car, without changing the models used to represent the different types of hazards and to compute the active support. On the other hand it seems obvious that a change in the modelization of the dangers does not affect the way they are detected. By changing that modelization it is possible to modify the reaction of the driving assistant in order to obtain a behavior closer to what is expected of it.

In this thesis the assisting torques to apply on the steering wheel and pedal are obtained by a short range path planning. The used method is based on virtual potential fields representing the different dangers that can be encountered on the road. This approach was created to simplify the trajectory planning task and was used in several fields such as the control of manipulators[54] [55], mobile robots[56] [57] and even driving assistance[55] [58]. The
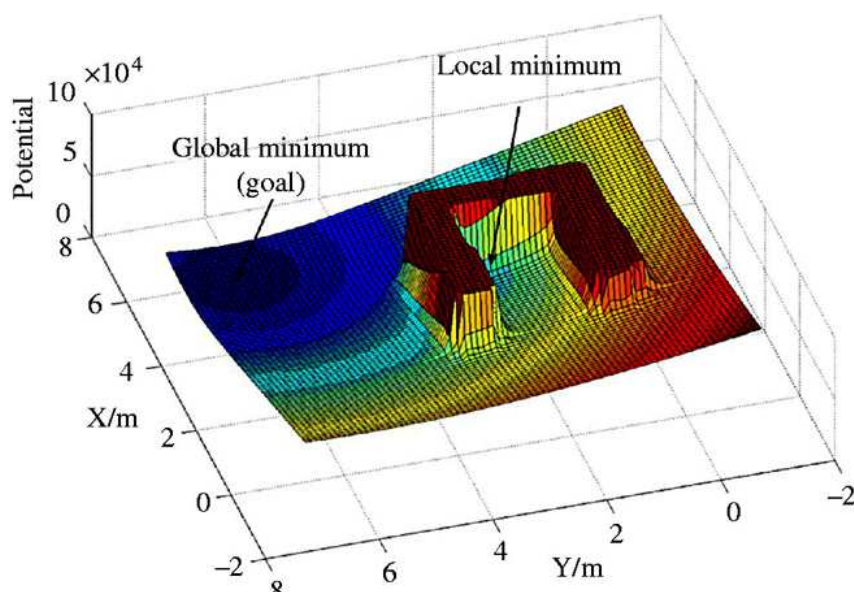
Fig. 3-1: Example of hazard map.

principle of virtual force fields is to assign to each point of the space in which the controlled object is evolving, a measurement representing the level of hazard at this point. At each type of detected hazard corresponds a particular potential field with a specific shape to allow the assistant to react correctly depending of the surrounding of the controlled car. As the potential fields are additive it is possible to create a hazard map, as shown in Fig.3-1, expressing all of the detected dangers. A local derivation on the location of the car on the hazard map allows a quick computation of a short range path planning. Torques corresponding to the desired trajectory are then applied on the steering wheel and pedal. This method allows a better cooperation with the human driver that is informed of the reactions of the driving assistant and can have an increased control feeling over the trajectory and speed of the car, compared to what would happen if no feedback was offered on the interfaces with the user. It is expected, by then, to increase the acceptability of the proposed system by road users, conversely to a certain reluctance toward autonomous vehicles. The main problem of this approach is caused by the possible appearance of local minima. However as the proposed system is a driving support this problem can be tackled by the driver who can choose to leave a local minima to reach a better location.

This approach is characterized by its local aspect. Indeed only the hazards close to the

controlled vehicle are taken into account by the path planning and then the computation of the support to the driver. The main interest of this propriety is that it has a good symbiosis with stereo cameras. Indeed with that kind of reprojection the accuracy goes worse as the distance is increased. The use of virtual potential fields enable to consider a danger only when it is relatively close to the controlled car, corresponding to when its location is estimated with the best accuracy.

3.2   Control of the vehicle

This section will describe how the vehicles used to test the efficiency of the proposed method are controlled in two different conditions, with the driver inside the car, in a typical case of embarked driving assistant, and in case of remote driving by controlling the car from a distant driving station. This should enlighten how the assisting torques are applied by the driving support.

3.2.1   Driver in the vehicle

Fig.3-2 is a representation of the control applied to the vehicle. The used variables are listed in Table.3.1. In this figure we can see how the driving assistant torques are applied. It can be divided in two main parts. One controlling the direction of the vehicle and the other controlling its speed. Those parts both use Disturbance Observers[59] to correct the disturbances applied on the motors and Reaction Torque Observers[60] to estimate the intensity of the torques applied by the driver.

It can be observed that three torques are applied on the pedal. The first one, τ_{daped} is created by the driving assistant from the results of the modelization of the detected hazards, and will be described with more details in the next section. The second, $\tau_{driverped}$, represents the interaction of the driver with the pedal system. Finally the last one, τ_{re} is a torque aiming at returning the pedal in its original position, corresponding to a speed of the controlled vehicle equal to 0. It can be expressed as follows.

$$\tau_{re} = -\left(K_{re}\theta_{ped} + D_{re}\dot{\theta}_{ped} \right) \tag{3.1}$$

Where K_{re} is a proportional gain and D_{re} a damping term.
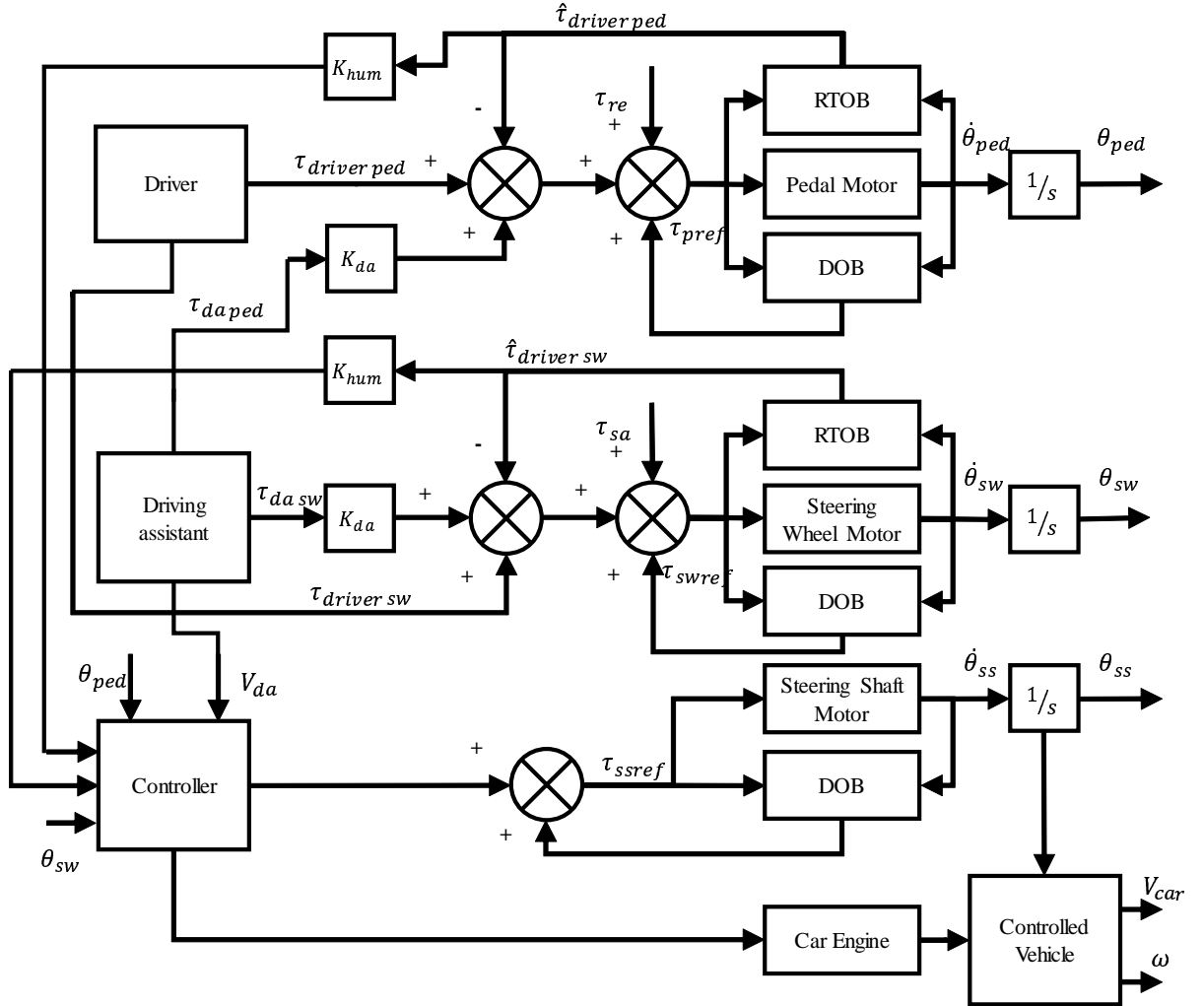
Fig. 3-2: Block diagram of the control of the car, driver in the vehicle.

The same structure is implemented on the other master motor that is connected to the steering wheel. Two torques τ_{dasw} and $\tau_{driversw}$ respectively correspond to the support offered by the driving assistance and to the action of the human user on the steering wheel. The last one, τ_{sa} is a self alignment torque. Its purpose is to return the steering wheel in a neutral position. Its behavior is described in Fig.3-3. It behaves as spring term for $\theta_{sw} \in [-\theta_{swlin}, \theta_{swlin}]$. The torque is then constant if $|\theta_{sw}| < \theta_{swmax}$. The purpose of that phase is to prevent the self aligning torque to become so strong it would prevent the driver to move the steering wheel. And finally if $|\theta_{sw}| > \theta_{swmax}$ the torque is increased rapidly. θ_{swmax} correspond to the maximum angle that can be reached by the steering

Table 3.1: Parameters of the block diagram, driver in the vehicle.

Variable	Meaning
$\tau_{driverped}$	Driver's torque on the pedal
$\widehat{\tau}_{driverped}$	Estimated driver's torque on the pedal
τ_{re}	Return torque of the pedal
τ_{pref}	Command torque of the pedal
τ_{daped}	Driving assistant's torque on the pedal
$\tau_{driversw}$	Driver's torque on the steering wheel
$\widehat{\tau}_{driversw}$	Estimated driver's torque on the steering wheel
τ_{sa}	Self aligning torque on the steering wheel
τ_{swref}	Command torque of the steering wheel
τ_{dasw}	Driving assistant's torque on the steering wheel
τ_{ssref}	Command torque of the steering shaft
θ_{ped}	Pedal angle
θ_{sw}	Steering wheel angle
θ_{ss}	Steering shaft angle
V_{da}	Speed commanded by the driving assistant
V_{car}	Speed of the car
ω	Car's orientation

shaft, the purpose of that part is then to prevent the driver to reach a steering wheel position that could damage the system. In fact τ_{sa} also include a damping term that is not represented Fig.3-3.

In the block diagram, K_{da} and K_{hum} are gains used to control the influence of both the driving assistant and human driver on the trajectory of the car. They will be described later in this chapter.

On the slave part of the diagram, the τ_{ssref} torque is obtained through a PD control on θ_{sw} and the desired speed is computed from the following relation.

$$V_{cmd} = C_1 \frac{|\theta_{ped}|\theta_{ped}}{\theta_{pedmax}^2} \tag{3.2}$$
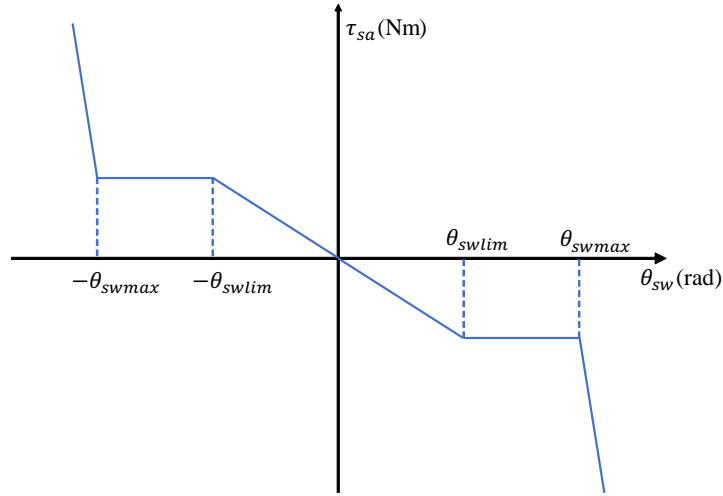
Fig. 3-3: Self aligning torque.

Where θ_{pedmax} is the maximal angle that can be reached by the pedal and C_1 a constant used to determine the maximum speed of the car. This expression allows a better accuracy of the speed selection at small angles compared to a linear expression.

3.2.2 Remote control

This section will describe how the remote control was implemented on the systems used to test the efficiency of the proposed driving assistant. The block diagram representation was split in two figures Fig.3-4 and Fig.3-5, and the used variable are listed in Table.3.2.

The realization of the steering will be studied first. As it can be seen, the support torque, τ_{dasw}, is computed directly in the controlled vehicle. This enable the driving assistant to correct the trajectory of the car without being impacted by the communication time delay caused by the network and expressed as $\exp^{-Ts}$. The direction of the car is handled through a virtual angle θ_{ss}. This angle does not represent any physical value but is used as a command to the steering shaft motor. The variation of this angle, $\dot{\theta}_{ss}$, is modified by three factors. The fist one is produced by the assisting torque through an impedance Z_{sw}. This impedance enable to estimate the variation of the steering wheel angle that would be caused by τ_{dasw} without other action on the steering wheel. $\dot{\theta}_{ss}$ is also modified by $\dot{\theta}_{swcmd}$ that correspond to the command of the variation of steering shaft angle. This value is obtained from the variation of position of the steering wheel on the driving station, by
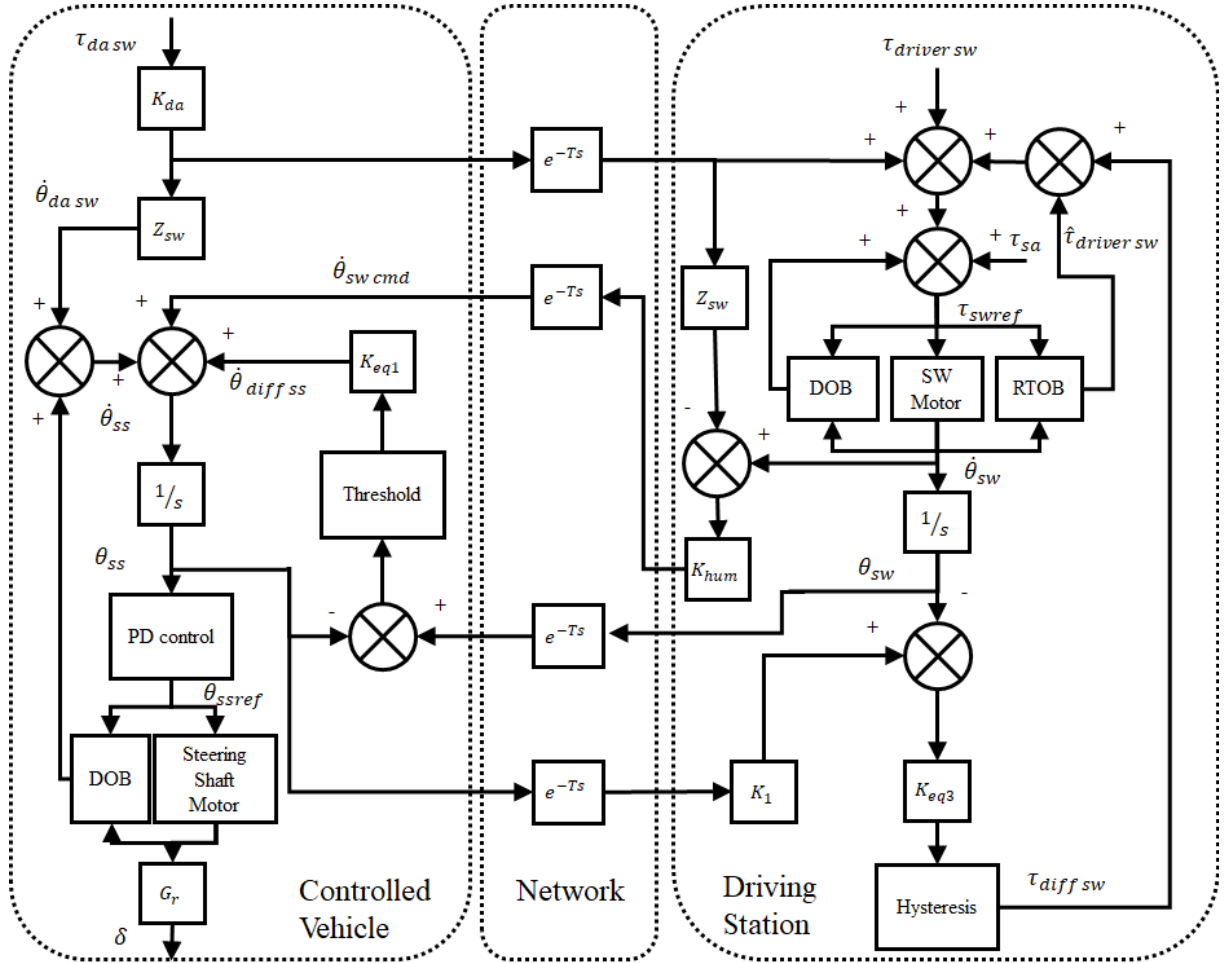
Fig. 3-4: Block diagram of the remote control of the car, steering.

subtracting $Z_{sw}\tau_{dasw}$ to $\dot{\theta}_{sw}$ in order to avoid applying the effect of the support twice. The last factor modifying $\dot{\theta}_{ss}$ is $\dot{\theta}_{diffss}$. This variation is computed from the difference between θ_{ss} and θ_{sw}. Its purpose is to ensure that those two angles tend to be equal after the end of the application of an assistance. This is why this difference goes through a threshold and is only applied by a proportional gain. By this mean the equalization is made slow and is not able to prevent the application of the driving assistant.

From the driving station point of view, the torques applied to the steering wheel are the same that were implemented in the case of the local driving. The differences are the delay in the application of the support torque and the addition of τ_{diffsw}. This torque is similar in its purpose to $\dot{\theta}_{diffss}$. A hysteresis filtering is applied to this torque to avoid
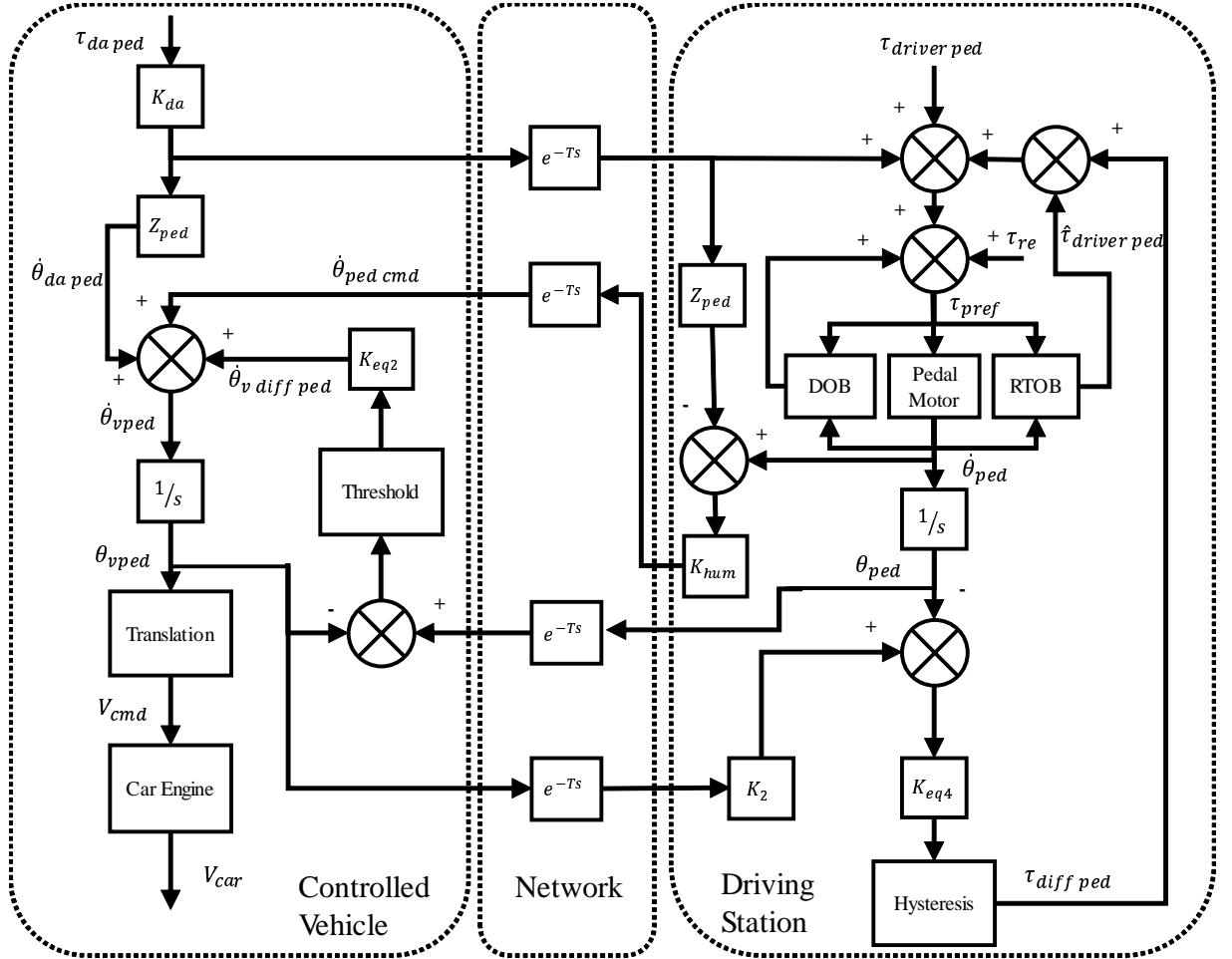
Fig. 3-5: Block diagram of the remote control of the car, speed control.

to counter τ_{sa} if the difference between θ_{ss} and θ_{sw} is small. The actual computation of τ_{diffsw} is performed as follows.

$$\tau_{diffsw} = K_{eq3} \left(\frac{K_{eq3} + K_{sa}}{K_{eq3}} \theta_{ss} - \theta_{sw} \right) \tag{3.3}$$

Where K_{sa} is the spring gain used to compute τ_{sa}. The purpose of this computation is to compensate τ_{sa} when trying to equalize the position of the steering wheel and of the virtual steering wheel angle.

The architecture used for the speed control is analogue to what was performed for the direction control.

Table 3.2: Parameters of the block diagrams, remote control.

Variable	Meaning
$\tau_{driverped}$	Driver's torque on the pedal
$\widehat{\tau}_{driverped}$	Estimated driver's torque on the pedal
τ_{re}	Return torque of the pedal
τ_{pref}	Command torque of the pedal
τ_{daped}	Driving assistant's torque on the pedal
$\tau_{driversw}$	Driver's torque on the steering wheel
$\widehat{\tau}_{driversw}$	Estimated driver's torque on the steering wheel
τ_{sa}	Self aligning torque on the steering wheel
τ_{swref}	Command torque of the steering wheel
τ_{dasw}	Driving assistant's torque on the steering wheel
τ_{ssref}	Command torque of the steering shaft
θ_{ped}	Pedal angle
θ_{sw}	Steering wheel angle
θ_{ss}	Virtual Steering Shaft angle
V_{car}	Speed of the car
δ	Car's wheels orientation
$\dot{\theta}_{pedcmd}$	Command of the pedal angle variation
$\dot{\theta}_{daped}$	Variation of the pedal angle caused by the DA
$\dot{\theta}_{vdiffped}$	Variation of the pedal angle caused by the angle equalization
θ_{vped}	Virtual pedal angle
V_{cmd}	Command speed
$\tau_{diffped}$	Equalization torque, pedal
$\dot{\theta}_{swcmd}$	Command of the SW angle variation
$\dot{\theta}_{dapsw}$	Variation of the steering shaft angle caused by the DA
θ_{ssref}	Command angle of the steering shaft
$\dot{\theta}_{diffss}$	Variation of the steering shaft angle caused by the angle equalization
τ_{diffsw}	Equalization torque, SW

3.3 Computation of the assistance

3.3.1 Line Crossing

In this thesis, the detected lines are modelized by Gaussian like potentials as shown in Fig.3-6. This figure represents an example of road on witch two lines were detected. At each point of the road it is possible to determine a strength to apply on the controlled car by performing a spatial derivation as shown by the red arrow. Those potentials can be expressed as follows:

$$P = K_{lw1} \exp\left(\frac{-D_\perp^2}{2S_{lw}^2}\right) \tag{3.4}$$

With K_{lw1} a scaling factor, S_{lw} a slope factor and $D_\perp$ the orthogonal distance between the center of the car and the line.

Fig3-7 shows a situation where a car is approaching a line. The position of the line is obtained through the coordinates of its extremities, as described in the previous section, and the position of the car is estimated with the previous cinematic model. In this figure, θ_C is the orientation of the car in the absolute referential, P the orthogonal projection of V, the car center, on the line and θ_F the orientation of $\overrightarrow{PV}$ in the absolute referential, representing the assisting force direction.

Using the previously defined parameters a support torque is applied on the steering wheel. Its purpose is to prevent undesired line crossing and to assure that the car remains in its lane. In this section the computation of the assisting torque applied on the steering wheel is described for a single line. In real use conditions this process is repeated for each lines, and the corresponding torques are added. First the norm and orientation of $\overrightarrow{PV}$ are computed. Then the difference angle $\theta_D = \theta_c - \theta_F$ is used to determine the direction of the torque to apply on the steering wheel. A positive torque correspond to a positive increase of δ. So we can define the direction d as:

$$d = \begin{cases} 1 & \text{if } \theta_D \in [-175°, -5°] \\ -1 & \text{if } \theta_D \in [5°, 175°] \\ 0 & \text{else} \end{cases} \tag{3.5}$$
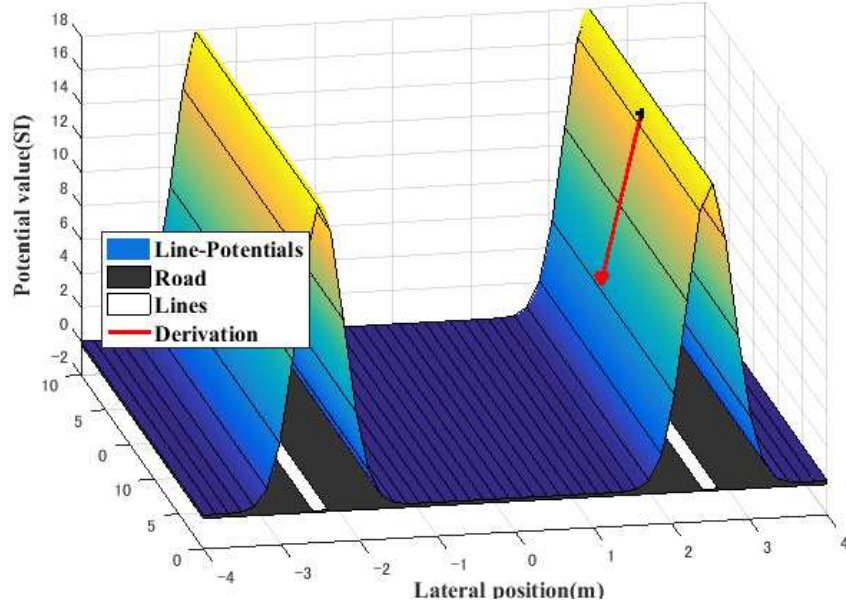
Fig. 3-6: Line Potentials representation.

The 0 case was created to handle the scenario where the car is completely orthogonal to the line. Indeed it is safer to let it go straight to avoid unpredictable direction changing. The next step is the computation of the desired steering wheel angle θ_{da} from the derivation of the line's potential.

$$\theta_{da} = dK_{lw1} \parallel \overrightarrow{PV} \parallel \exp\left(\frac{-\parallel \overrightarrow{PV} \parallel^2}{2S_{lw}^2}\right) \tag{3.6}$$

Then, with θ_{sw} the steering wheel angle, a gain is computed:

$$K_{dar} = \begin{cases} 0 & \text{if } \theta_{da}\theta_{sw} = 1 \text{ and } |\theta_{sw}| > |\theta_{da}| \\ \sqrt[3]{\left|\frac{\Delta \parallel \overrightarrow{PV} \parallel}{\Delta t}\right|} \; |\theta_{da}| & \text{else} \end{cases} \tag{3.7}$$

This gain is null if the current steering wheel angle is in the same direction than the one computed by the driving assistant and of greater value. Finally the driving assistance on the steering wheel is defined as follows:
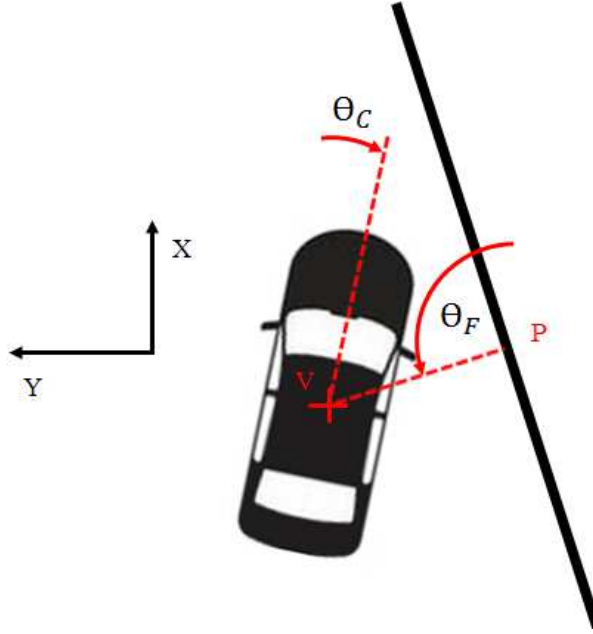
Fig. 3-7: Geometric model for the Line Driving Assistant computation.

$$\tau_{dasw} = \begin{cases} K_{rd}K_{lw2}K_{dar}\left(\theta_{da} - \theta_{sw}\right) & \text{if } \dfrac{\Delta \parallel \overrightarrow{PV} \parallel}{\Delta t} < 0 \\ -K_{rd}\dfrac{K_{lw2}}{1.8}K_{dar}\left(\theta_{da} - \theta_{sw}\right) & \text{else} \end{cases} \tag{3.8}$$

Where K_{lw2} is an adjustable gain and K_{rd} a gain used to modulate the effect of the road potentials in the driving assistant. The purpose of this final condition is to help the driver to align the car with the line when the vehicle is getting farther from it.

The driving assistant also has an impact on the speed control of the car. However to avoid to break suddenly if the angle between the line and the car orientation is small, the speed control is only applied when θ_D is bigger that 165° or smaller than −165°. With K_{lp} a scaling factor and S_{lp} a slope factor it is possible to define the applied support torque:

$$\tau_{daped} = -K_{lp}\theta_p \parallel \overrightarrow{PV} \parallel \exp\left(\frac{\parallel \overrightarrow{PV} \parallel^2}{2S_{lp}^2}\right) \tag{3.9}$$

This torque helps the driver to reduce the speed of the car, as this one only depends of the position of the pedal and is null when the pedal angle is equal to 0.
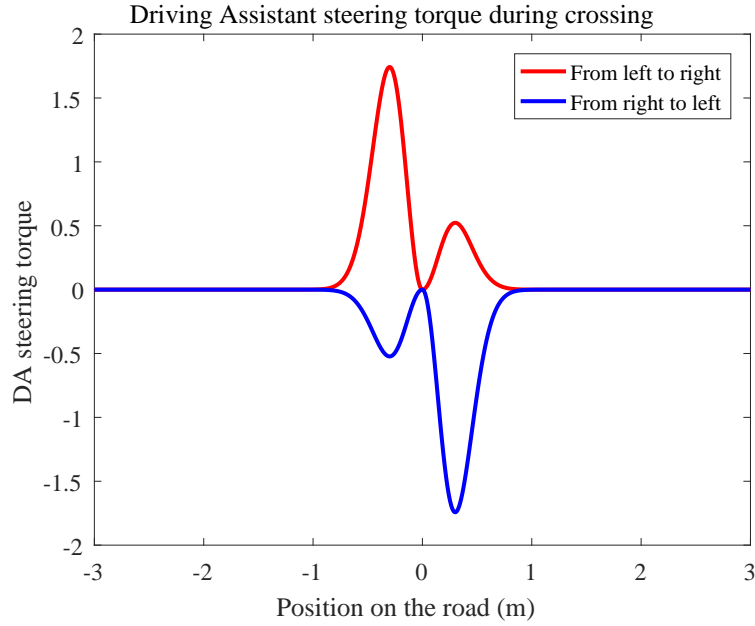
Fig. 3-8: τ_{dasw} during a crossing.

Fig.3-8 represents results obtained with Matlab and representing the assisting torques during crossing motions from both sides of the line. The steering angle is supposed to be constant, corresponding to a driver that would completely compensate the support, and equal to zero. Two phases can be noticed. The first one corresponds to an opposition of the crossing motion as the car get closer to the line. It is represented by the highest peak on the figure. In the second phase the driving support aims to realign the car with the line and produces a smaller torque. This behavior can be used to evaluate the efficiency of the implementation.

Fig.3-9 describes an example of the support torque of the pedal offered in a simulation where the car get perpendicularly closer to a line, from both of the road side. It can be observed that this torque is increasing as the car get closer, and is maximum when the center of the car is located at around 80 cm of the line.

The choice of the cubic root in the expression of K_{dar} was conducted with the idea of selecting a correct scaling between the torques obtained at high speed and the torques obtained at low speed. Tests were conducted in Matlab simulations, with different powers applied to the lateral speed, 2, 1, 1/2 and 1/3. The results are gathered in Fig.3-10. It
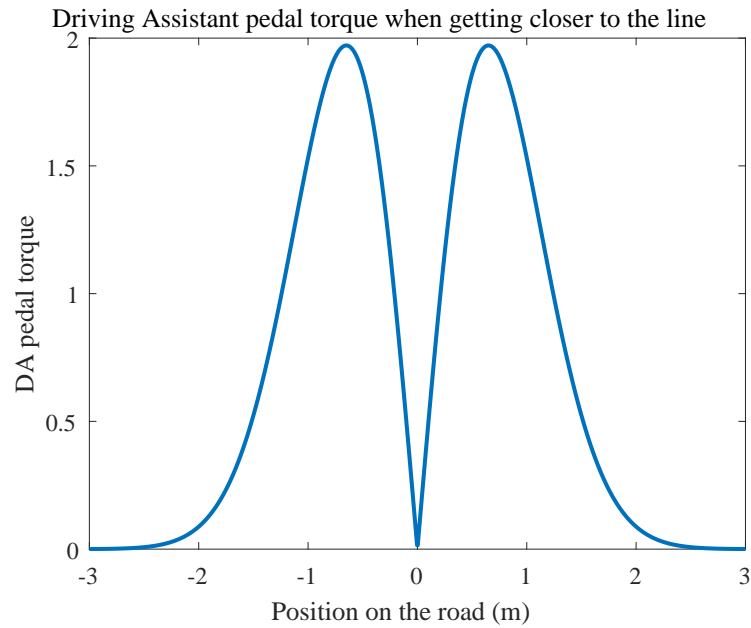
Fig. 3-9: τ_{daped} during a crossing.

can be observed that the highest the selected power, the biggest the difference of behavior between low and high speed. A cubic root was chosen because it suits the best to what was expected of the driving assistant. Indeed conversely to what is obtained with power applied to the lateral speed superior to 1 even at low speed the assisting torque can still be felt. Moreover an increase of speed provokes an increase of the support torque that remains in the same scale encountered at low speed.
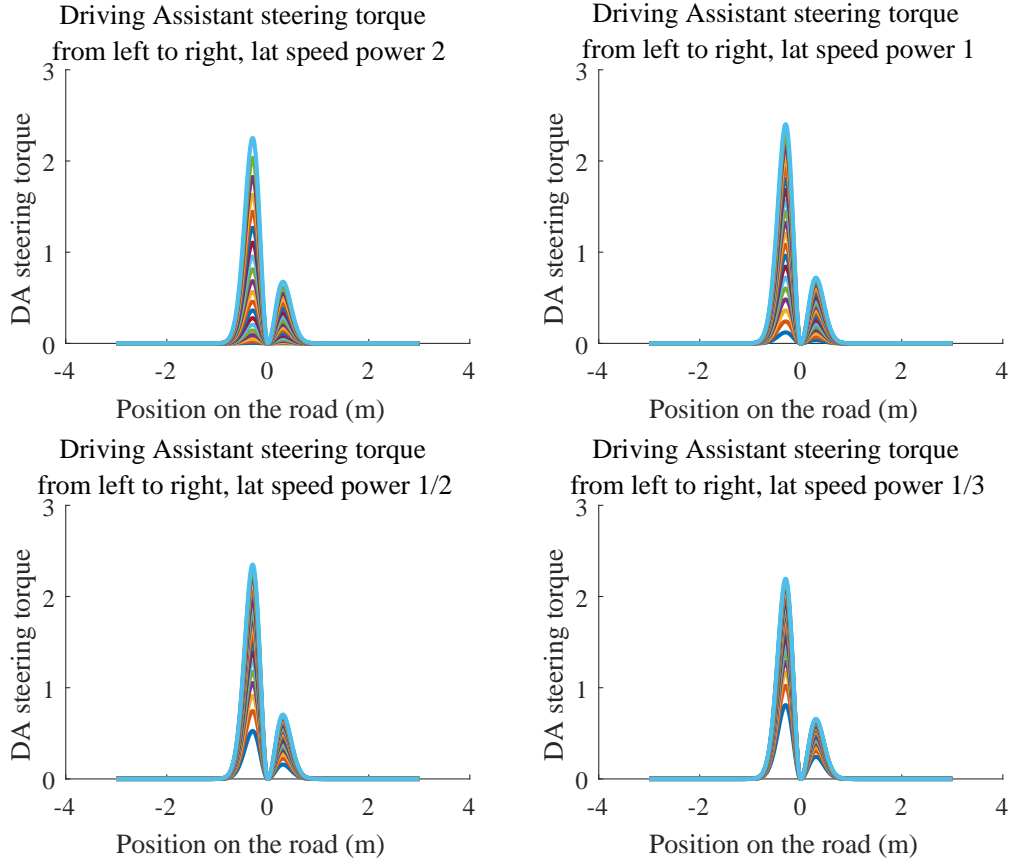
Fig. 3-10: Effect of the lateral speed on τ_{dasw} with different power of the lateral sped in K_{dar} computation, lateral speed between 0.01m/s and 0.2m/s.

3.3.2 Collision Avoidance

The potential created by a car type obstacle depends of the distance between the controlled car and the obstacle car, in order to create a shape as described in Fig.3-11. This shape is based on a rectangle describing the group of points located at the same distance of the obstacle car with the addition of a triangular shape at the rear of the car to help the controlled car passing the obstacle.

This is why, the first step of the collision avoidance is to estimate the distance between the car, and by then to determine if the two cars are colliding.

Two polygons are colliding if it is not possible to find a side on one of the two polygons that separate the vertices of the two polygons. It is then required to inspect each side
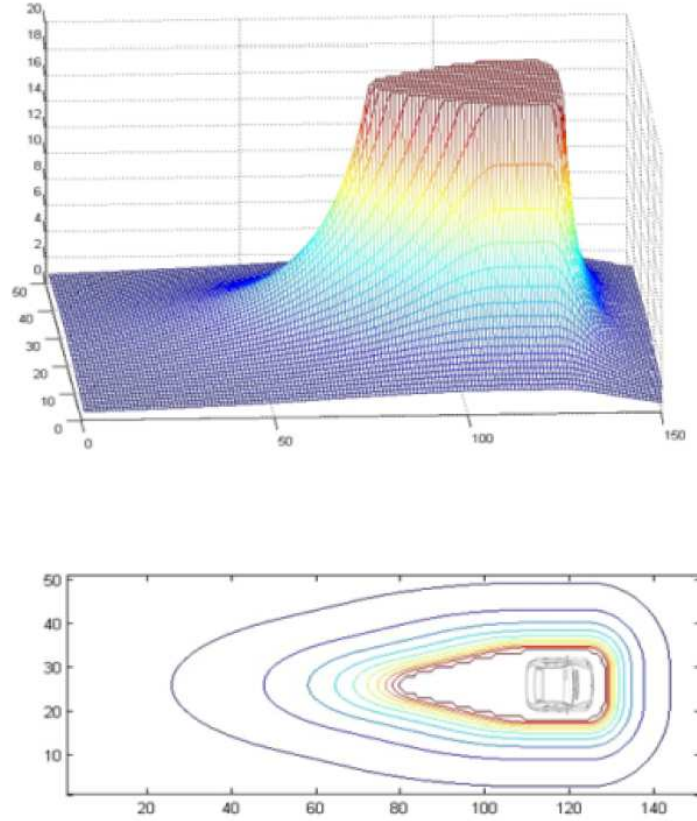
Fig. 3-11: Shape of the potential used to represent a car.

on both of the polygons to find such a separator. In Fig.3-12 the AD line separates the two cars indicating that there is no collision. In that situation the distance between the two cars can be estimated by checking for each vertex of the two polygons, the distance to the other car's vertices and its orthogonal distance to each side of the other car, if its orthogonal projection on that side is located between its two extremities. The minimum distance obtained corresponds to the distance between the two cars, d_{car}.

The potential is computed as follows:

$$P = \frac{K_{car}}{d_{car}} \exp\left(-S_{car} d_{car}\right);$$ (3.10)

With K_{car} a scaling coefficient and S_{car} a slope coefficient. This potential is maxed to a certain value as it could tend to the infinity.
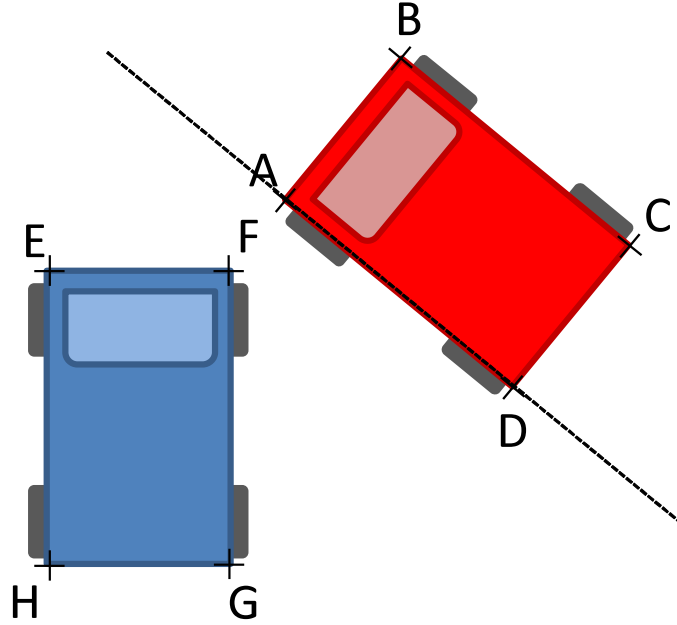
Fig. 3-12: Geometric model for collision avoidance.
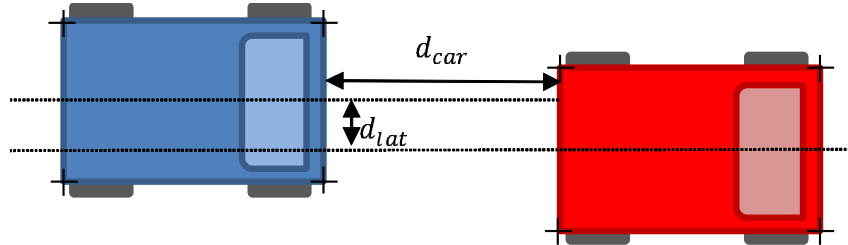
Fig. 3-13: Lateral distance.

To obtain the shape described in Fig3-11 designed to help the lane change, the distance used to compute the potential value is modulated when the controlled vehicle is located behind the obstacle car according to the following equation.

$$\widehat{d_{car}} = \left(K_{pp} \left(\exp\left(-K_{ps}|V|\right) - 1.0 \right) \left(1.0 - \frac{2.0|d_{lat}|}{W} \right) + 1 \right) d_{car} \qquad (3.11)$$

Where K_p and K_{ps} are scaling factors, V is the speed of the controlled car, W the width of the obstacle and d_{lat} the lateral distance between the centers of the two cars, as shown in Fig.3-13. The $\left(1.0 - \frac{2.0|d_{lat}|}{W} \right)$ part is here to give the rectangular shape of the potential. The $K_{pp} \left(\exp\left(-K_{ps}|V|\right) - 1.0 \right)$ is used to determine the length of the tail
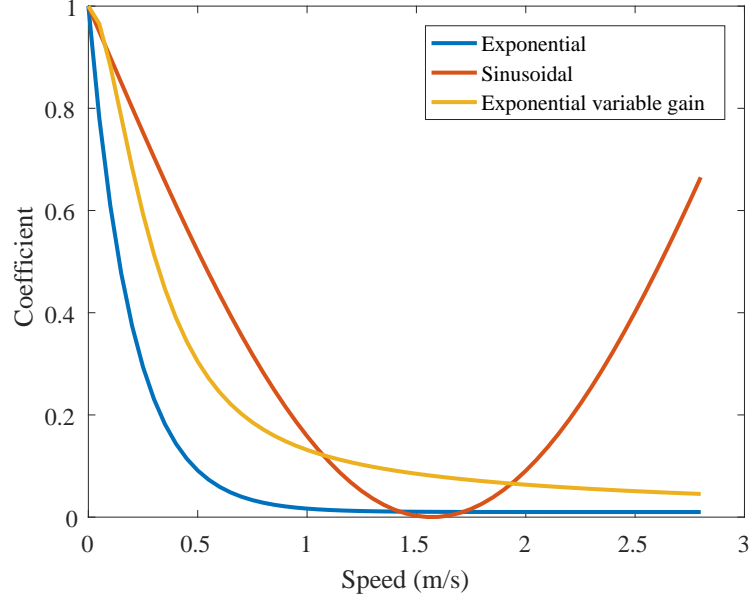
Fig. 3-14: Pseudo distance coefficient for different tail length method.

behind the obstacle car in function of the speed difference between the two cars.

The tail length determination was chosen among several choices, among them were the following options.

- $K_{pp} \left(\exp \left(-K_{ps}|V| \right) - 1.0 \right)$

- $K_{pp} \left(-\sin \left(K_{ps}|V| \right) \right)$

- $\dfrac{2}{\pi} \arctan(3K_{ps}|V|) \left(\exp \left(-K_{ps}|V| \right) - 1.0 \right)$

The results of the application of those expressions are shown in Fig.3-14 with a lateral distance equal to 0. The first expression offers a quick decrease of the pseudo distance with the speed but K_p should remain strictly inferior to 1. The second is less affected by the speed increase but can reach a value of 0. The periodic aspect is not a problem as it could easily be filtered. The last one is more complex but can have a softer decrease than the first one. The selected solution is the first one for the increased safety it offers as the coefficient is decreasing rapidly with the speed.

The effect of a change of K_{pp} and K_{ps} are shown in Fig.3-15 and Fig.3-16. On these figures, each choice of constant is represented by three lines of the same color. Those lines represent the distance at which the controlled car reach 25% of the maximum potential
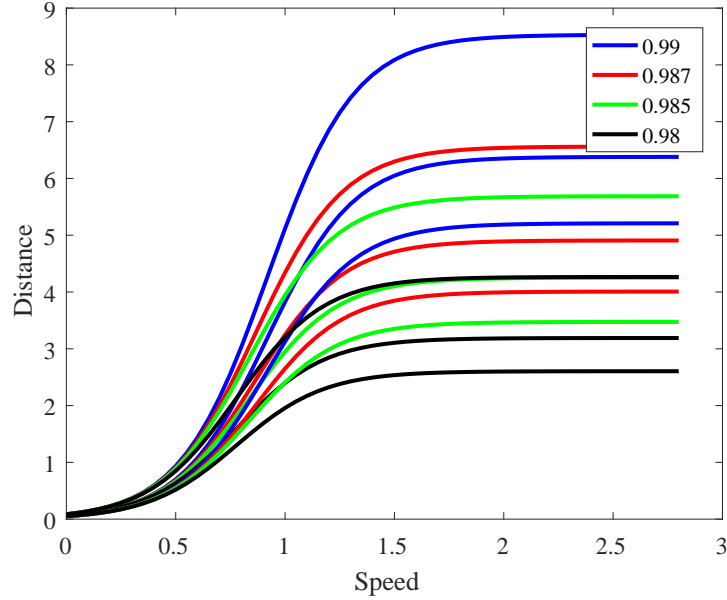
Fig. 3-15: Influence of K_{pp}.

value, the highest line, 50%, the middle one, and 75%, the lowest. It can be seen that increasing K_{pp} increases the distance at which the driving assistant begin to have en effect on the controlled car. On the other hand K_{ps} has an impact on the speed at which the previously described distances stop to grow. The bigger K_{ps}, the smaller the speed required to reach that limit is. Once the shape of the potential is decided through the choice of all the previously cited constants, it is possible to compute the assisting torque to offer on the pedal and on the steering wheel.

The driving assistant torque applied to the pedal is determined as follows. Its purpose is to slow down the car to avoid collision.

$$\tau_{daped} = P K_{cp} K_{ve} \tag{3.12}$$

With K_{cp} a scaling factor and K_{ve} a gain used to modulate the effect of the car potential in the driving assistant. This last gain will be discussed in the following section.

Concerning the support torque applied on the steering wheel, the direction of this one depends of the sign of d_{lat}. It is then possible to define this direction d as follows.
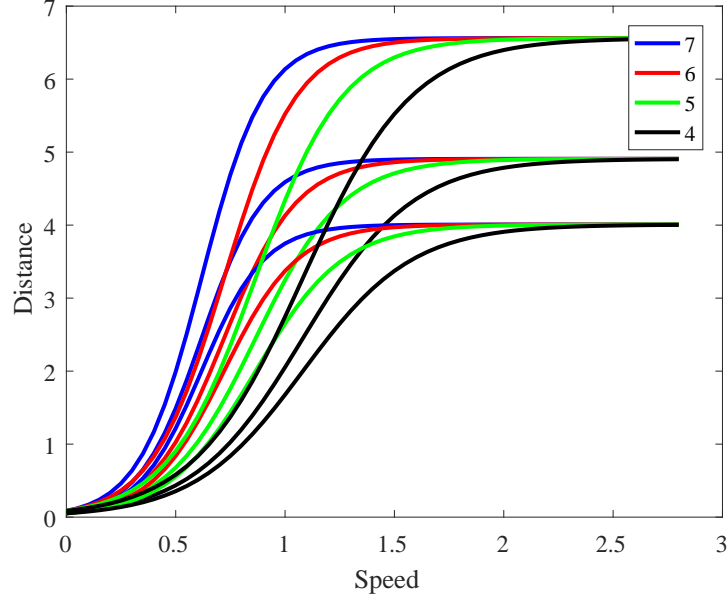
Fig. 3-16: Influence of K_{ps}.

$$d = \begin{cases} 1 & \text{if } d_{lat} > 0 \\ -1 & \text{else} \end{cases} \tag{3.13}$$

Then the lateral force to apply on the car to avoid the collision, F_{lat}, is defined in the next equation.

$$F_{lat} = \begin{cases} 2dP \left| \dfrac{dd_{car}}{dt} \right| & \text{if } \dfrac{dd_{car}}{dt} < 0 \\ -dP \left| \dfrac{dd_{car}}{dt} \right| & \text{else} \end{cases} \tag{3.14}$$

The smaller force aims at realigning the controlled car with the obstacle when getting the distance between the two is getting bigger.

From the force, a desired steering angle is computed, with K_{cw1} a scaling factor.

$$\theta_{dac} = K_{cw1} F_{lat} \tag{3.15}$$

Moreover to avoid oscillations of the assistance when d_{lat} is close to zero the following gain is added.
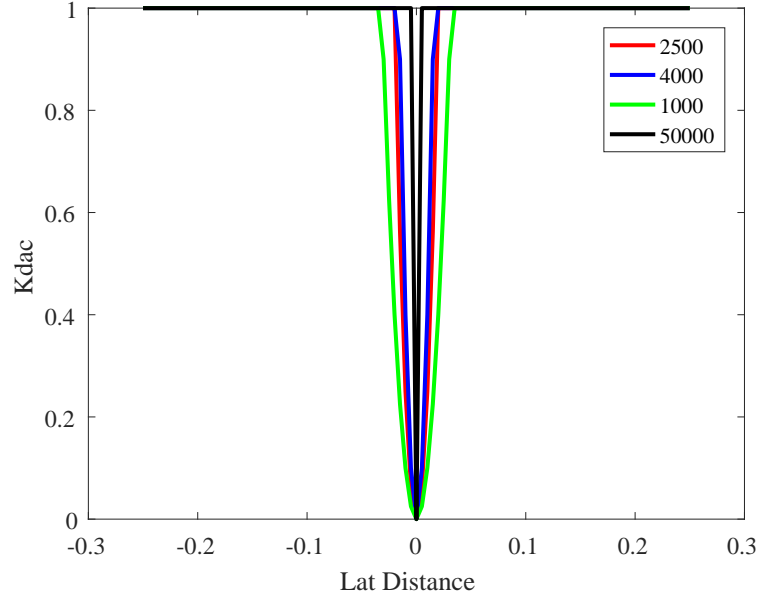
Fig. 3-17: Effect of k on K_{dac}.

$$K_{dac} = \begin{cases} kd_{lat}^2 & \text{if } |d_{lat}| <= \dfrac{1}{\sqrt{k}} \\ 1 & \text{else} \end{cases} \quad (3.16)$$

Where k is a constant that can be chosen to determine the scale at which K_{dac} should soften the sign transition. Fig.3-17 represents the values of K_{dac} for different values of k. In this figure the purpose was to determine the correct value of k in the case a a 1/10th scale car. This is why the effect of K_{dac} is so restrained.

And finally the assisting torque to apply on the steering wheel is computed as follows.

$$\tau_{dasw} = \begin{cases} K_{cw2}K_{ve}K_{dac}\theta_{dac}\left(\theta_{dac} - \delta\right) & \text{if } \theta_{dac} > 0 \\ -K_{cw2}K_{ve}K_{dac}\theta_{dac}\left(\theta_{dac} - \delta\right) & \text{else} \end{cases} \quad (3.17)$$

Where K_{cw2} is a scaling factor and δ the angle of the car's wheel.

The purpose of this torque is to avoid the collision by making the car turn before reaching the obstacle.
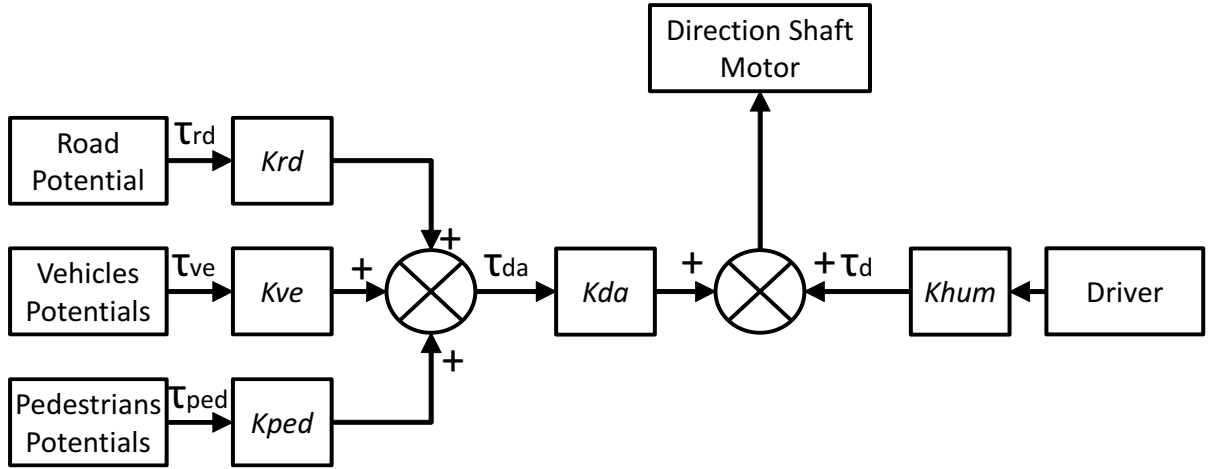
Fig. 3-18: Effect of the driving assistant and driver on the direction.

3.4 Modulation of Control Sharing

3.4.1 Control Sharing

As a result of the application of the driving assistant, the control of the vehicle is shared between two entities, the human driver and the support algorithm. The torques created by the driving assistant for every type of detected hazards are applied on the direction shaft motor, as well as the driver's one. From the driver's point of view, the driving assistant acts like a second driver that would handle the steering wheel and pedal. From that image it is easy to understand that some conflicts can appear if the will of the driver is opposed to the support offered by the driving assistant. Of course in dangerous situations the late one should prevail, but in more normal situations it is better to let to the driver a feeling of liberty. Indeed the driving assistant is more easily accepted if the user does not feel restrained in every of his actions. Therefore the assistance is accepted more willingly in critical situations, when it is really needed. Moreover depending of the situation, the same object can be dangerous or not. It is typically the case of line marks. If involuntary lane changes should be prevented, in some conditions lane changing is completely safe. On the other hand, if the driver is detected as sleeping or in other similar cases, the driver's inputs should be ignored.

From that statement, several modulating coefficients were added to adapt the offered

support to the situation. Fig.3-18 describes those constants in the case of the direction control. Each torques produced by a certain type of potential are modulated by specifics coefficients, K_{rd}, K_{ve} and K_{ped}. Then more global coefficients are applied to the final support torque and to the human torque, K_{da} and K_{hum}. In previous work[61] a modulation process was proposed. Using a driver's face analysis, the status of this one was estimated using thresholds and boolean conditions. The driver could be detected as awake, drowsy, speaking, distracted or wanting to cross a line. For each of these states, a corresponding set of coefficients was defined. If this proposal was able to solve the conflicts caused by the control sharing, the transitions between the different states were too sudden and could lead to uncontrolled reactions of the driver. Moreover the definition of the thresholds was subject to discussions as it is impossible to define absolute threshold values to any physiological parameter. Thus a new method of modulation is proposed and described in the next subsection.

3.4.2 Fuzzy Logic Engine

This modulation was performed using fuzzy logic. Fuzzy logic is an extension of the classical logic aiming to a better modelization of imperfect data and trying to mimic the flexible human logic described in 1965 by L.A Zadeh[62]. It is a form of many-valued logic where the truth value of a variable is not restricted to 0 or 1 but can be any number between those two. It can be used to deal with partial truth where the truth of an assertion can be completely true, completely false or anything between that limits. It is possible to use linguistic variables, which degrees are managed by membership functions. A linguistic variable is a set of terms describing a specific variable. For example considering the distance to an object, linguistic variables could be far and close, that can be intersecting on certain values of that distance. The input and outputs variables are connected through inference rules. Those rules define the certainty of different linguistic variables on the output variables. From that, a crisp value is determined for each output. This method was applied to numerous systems[63], including control of mobile robots[64][65][66] and path planning[67].

The first step of the fuzzy engine creation is the selection of the pertinent parameters.
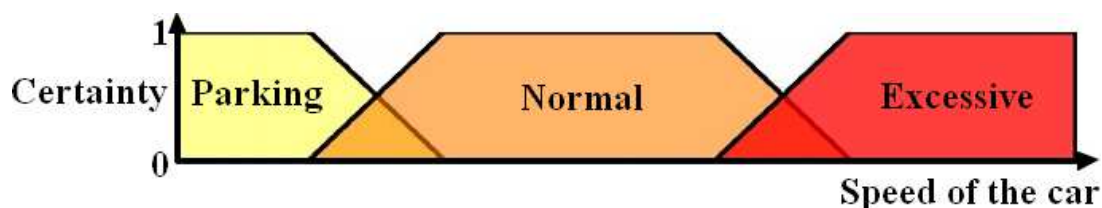
Fig. 3-19: Example of fuzzified variable.

The purpose of this selection step is to describe the most efficiently as possible the driving situation. This one can be described by the car environment, that is analyzed through the stereo camera system, by the state of the car, obtained by the embarked sensors, or by the status of the driver, that is analyzed by a camera oriented toward the driver's face[61]. In this proposal, those parameters are the speed of the car, the yaw and blink frequency and their mean duration, the amplitude of the driver's gaze movements, and finally the time spent looking at the mirrors. The outputs of this engine are the previously described modulation variables.

The behavior of this engine is defined by two critical steps. The first one is the "fuzzification" of its inputs and outputs. That means the creation and definition of the linguistic variables for all of the inputs and outputs. Their definition consists in creating geometric shapes to set their certainty level, a value between 0 and 1. Fig.3-19 illustrates an example of fuzzified variable. In the speed case, the linguistics terms are "Parking", "Normal" and "Excessive" and their certainties are described by the geometric shapes on the figure. Table.3.3 enumerates all of the used parameters as well as their associated linguistic variables. A last output of the fuzzy logic engine is $K_{warning}$. It aims at giving to the driver information about dangerous situation. If it is set to warning a visual warning is displayed. If set to Haptic, vibrations are sent through the steering wheel to send an impulse to the driver, by instance in case of slumbering.

The second step is the definition of the rules used by the fuzzy logic engine. They are expressed, by instance as:

if(Blink Mean Duration is Drowsy or Blink Mean Duration is Micro Sleep) and Yaw Mean Duration is Drowsy and Gaze Movement Amplitude is Fixed Gaze then Kda is High

Finally, using a set of 32 rules, the output values are computed, enabling a high flexibility of the control sharing and soft transitions between the different states of the outputs.

Table 3.3: Fuzzy Logic Engine variables.

System variables	Linguistic variables
Speed of the car	Parking, Normal, Excessive
Communication Delay	Long
Distance to pedestrian	Close, Normal, Remote
Evolution of Distance to pedestrian	Negative, Null, Positive
Distance to vehicle	Close, Normal, Remote
Evolution of Distance to vehicle	Negative, Null, Positive
Blink Frequency	Focused, Normal, Stressed
Blink Mean Duration	Normal, Drowsy, Micro Sleep
Yaw Frequency	Speaking
Yaw Mean Duration	Drowsy
Gaze Movement Amplitude	Fixed gaze, Moving gaze
Time spent looking at the mirror	Checked, Not checked
K_{da}	Weak, Normal, High
K_{ve}	Weak, Normal, High
K_{rd}	Weak, Normal, High
K_{ped}	Weak, Normal, High
K_{hum}	Weak, Normal, Intermediary
$K_{warning}$	None, Warning, Haptic

The rules and terms are defined in order to strengthen the influence of the assistant in case of hazardous situations, by instances an excessive speed or a drowsy driver, and to let the driver pilot freely the car in safe situations, for example if the driver checked its mirror before changing lane. More information about the used variables and the rules of the engine are given in Appendix C.

3.4.3 Effect of the Engine

Fig.3-20 demonstrates the evolution of the road coefficient in function of the speed of the car and of the time spent by the driver looking at the mirror. It shows that the evolution of the coefficient is continuous. If the driver checked the mirror, a crossing
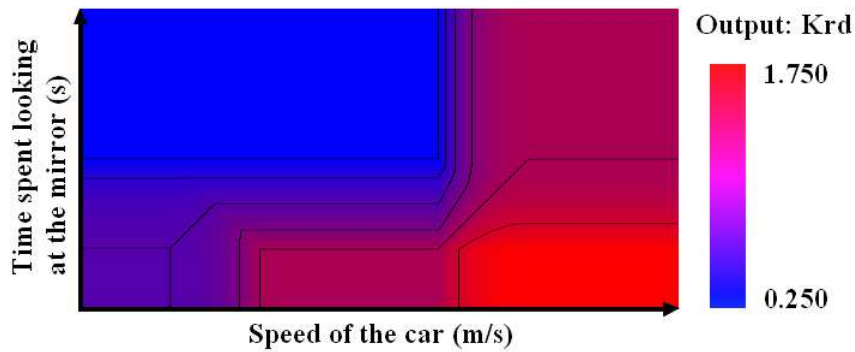
Fig. 3-20: Effect on K_{rd} of the speed of the car and of the time spent looking at the mirror.
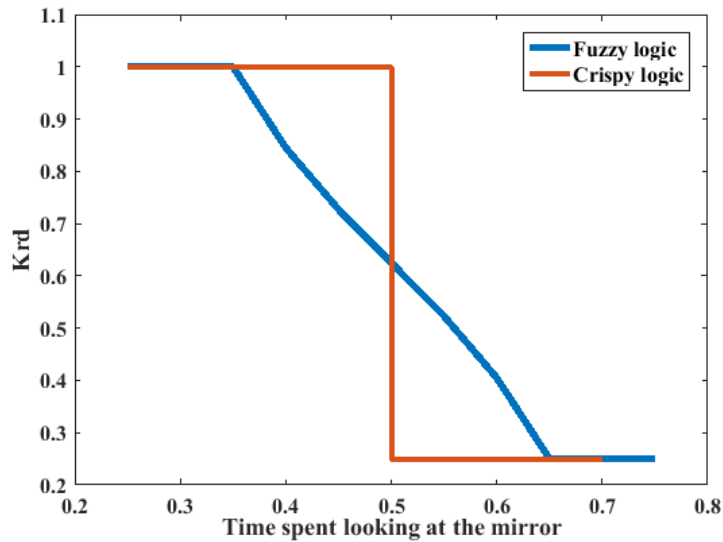
Fig. 3-21: Effect on K_{rd} of the time spent looking at the mirror.

intention is detected and K_{rd} is lowered. If the speed of the car is very low, indicating a parking situation, K_{rd} is also reduced in order to allow easy line crossing, as those one can often happen in parking situation. But if that speed becomes too high, the coefficient is strengthen to compensate for the shorter reaction time required from the driver in that situation. Finally Fig.3-21 compares the current modulation method using fuzzy logic and the previous one based on thresholds. The effect of time spent looking at the mirror on the Krd coefficient is plotted for the two modulation algorithms. It appears clearly that the new method offers a continuous evolution of the coefficient, preventing sudden changes of the assistance intensity that could be dangerous and enabling a softer estimation of the

required time spent on the mirror to consider that the driver is aware of his environment.

Finally, Table 3.4, Table 3.5 and Table 3.6 gather examples of results obtained with the fuzzy logic engine in different situations. In those table, the certainty of the different linguistic variables are expressed and the corresponding modulation coefficient are listed.

3.5 Summary

This section described how the driving support is applied on the controlled car and how the computation of the support torques is conducted. First the control method used to implement the driving assistant was describe both in local driving and remote driving situation. The late case is based on the use of virtual steering and throttle angles in order to apply the active driving assistant directly on the controlled car without disturbance of the communication time delay. It also take into account the possible shift between the master and the slave parts of the control and try to correct it without disturbing the application of the driving support. Moreover the computation methods used to estimate the intensity of the offered support were detailed. The determination of the computation method was described and its impact on the behavior of the driving assistant demonstrated. Finally, to solve the problem of control sharing between the driver and the driving assistant, a fuzzy logic engine was designed. Its purpose is to strengthen the influence of the support compared to the human driver in hazardous situations, while letting the late one as free as possible in other cases. It was conceived to offer smooth transitions between the different states and to try to imitate the human way of evaluating situations, especially on variables barely compatible with boolean logic.

Table 3.4: Examples of fuzzy logic engine results in different situations.

		Standard situation			High speed, getting closer ped.		
Inputs	Car Speed	Parking	Normal	Excessive	Parking	Normal	Excessive
		0	1	0	0	0.4	0.6
	Communication time delay	Long			Long		
		0			0		
	Distance to closest ped.	Close	Normal	Remote	Close	Normal	Remote
		0	1	0	0	0.5	0.5
	Rel. speed to closest ped.	Negative	Null	Positive	Negative	Null	Positive
		0	1	0	1	0	0
	Distance to closest car	Close	Normal	Remote	Close	Normal	Remote
		0	1	0	0	1	0
	Rel. speed to closest car	Negative	Null	Positive	Negative	Null	Positive
		0	1	0	0	1	0
	Blink Freq.	Focused	Normal	Stressed	Focused	Normal	Stressed
		0	1	0	0	1	0
	Blink mean duration	Normal	Drowsy	Micro-sleep	Normal	Drowsy	Micro-sleep
		1	0	0	1	0	0
	Yaw Freq.	Speaking			Speaking		
		0.035			0.035		
	Yaw mean duration	Drowsy			Drowsy		
		0.01			0.01		
	Gaze mvt Amplitude	Fixed	Moving		Fixed	Moving	
		0	1		0	1	
	Time spend on mirror	Checked	Not Checked		Checked	Not Checked	
		1	0		1	0	
Outputs	K_{da}	Weak	Normal	High	Weak	Normal	High
		0	1	0	0	0.374	0938
	Value	1			1.469		
	K_{ve}	Weak	Normal	High	Weak	Normal	High
		0	1	0	0	1	0
	Value	1			1		
	K_{rd}	Weak	Normal	High	Weak	Normal	High
		0	1	0	0	0.55	0.45
	Value	1			1.337		
	K_{ped}	Weak	Normal	High	Weak	Normal	High
		0	1	0	0	0.5	0.5
	Value	1			1.375		
	K_{hum}	Weak	Inter.	Normal	Weak	Inter.	Normal
		0.015	0.031	0.985	0.015	0.031	0.985
	Value	0.985			0.985		
	$K_{warning}$	None	Warning	Haptic	None	Warning	Haptic
		0.975	0	0	0.4	0.614	0
	Value	None			Warning		

Table 3.5: Examples of fuzzy logic engine results in different situations.

		Time delay, getting farther car			Stressed and speaking driver		
Inputs	Car Speed	Parking	Normal	Excessive	Parking	Normal	Excessive
		0	1	0	0	1	0
	Communication time delay	Long			Long		
		0.74			0		
	Distance to closest ped.	Close	Normal	Remote	Close	Normal	Remote
		0	1	0	0	1	0
	Rel. speed to closest ped.	Negative	Null	Positive	Negative	Null	Positive
		0	1	0	0	1	0
	Distance to closest car	Close	Normal	Remote	Close	Normal	Remote
		0.752	0.248	0	0	1	0
	Rel. speed to closest car	Negative	Null	Positive	Negative	Null	Positive
		0	0	1	0	1	0
	Blink Freq.	Focused	Normal	Stressed	Focused	Normal	Stressed
		0	1	0	0	0.360	0.640
	Blink mean duration	Normal	Drowsy	Micro-sleep	Normal	Drowsy	Micro-sleep
		1	0	0	1	0	0
	Yaw Freq.	Speaking			Speaking		
		0.035			0.783		
	Yaw mean duration	Drowsy			Drowsy		
		0.01			0.023		
	Gaze mvt Amplitude	Fixed	Moving		Fixed	Moving	
		0	1		0	1	
	Time spend on mirror	Checked	Not Checked		Checked	Not Checked	
		1	0		1	0	
Outputs	K_{da}	Weak	Normal	High	Weak	Normal	High
		0	0.463	0.806	0	1	0
	Value	1.403			1		
	K_{ve}	Weak	Normal	High	Weak	Normal	High
		0.288	0.712	0	0	1	0
	Value	0.784			1		
	K_{rd}	Weak	Normal	High	Weak	Normal	High
		0	1	0	0	1	0
	Value	1			1		
	K_{ped}	Weak	Normal	High	Weak	Normal	High
		0	1	0	0	1	0
	Value	1			X		
	K_{hum}	Weak	Inter.	Normal	Weak	Inter.	Normal
		0.015	0.031	0.985	0.166	0.332	0.834
	Value	0.985			0.833		
	$K_{warning}$	None	Warning	Haptic	None	Warning	Haptic
		1	0	0	0	1	0
	Value	None			Warning		

Table 3.6: Examples of fuzzy logic engine results in different situations.

		Drowsy driver			Low speed, checked mirror		
Inputs	Car Speed	Parking	Normal	Excessive	Parking	Normal	Excessive
		0	1	0	0.627	0.373	0
	Communication time delay	Long			Long		
		0			0		
	Distance to closest ped.	Close	Normal	Remote	Close	Normal	Remote
		0	1	0	0	1	0
	Rel. speed to closest ped.	Negative	Null	Positive	Negative	Null	Positive
		0	1	0	0	1	0
	Distance to closest car	Close	Normal	Remote	Close	Normal	Remote
		0	1	0	0	1	0
	Rel. speed to closest car	Negative	Null	Positive	Negative	Null	Positive
		0	1	0	0	1	0
	Blink Freq.	Focused	Normal	Stressed	Focused	Normal	Stressed
		0	1	0	0	1	0
	Blink mean duration	Normal	Drowsy	Micro-sleep	Normal	Drowsy	Micro-sleep
		0	1	0	1	0	0
	Yaw Freq.	Speaking			Speaking		
		0.033			0.33		
	Yaw mean duration	Drowsy			Drowsy		
		0.680			0.008		
	Gaze mvt Amplitude	Fixed	Moving		Fixed	Moving	
		0.830	0.170		0	1	
	Time spend on mirror	Checked	Not Checked		Checked	Not Checked	
		1	0		0.303	0.697	
Outputs	K_{da}	Weak	Normal	High	Weak	Normal	High
		0	0.520	0.720	0.603	0.397	0
	Value	1.360			0.548		
	K_{ve}	Weak	Normal	High	Weak	Normal	High
		0	1	0	0	1	0
	Value	1			1		
	K_{rd}	Weak	Normal	High	Weak	Normal	High
		0	1	0	0.662	0.338	0
	Value	1			0.503		
	K_{ped}	Weak	Normal	High	Weak	Normal	High
		0	1	0	0	1	0
	Value	1			1		
	K_{hum}	Weak	Inter.	Normal	Weak	Inter.	Normal
		0.904	0.096	0	0	0.024	0.988
	Value	0.096			0.988		
	$K_{warning}$	None	Warning	Haptic	None	Warning	Haptic
		0	0	1	1	0	0
	Value	Haptic			None		

Chapter 4

Small and Large Scale Vehicle Systems

4.1 Introduction

The previous chapters introduced the methods used by the driving assistant to detect and locate objects in the surrounding of the car and to model these dangers in order to offer to the driver the proper level of assistance. Processes were proposed to detect as efficiently as possible hazards that could occur in driving situations mainly based on computer vision analysis, and to compute from the information extracted from the car environment assisting torques aiming at avoiding collisions or at ensuring lane keeping. Naturally, the next step in the process of creating such an active driving assistant is the test of the efficiency of the proposed methods. If that kind of test can partially be conducted through simulations[61], it is necessary, in order to obtain a true validation of the method, to verify how the proposed active driving assistant operates on real cruising systems. For that purpose systems have to be created keeping several concerns in mind. Their ultimate purpose being to evaluate the efficiency of the driving support, the designed experimental systems should be as close as possible of what a commercial car including a driving assistant would be. This is why one of the system is based on a single seat electric car. With this electric vehicle it is possible to verify the behavior of the proposed driving assistant at a real scale, and confirm that the execution speed of the different programs involved are compatible with real cruising conditions. However some verification could

be dangerous if conducted in such conditions. Indeed if line crossing experiments can be performed safely on an electric vehicle, its dimensions, mass and the scale at which the experiments involving such a vehicle are conducted make it dangerous to test collision avoidance. In case of failure a collision between the controlled car and any kind of obstacle could provoke injuries, destruction or deterioration of the test system, obstacle or other vehicles or persons in the test environment. This is why an other experimental system was operated in collision avoidance experiments. This system is a 1/10th scale car reproducing the behavior of a standard car. Of course this kind of system cannot be locally driven by a human driver, and can only be remotely controlled. However the small size required for the experimental setup it take part in, allows to conduct experiments with a very small communication time delay, enabling to emulate the behavior of that car if it were piloted from the inside. The following sections will describe more deeply those two experimental systems.

4.2 Takeoka Milieu R

4.2.1 Presentation

The electric vehicle that was modified in order to conduct the presented research is a commercial vehicle sold by Takeoka, the Milieu R[7]. This vehicle is represented in Fig.4-1 and some of its characteristics are listed in Table.4.1. It is mainly a one seated electric vehicle. The tests conducted using that vehicle are, as mentioned before, related to the line crossing and lane keeping. This vehicle can be used both in local driving, with a human driver inside of the vehicle and in remote controlled application. However it is not suitable for such use in its factory state. Even if it easily possible to connect any compatible device on its battery, the power transmission of the direction shaft and the control of the electric motor mastering the speed of the car should be modified in order to enable the addition of the driving assistant. Moreover the realization of such assistant implies to add sensors in order to be able to control the direction and speed of the car, estimate the drivers inputs and use the cinematic model.

Finally the Fig.4-2 gives the correspondence between the direction shaft angular position and the orientations of each wheels. It can be observed that the relation is not

Fig. 4-1: Takeoka Milieu R.

Table 4.1: Takeoka Milieu R, characteristics[7].

Length	2.15m
Width	1.14m
Height	1.35m
Weight	295kg
Maximum speed	50km/h (Eco mode), 60km/h (Power mode)
Smallest radius of gyration	2.5m
Maximum reachable distance in one charge in urban condition	50km (at 45km/h) 45km in winter
Electric Motor	AC-motor, 600W 48V
Battery	Lead battery, 60Ah 12Vx4

proportional and is asymmetrical.

4.2.2 Conducted Modifications

All of the modifications conducted on the Milieu R have the secondary objective to be non destructive of the original vehicle. That means all of the addition to the car should be reversible. In order to be able to apply the driving assistant, the car was modified
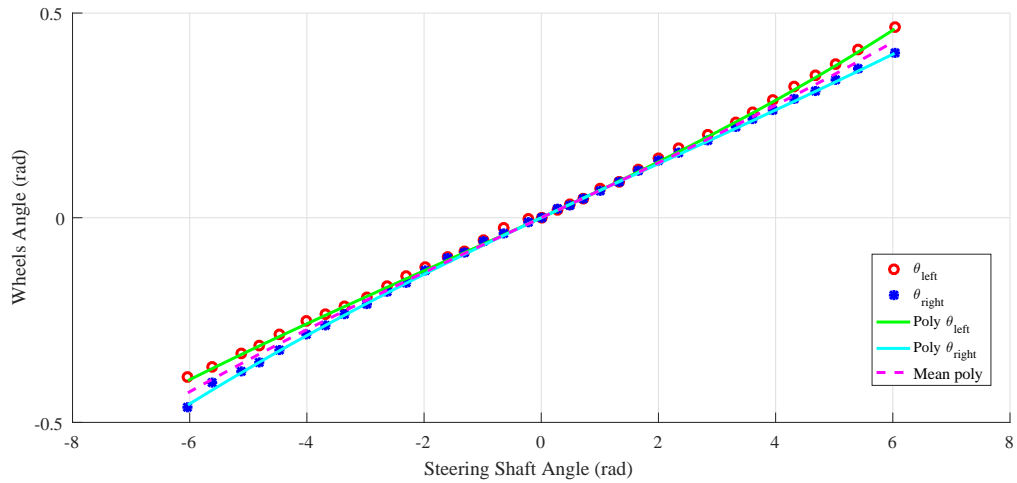
Fig. 4-2: Wheels orientations relation to Steering Shaft angle.
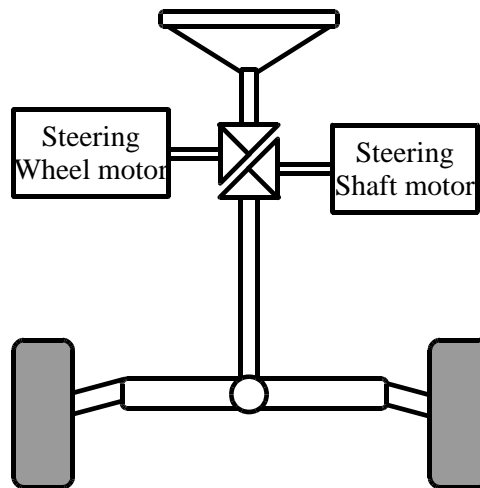
Fig. 4-3: Steer by wire system.

to include a driver by wire system. Such system suppress the mechanical connection of the direction shaft with the steering wheel and the direct relation between the pedal and the controller of the car engine. It is then possible to control the master parts of the vehicle, steering wheel and pedal, independently from the slave parts, the direction shaft and the engine controller. For that purpose the steering wheel was removed from the direction shaft and replace by bevel gears connected to a motor. A new steering wheel, connected to an other motor through bevel gears, was placed as close as possible of the position of the original steering wheel. Fig.4-3 represents the configuration of the created
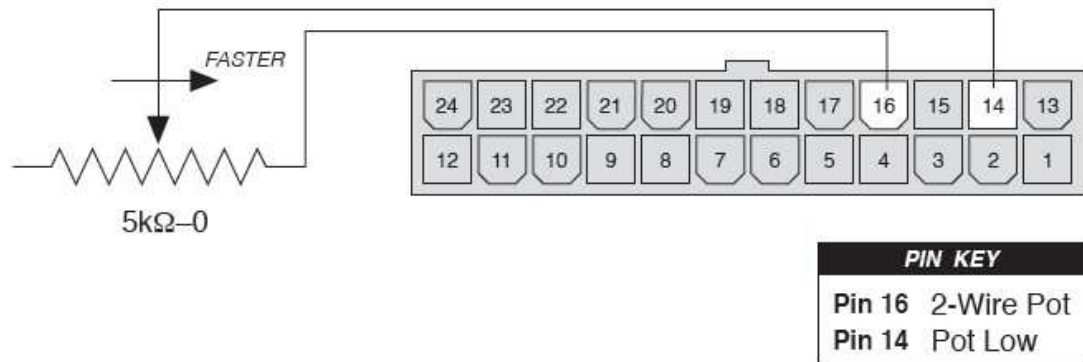
Fig. 4-4: Original throttle system.

system. The steer-by-wire presents the advantage of easily enabling the implementation of the driving assistant that can be applied on the steering wheel directly in case of local driving, or on the direction shaft in case of remote control to avoid the communication time delay. Thus the system and control are not impacted by the use or not of remote control. Indeed with a steer-by-wire system the instruction can come from outside of the car without need to change the control method. The bevel gears solution was chosen to reduce as much a possible the space required by the physical implementation of the system, as the car being one seated is quite narrow.

To realize the pedal-by-wire, which principle is similar to the steer-by-wire but adapted to the pedal, it was necessary to determine the method used by the car engine controller to translate the position of the pedal into a speed command. Fig.4-4 is an extract of that controller manual. The actual system make variate a resistor with the position of the throttle pedal. The controller translate that resistor value into a speed instruction. The created pedal-by-wire system is then composed of two parts. A new pedal was created and connected to a motor, in order to apply assisting and other torques on it. The slave part of the system is composed of a microprocessor that translate the instruction received from the driving assistant program as a tension to SPI instructions sent to a digital resistor connected to the engine controller. The created circuit is represented in Fig.4-5 and enables to switch at any time between the original throttle system and the pedal-by-wire system.

Moreover, in order to be controllable, the car had to be equipped with different sensors.
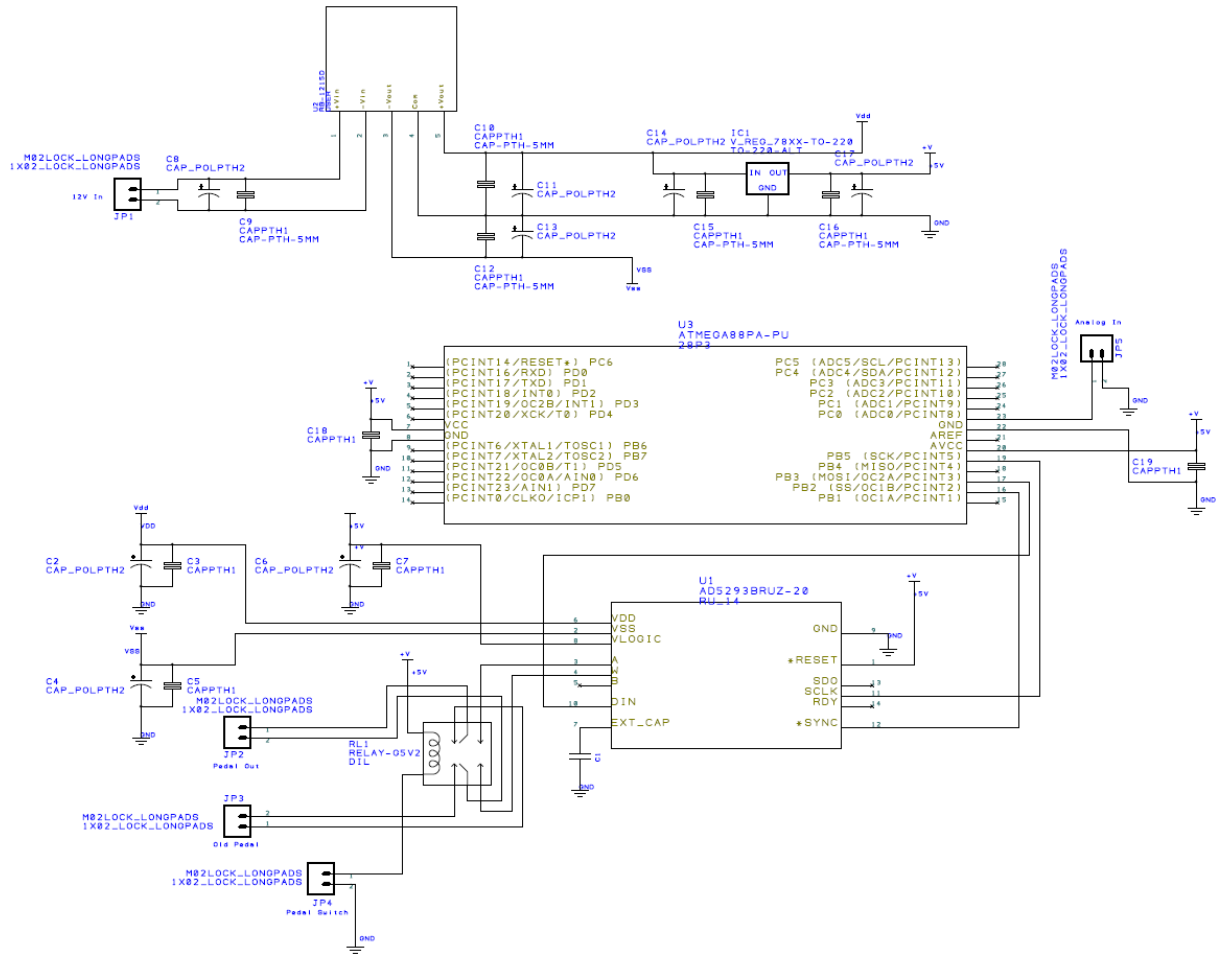
Fig. 4-5: Pedal Emulator circuit.

Each of the previously cited motor are mounted with encoders. That mean that the position of the steering wheel, pedal and steering shaft are known. It is then possible to estimate the orientation of the wheels as previously discussed. An other encoder was added to the speedometer cable in order to measure the speed of the car. From a cinematic point of view it is the possible to know the speed of the front wheels, but not separately, and the orientation of the wheels. This is why a simple cinematic model was chosen as it correspond to the data that can be acquired by the system. A more complex model would require the addition of other sensors that can be difficult to implement.

Of course the computer vision module including the stereo camera and the Jeton Development Kit was also included in the car, the late one being also the controller used to
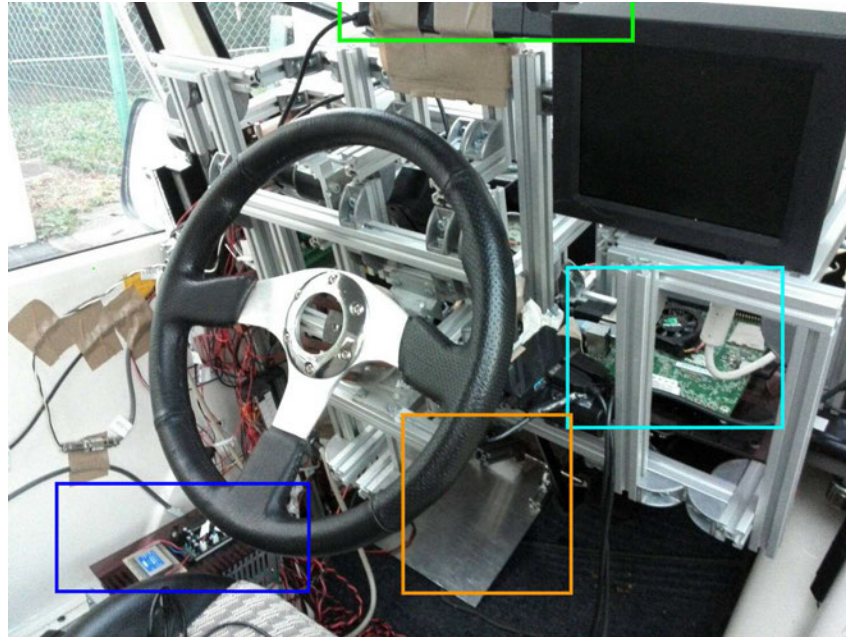
Fig. 4-6: Inner picture of the modified car.

run the program of the driving assistant and communicate with the motors controller.

Fig.4-6 and Fig.4-7 are pictures of the final implementation taken from outside and inside of the car. In green is the used PlayStation® 4 camera, in light blue the used Jetson TK1, in orange the master part of the pedal-by-wire system including the pedal, in deep blue the slave part of the pedal-by-wire system with the digital resistor and in red the transmission system between the steering shaft and its associated motor.

4.2.3 Internal Programs Communications

Fig.4-8 represents the different programs involved in the line crossing driving assistant tests conducted with the Milieu R and the communication between them. In case of local driving only the electric car part is considered. In that situation the Jetson is running two programs. The first one is the computer vision program that analyses the environment of the car in order to detect and locate the line. It communicate through UNIX socket with the interface program. The artificial vision program send the location of the detected hazards, and the interface program send the current position and orientation of the car in order for the line detection program to compute the location of the lines in
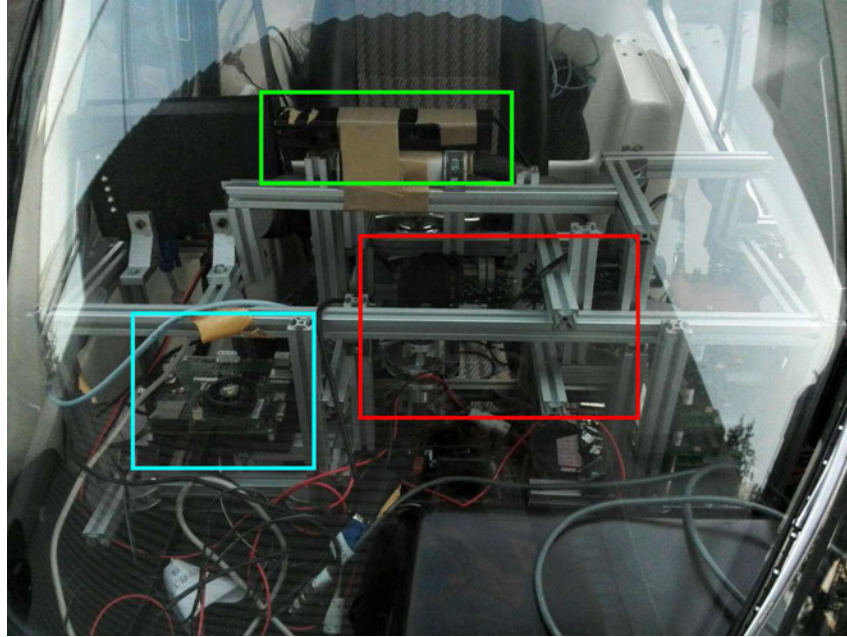
Fig. 4-7: Front picture of the modified car.

the absolute referential of the experiment. The interface program computes the driving assisting torques and send them to the motor control program running on the iBIS controller. This program handles the real time control of the motor and reads the values of the encoders. It also sends those data to the interface program. In case of remote control a very similar architecture is added to realize the remote controller based on an interface computer connected to an iBIS controller on which are connected the steering wheel and the pedal. The controller program of he driving station send the instruction of the driver to the interface program of the Jetson and receives the assisting torques and the encoders readings.
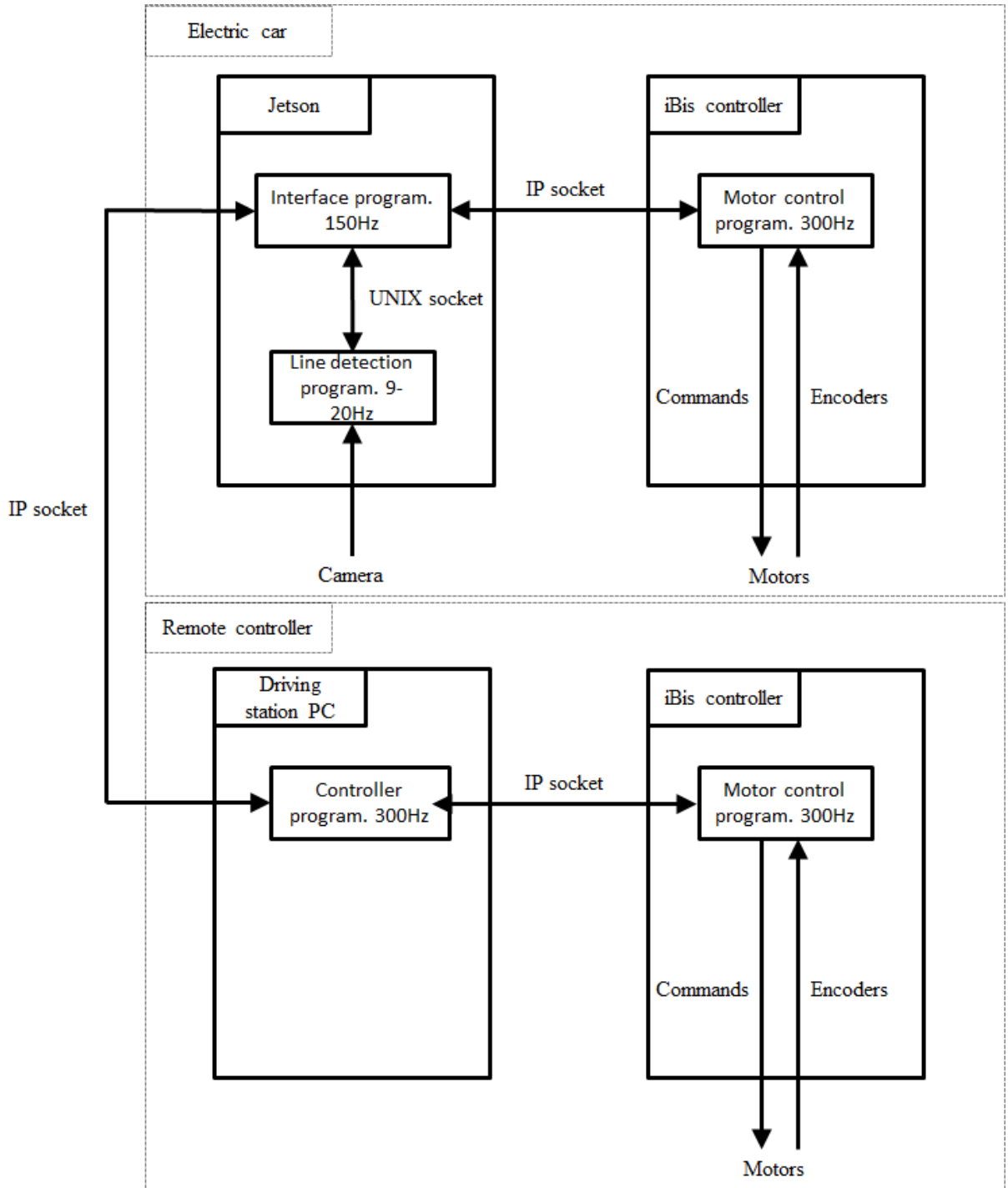
Fig. 4-8: Communication architecture in the Milieu R.

4.3 RoboCar® 1/10th Scale

4.3.1 Presentation

In order to be able to conduct tests implying collisions, the used 1/10th scale vehicle is a product of ZMP®[8] that was modified to enable the application of a driving assistant. The commercial solution can be observed in Fig.4-9 and Table.4.2 gathers some of its characteristics. As it can be observed, the Robocar® is well suited for any application of remote control. Thanks to its high number of sensors, it is possible to know the speeds of each wheel and the different accelerations of the car, the orientation of the front wheels can be measured accurately and directly. However to ensure that the different tests were conducted in the same conditions, only information also available on the electric vehicle were used, i.e. the orientation of the front wheels, and their speeds. Moreover the Robocar® is equipped with a fish eye camera located at its front allowing to easily stream a video with a wide field of view of what is located in front of the car for the remote control. The Robocar® can be easily controlled through its API accessible from its main controller. As this controller is running on a Linux OS it is also simple to connect it with other experimental system, through its Ethernet and Wifi connections. The main purpose of this system is to test the collision avoidance of other vehicles as it is resilient to collisions thanks to its small weight and its foam bumpers. The main modifications that have to be conducted on it in order to apply the driving assistant are the addition of the Jetson development kit, PS4 camera, and the power supply of that computer vision module.
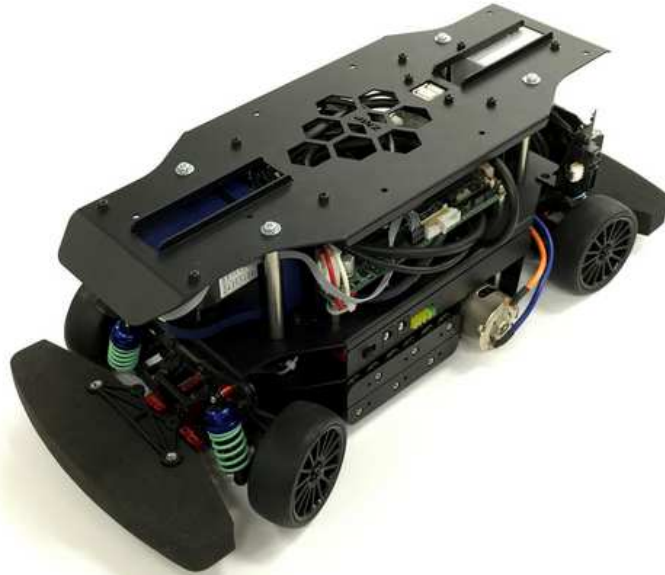
Fig. 4-9: 1/10 scale RoboCar®.

Table 4.2: 1/10 scale RoboCar®, characteristics[8].

Length	0.429m
Width	0.2122m
Height	0.195m
Weight	3kg
Maximum speed	3.8m/s
Main controller CPU	AMD Geode LX800 Processor 500MHz
Sensors	1 axis gyro
	3-axis accelerometer
	Rotary encoder (x4 wheels, x1 axis drive motor)
Direction control	Servo Motor for Robot
Drive motor	Small DC motor
Batteries	Control system: AA Ni-MH batteries (x12)
	Power: Nickel Metal Hydride battery pack (x1) 7.2V
Camera	Fish eye camera at the front

4.3.2 Conducted Modifications

Compared to the electric vehicle the modifications that had to be conducted were lighter. Indeed in its original state the RoboCar® was already fully controllable and the addition of driving assistant can be operated easily. The principal lack of the system is the artificial vision module. However as seen in Fig.4-9 the chassis of the RoboCar® includes a lot of holes used to fix some modules, by instance infra red sensors. Consequently it is possible to create fixations to hold the required hardware. Fig.4-10 represent the CAD model of a part designed to hold the PlayStation® 4 camera. It was created with the purpose of elevating the PS4 camera to get a better vision of what is located in front of the car. It is rigidly fix on the front of the chassis ensuring that the position of the camera on the vehicle is constant . It is also a way to protect the camera during possible collisions. This part was created through 3D printing. A battery holder was similarly designed and fixed on the rear part of the chassis to enable the use of a battery powering the Jetson. The chosen battery is a 4 cell lithium polymer one usually used on drones. The Jetson is fixed on the top of RoboCar® chassis.

Fig.4-11 and Fig.4-12 are pictures of the final state of the modified RoboCar®. In red it is possible to see the battery, in green the PlayStation® 4 camera, in orange the fish eye camera of the RoboCar® and in blue the used Jetson TX1.

However in order to control the RoboCar® a driving station as to be used. This one is represented in Fig.4-13. It is basically composed of the master parts of the drive by wire-system, i.e. a steering wheel and a pedal connected to an iBIS motor controller it self connected to a computer. This driving station can be used both to control the RoboCar® or to conduct remote control with the electric vehicle.

4.3.3 Internal Programs Communications

The architecture of the programs used to conduct the collision avoidance on the Robo-Car® and of the communications between them is represented on Fig.4-14. It is quite similar to the architecture used in the Milieu R, with a separation in two main parts, the master part represented by the remote controller with its steering wheel and pedal and the slave part, composed of the RoboCar® and the Jetson mounted on it. The late one is
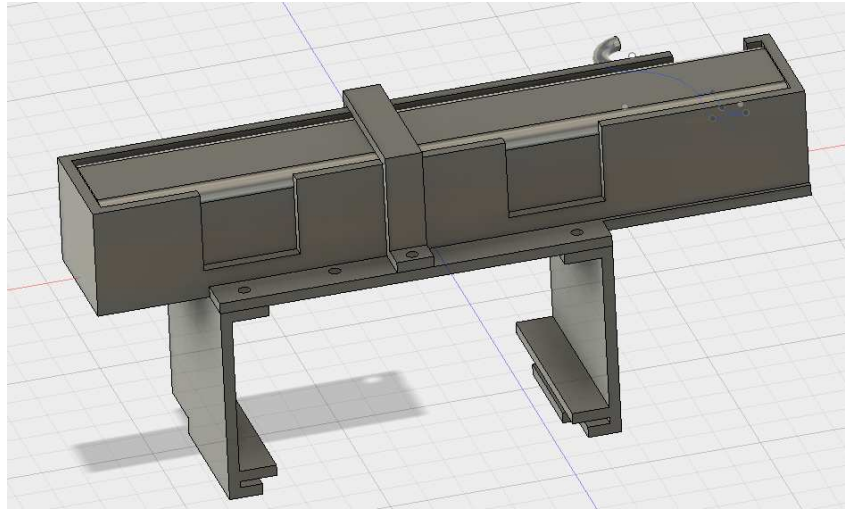
Fig. 4-10: PlayStation® 4 Camera Holder.
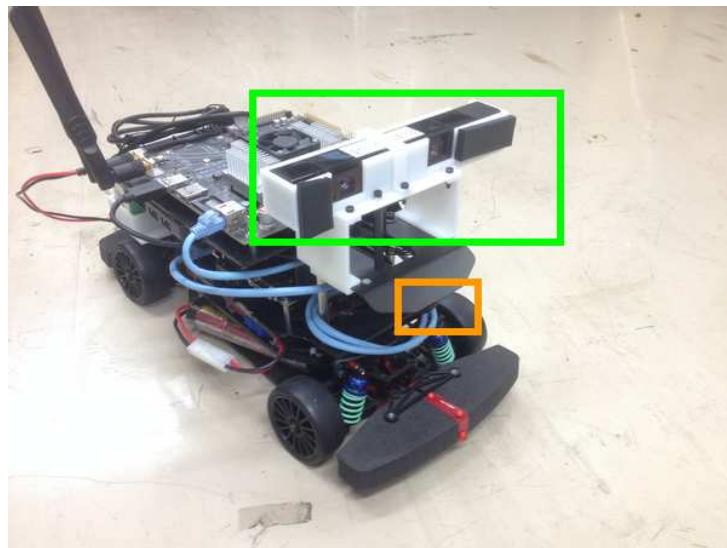
Fig. 4-11: Modified RoboCar®.

in charge of the obstacle detection and transmit the information about the found hazards to the RoboCar® controller, through a LAN connection, that return to the Jetson the position of the vehicle estimated by the cinematic model. This controller then computes the assistance to apply on the car, but also to send to the driving station thanks to a Wifi connection. The driving station also sends the instruction of the driver to the controlled car thanks to the control method discussed in the previous chapter.
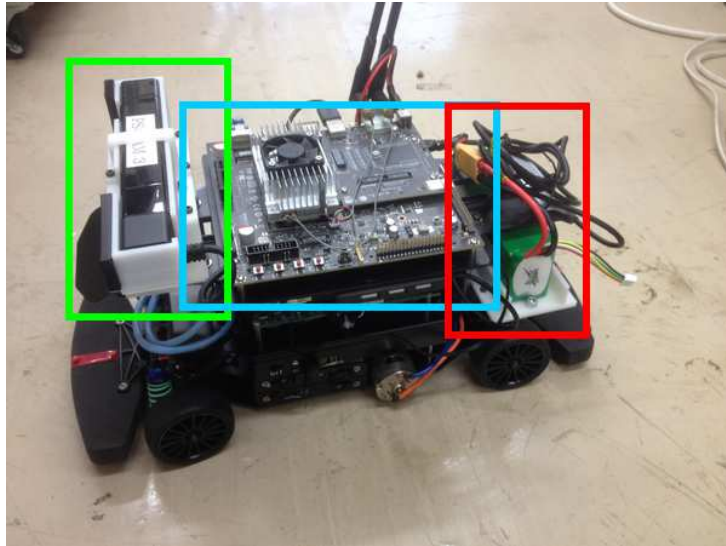
Fig. 4-12: Modified RoboCar®.
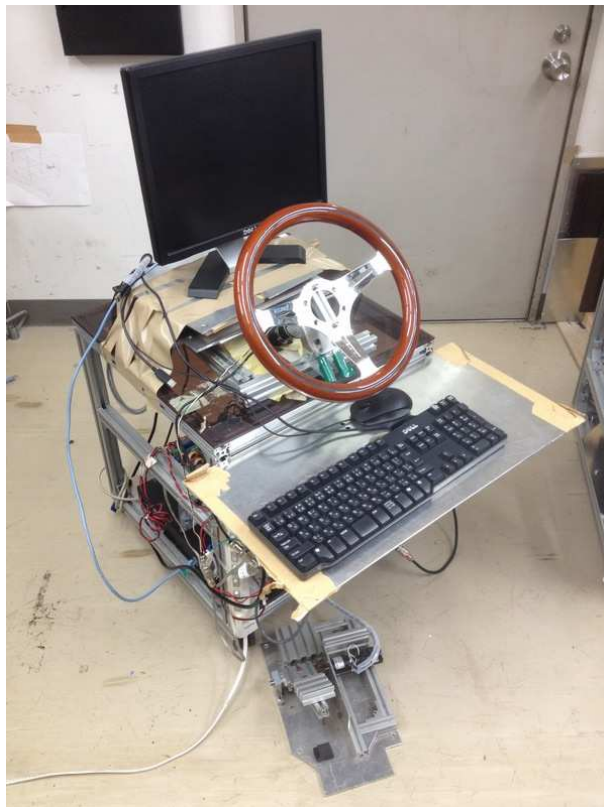
Fig. 4-13: Driving Station.
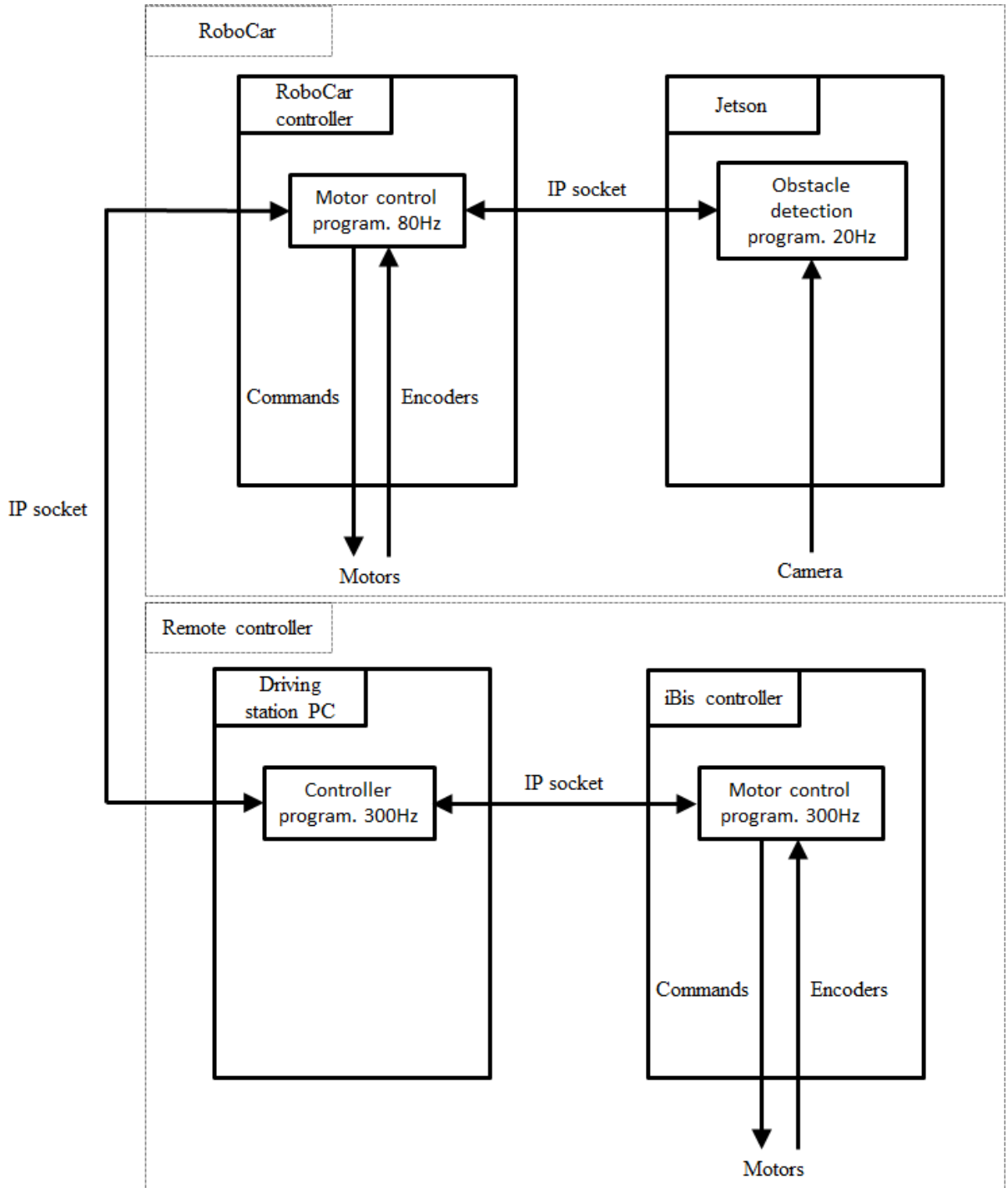
Fig. 4-14: Communication architecture in the RoboCar®.

4.4 Experimental Processes

Fig. 4-15: Line crossing tests conduction place.

This chapter described the different experimental system used to conduct tests in order to validate the efficiency of the proposed active driving assistant. A one seated electric vehicle was modified to perform tests on a real scale of that kind of driving support. Moreover as collisions can be dangerous if happening on that kind of vehicle a 1/10th model of car was customized to enable the conduction of experiments.

The experiments using the electric vehicle were performed on a campus road, as represented in Fig.2-13. During those ones, several drivers were asked to crossed the line while the computer vision algorithm was analyzing the road to extract the location of the line. These tests were the occasion to confront the proposed methods, cinematic model, detection processes and assisting torques computation methods, with the imperfection of a real driving situation and at a correct scale on the speed and distance. It is then possible to verify if the hypothesis supposed in the computation of the assisting torques, for example the flatness of the road or two wheels cinematic model, allow to obtain a correct result in real conditions experiments.

The collision avoidance tests were performed inside of the laboratory. Except for the flatness of the ground, the conditions tried to mimic the real ones but on a smaller scale. The obstacle use in those test was a cardboard model of a car which dimensions were closed to the RoboCar®'s dimensions represented in Fig.4-16. A red plastic ball was put on the top of that obstacle to ease the detection, as it did not exactly correspond to a real car and was then difficult to detect with the previously described detection algorithm.
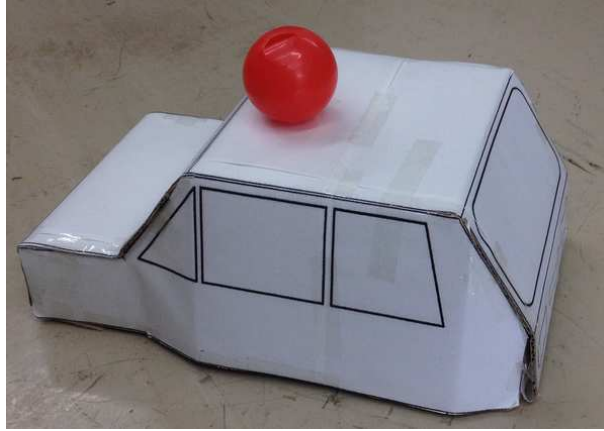
Fig. 4-16: Used cardboard obstacle.

To emulate the effect of the network status on the communication time delay, the packets send between the driving station and the controlled vehicles were delayed by a specified amount of time, as in the experiment condition the mere transmission time was the smallest as possible. Only the different instructions corresponding to a normal driving situation were delayed. Indeed, for safety reasons, all of the interruption signals were sent without delay. Moreover a person was always inside of the electric vehicle during remote control experiment to be able to manually stop the vehicle in case of problem. Finally in order to drive the vehicle while using the driving station, video streams were created using GStreamer[68] and were sent from the controlled vehicle to the driving station is a selected time delay corresponding to the chosen communication time delay.

4.5 Summary

This chapter presented the modifications operated on a one seated electric vehicle and on a 1/10th scale car in order to enable the application of active driving support. Those modifications are mostly related to the implementation of a drive by wire system in the one seated car, that is compatible with both active support and remote control, to the use of driving station in both case for remote control, and to the addition of the computer vision modules, composed of PS4 camera and Jetson development kits. This chapter also described the architecture of the communication of the different programs involved in the tests and conduction of the driving assistant. They are based on simple UNIX and

IP sockets, depending of the case, and are then modular and allows the to change any of the program independently as soon as the new program respect the communication protocol. The final architecture enable to select the communication time delay between the controlled vehicle and to delay the video streaming used to controlled the remote vehicle of the same duration.

Chapter 5

Evaluation Criteria and Experiments

5.1 Introduction

The previous chapters were dedicated to the description of different aspects of the creation of the proposed active driving assistant from its faculty to detect objects and to used that information to propose support torque to the driver, to the way systems were created to implement and test that assistant.

The current chapter will be focused on the analysis of the achieved performances and will, for that purpose be separated in two parts, each one focusing on a specific facet of this study. The first section will be dedicated to the raw analysis of the behavior of the driving assistant during the conducted experimental tests. The goal of that segment will be to evaluate if the offered assistance is conform to its expected behavior. More in details, its objective will be to ensure that the driving assistant actually increase the safety of the cruising and that all of the previously designed aspects of the driving assistant are working as expected. The second section of this chapter aims at creating a method allowing to evaluate the performances of the proposed active driving assistant based on computed criteria. The project of this section will be to design tools enabling the comparison of the performances of different designs of driving assistant depending of their purpose. It will also be the occasion to discuss of the pertinent criteria concerning the evaluation of a driving assistance.
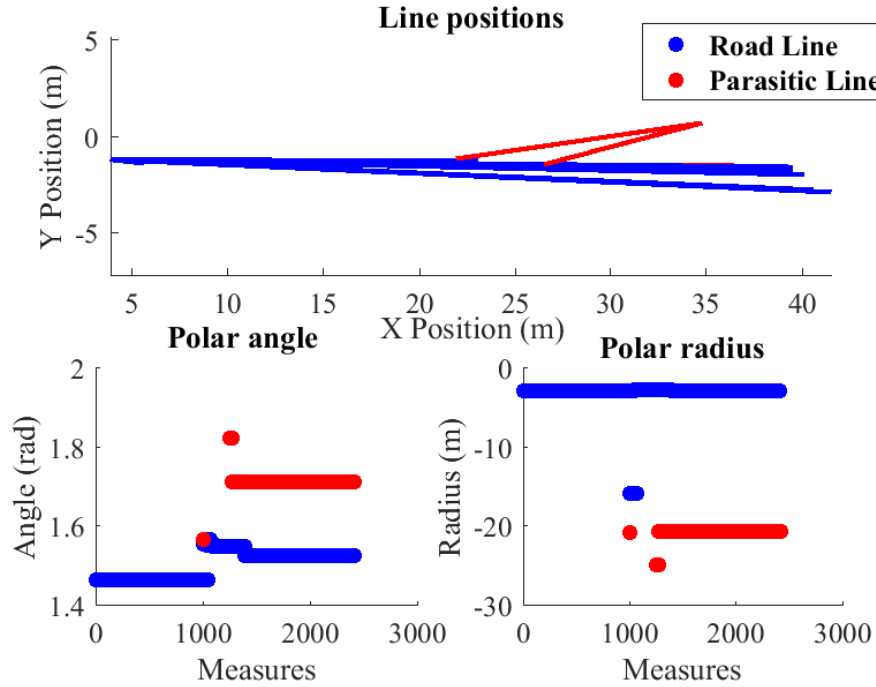
Fig. 5-1: Detection of a line during a crossing test.

Table 5.1: Line detection error.

Mean	5.06 rad
Standard deviation	2.07 rad

5.2 Behaviour Analysis

5.2.1 Efficiency of the Line Detection

The efficiency of the proposed driving assistant is dependent on the accuracy of the line detection. To evaluate this one, the evolution of the orientation in the absolute referential of a line was studied. The purpose of this evaluation is to measure the angular variation of the same line through the test. In perfect conditions, as the line is straight, this variation should be equal to 0. The experiment was conducted on the road shown in Fig.2-13 and Fig.4-15 and the process was the following. For each line detection performed by the computer vision algorithm, its results are fused with the previous detections to obtain the last up to date locations of the lines extremities. This list of extremities is then plotted to observe how the orientations of the lines are sliding through the experiment

process. In those tests the car was crossing a unique line and did not keep a straight trajectory. Fig.5-1 shows a typical result. The upper part of the figure represents the succession of positions of the lines, and the lower plots the polar coordinates of the detected lines. The colors indicate two different lines, the red one being the result of a parasitic detection. It can be easily filtered using the polar coordinates plots, as two coordinates at the same measure indicate two different line detections. The final results, obtained with several crossing and performed by different testers are the following. The mean deviation is of 5.06 degrees with a standard deviation of 2.07 degrees as shown in Table.5.1. This deviation can be explained by several factors. Of course the accuracy of the detection is not absolute and the location of the same line can slightly vary from one measure to the other. Moreover it is impossible to guarantee the simultaneity of the image acquisition and of the car coordinates estimation with the cinematic model. This lead to a loss of accuracy of the location estimation due to a small time gap. Other sources of that orientation variation are the differences with the used perfect models. The road is not completely flat and the car cannot be modeled perfectly as a two wheels vehicle. Finally in its current construction, the car has no absolute encoding of the position of its steering shaft. This can lead to small errors in the estimation of the wheels orientation. Nevertheless the current deviation is small enough for test purposes and the estimation errors are corrected during the driving by the real time estimation of the lines' locations.

5.2.2 Lane Changing Prevention

In the scenario of Fig.5-2 the driver approached the line with $K_{rd} = 1$, and let the driving assistant prevent the line crossing. This shows the expected reaction of the support in case of involuntary change of direction that could lead to an undesired lane changing. This can especially happen if the driver is not focused on his task, whether because of a distraction or because of drowsiness. In that situation the driving assistant should first correct the direction of the car to prevent the crossing, and then give to the car a direction parallel to the line, thanks to the inverted torque, when the vehicle get farther from it. This is what can be observed in this figure. Fig.5-3 represents a typical example of the torques obtained in that situation. We can see that the assisting torque is first positive

(a) Line crossing prevention trajectory
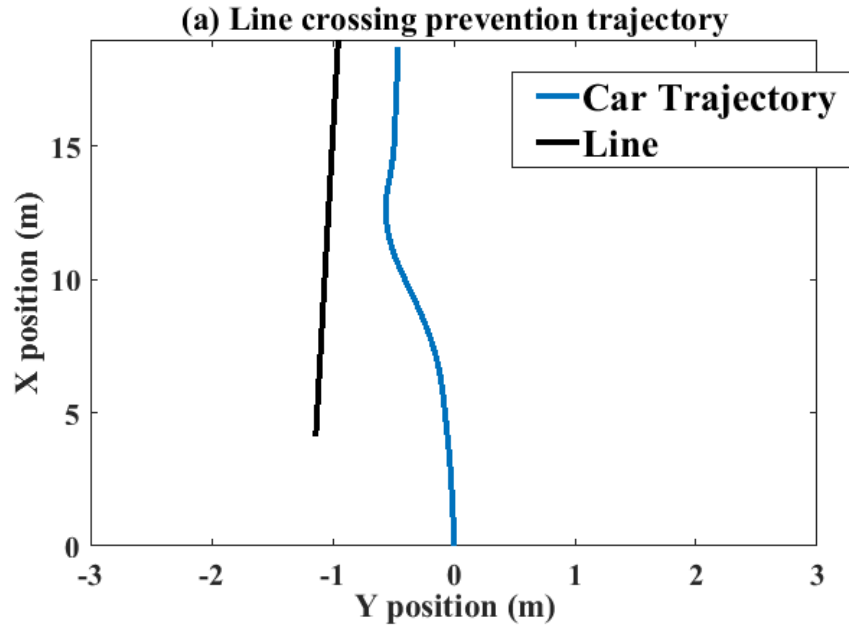
Fig. 5-2: Line crossing prevention trajectory.

in order to prevent the crossing. After that first peak, a smaller negative one is used to realign the car. We can also observe that the torque of the driver is very weak at first, until the assisting torque provoke a reaction of the driver who first try to counter the effect of this torque while staying at a lower intensity indicating that the driver holds the steering wheel but do not try to turn conversely to the driving support.

Moreover in every tests of this type, where the driving assistant was trusted to avoid the line crossing, this one has always been able to prevent the lane changing. It can then be stated that the driving assistant has the behavior expected of it when $K_{rd} = 1$, corresponding to a standard situation.
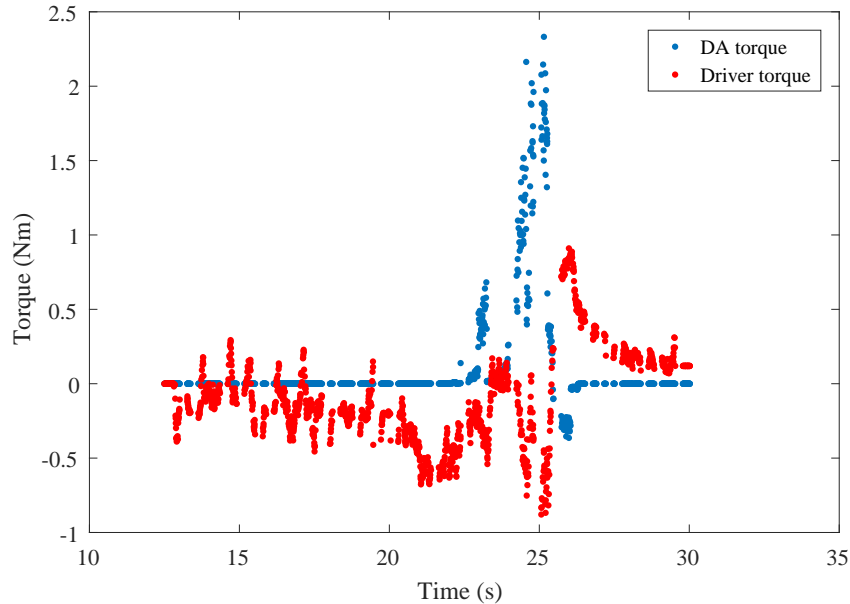
Fig. 5-3: Example of torque obtained during a line crossing prevention.

5.2.3 Lane Crossing Example

The Fig.5-4 shows a trajectory of the vehicle during a simulation that is typical of the trajectories followed during line crossing. It is possible to see that the car is first pushed from the line and that after the crossing it is aligned with the line. Several crossings like this one were performed and Fig.5-5 represents the different torques applied on the steering wheel during one of these. As we can see the driving assistant first try to prevent the crossing and then help the driver to realign the car with the road. The prevention torque, before 15s, is bigger that the aligning torque, after 15s, as expected from the support algorithm. As in this this situation the crossing is forced, the torque applied by the driver is almost the opposite of the driving assistant one, as the driver hold the steering wheel still, to force the crossing.
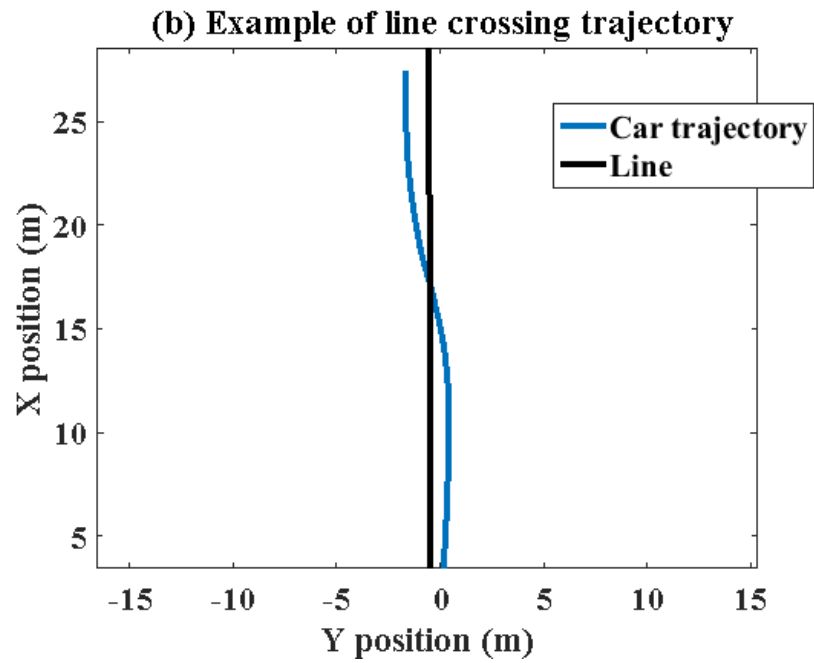
Fig. 5-4: Line crossing prevention trajectory.
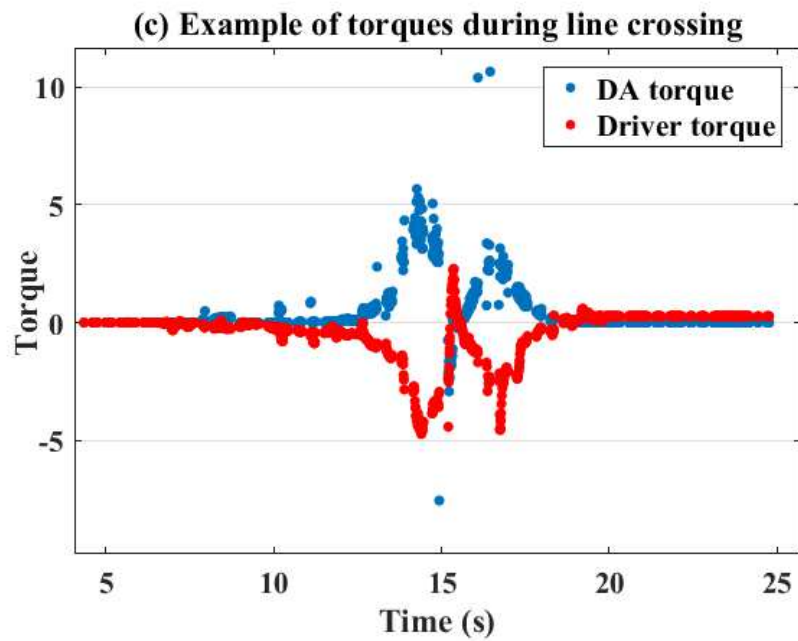
Fig. 5-5: Example of torque obtained during a forced line crossing.

5.2.4 Effect of K_{rd}
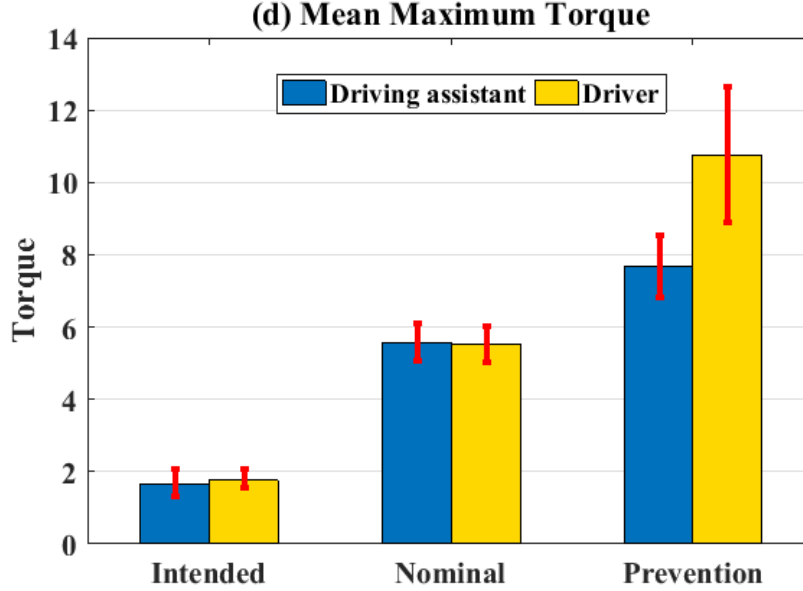
Fig. 5-6: Mean Maximum Torque obtained during a forced line crossing.

In order to evaluate the effect of the fuzzy logic output on the controlled car behavior, several human drivers were asked to performed line crossing with different values of K_{rd}, in order to estimate its impact on the control of the electric vehicle. The chosen values of K_{rd} were 1, to describe a normal driving situation, 0.25, to analyze the behavior of the driving assistant when a line crossing intention was detected and 1.75 to represent the potentials' effects in a dangerous situation. Each driver was asked to perform several crossings for each value of K_{rd}. Fig.5-6 gathers the results of all the crossing experiments to compute the mean maximal torques of the driving assistant and driver with different K_{rd} values and their standard deviations. When a crossing intent is detected the DA torque is too small to prevent the crossing but the driver is able to feel it and then obtain haptic information about the location of the line. On the other hand when the K_{rd} is high the torque required from the driver to perform the crossing is really high and should prevent even desired crossing in real driving situation. The behavior of the assistant is then conform to what was expected of it.

5.2.5 Influence of the Driving Assistant on the Car Direction During Line Crossing
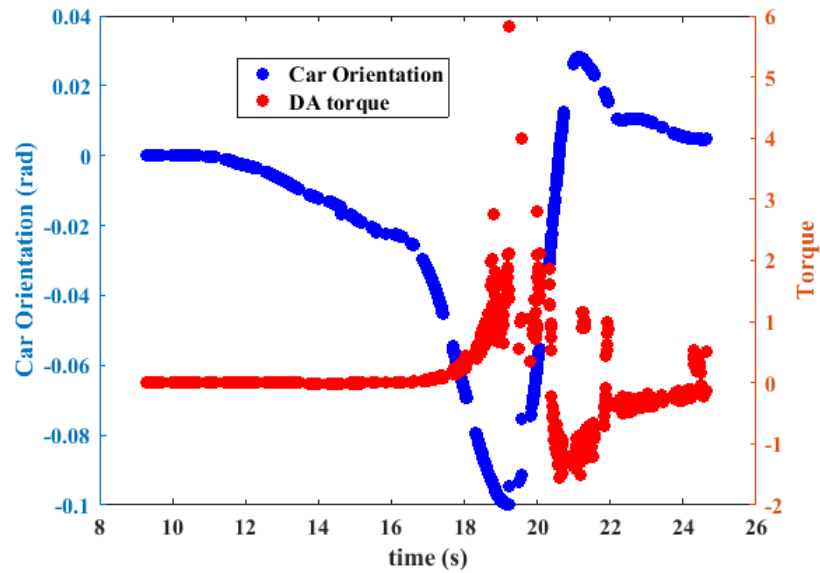
Fig. 5-7: Effect of the DA torque on the orientation of the car during crossing prevention.
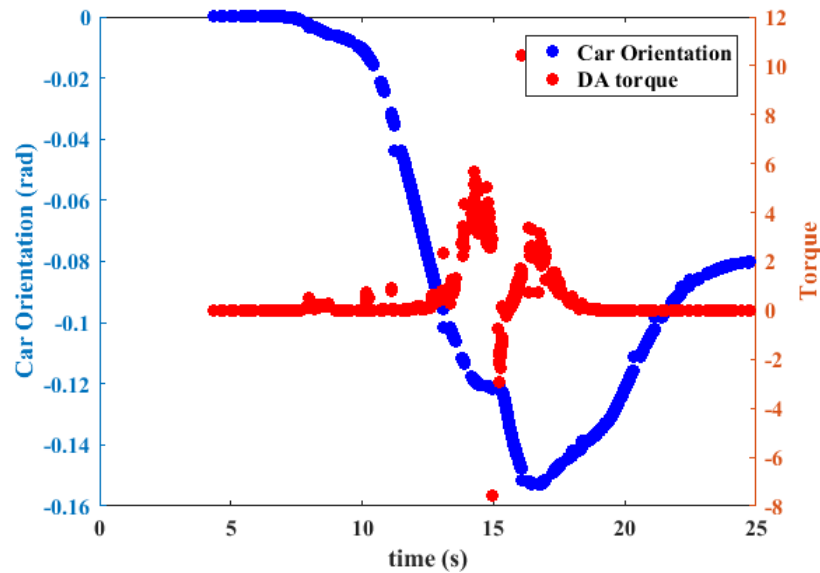
Fig. 5-8: Effect of the DA torque on the orientation of the car while crossing in normal condition.

An other important aspect of the driving support, except from the assistance it offers,
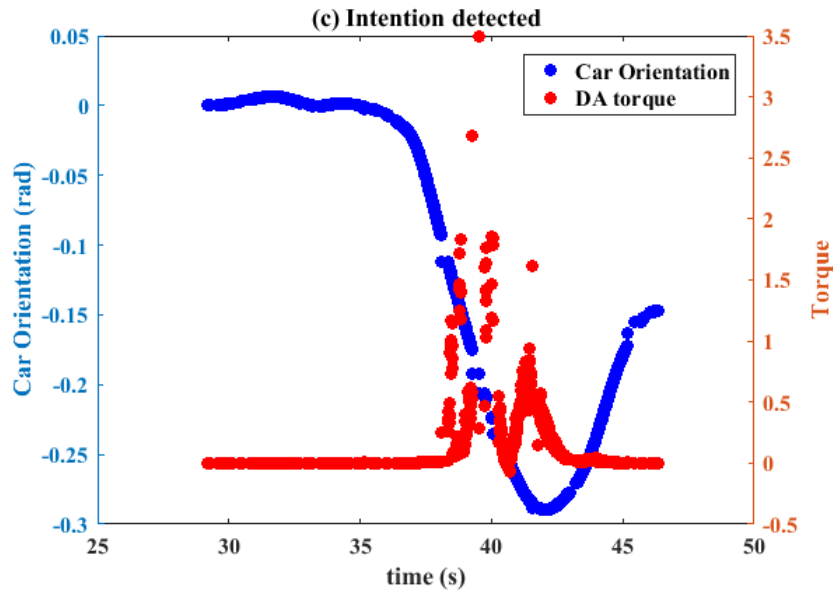
Fig. 5-9: Effect of the DA torque on the orientation of the car while crossing with crossing intention detected.

is its ability to reduce as much as possible its impact on the trajectory of the car when the support is not needed. This aspect is studied in Fig.5-7, Fig.5-8 and Fig.5-9. It represents simultaneously the orientation of the car and the torque applied by the driving assistant in different scenarios. Fig.5-7 describes a case where the driving assistant prevent a crossing, 5-8 a case where the driver forced a line crossing in normal condition and 5-9 a case where a line crossing was intended. As expected in the non crossing situation the DA assistant directly influences the direction of the car and first the DA torque modify the orientation of the car to prevent the crossing. Then a reversed torque is applied when the car begin to get farther of the line to align the vehicle, and it can be observed that finally the orientation of the car returned to a value closed to 0. In the normal conditions crossing, it can be observed that the DA torque has an influence on the car orientation that disturb the crossing motion. This behavior is expected but it should be different if a line crossing intent was detected. Indeed in this last situation, both to improve the acceptance from the driver but also to avoid dangers caused by a perturbed trajectory, the effect on the trajectory of the driving assistant should be minimal. It is what can be observed in 5-9. The first torque has no influence on the car's orientation but this
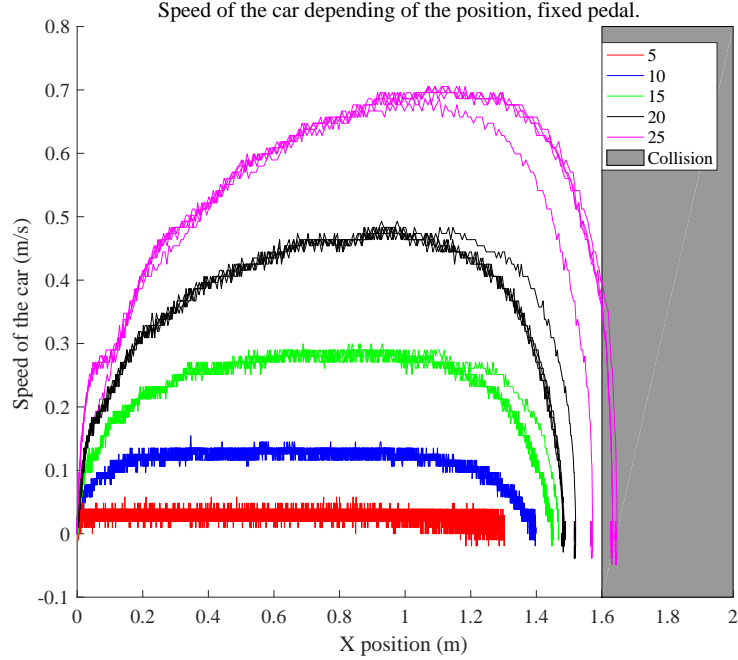
Fig. 5-10: Effect on the speed of the pedal torque, fixed pedal angle.

one varies after the second torque, the alignment one, indicating that the driver is not restrained by the DA in that situation but can use its haptic information if he wants to. The experiments were then able to demonstrate that the proposed driving assistant can, depending of the situation, offer the proper level of assist and do not disturb the driver.

5.2.6 Effect of the Pedal Assisting on Collision Avoidance

This subsection is dedicated to the analysis of the influence of the driving assistant on the speed control in case of collision avoidance. The corresponding tests were then conducted using the RoboCar®, in different conditions. The common point of the different test situations was that the steering of the car was blocked to specifically analyze the impact of τ_{daped}. First tests were conducted with a blocked position of the pedal on the driving station, emulating what would happen if a driver kept pressing the pedal to counter the effect of the driving assistant. Different angular positions of that pedal were used to perform the experiment. The results are gathered in Fig.5-10 where the speed of the car is indicated in function of its longitudinal coordinate in the experiment referential.
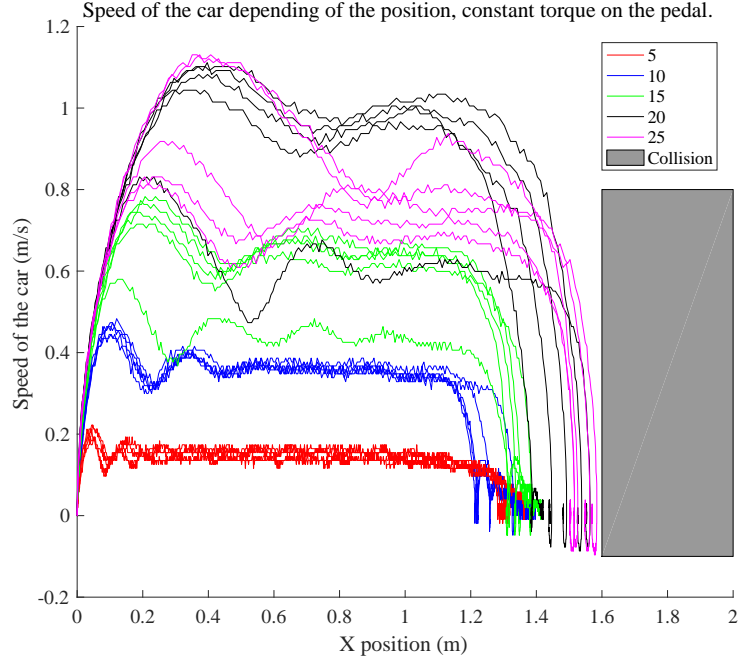
Fig. 5-11: Effect on the speed of the pedal torque, Constant Torque on the Pedal.

The obstacle car was located 2 meters in front of the controlled car so collisions occurred if the car entered the grey area. As it can be observed the driving assistant tends to stop the controlled car when this one is getting closer to the obstacle. Each tests conducted with the same pedal angle are represented using the same color. It can be seen that the faster the car goes, the closer the final distance to the obstacle is, and collisions can happen if the speed of the car is too important. Indeed as the position of the command pedal was artificially set to a constant value the estimated value of the driver torque could vary very strongly and the command based on the derivation of the driver input could become very strong compared with τ_{daped}. However as detailed in Chapter 3, at high speed the car potential aims at making the car turn to avoid the collision and does not only rely on the speed control.

The following tests were conducted with a constant command torque on the pedal, corresponding to what would happen if the driver pressed the pedal with a constant intensity. Those torques correspond to the torques to apply in order to maintain specific angular positions of the pedal without assisting torque but only the spring torque. The
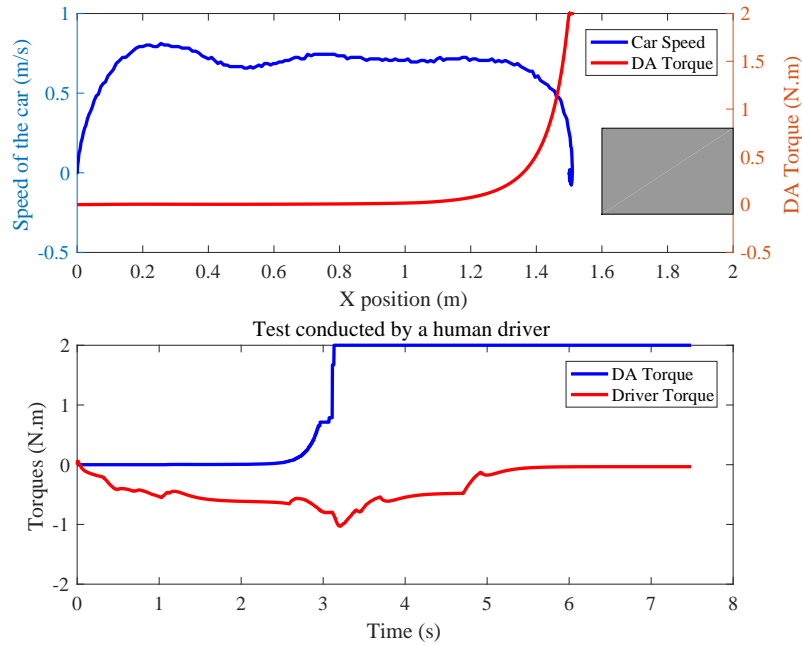
Fig. 5-12: Example of collision avoidance conducted with a fixed steering wheel.

results of that test procedure are gathered in Fig.5-11. This figures shows the effects of the driving assistant on the speed, as the car goes closer to the obstacle. As it can be observed, the car is stopped before collision even if that distance get smaller as the speed is increasing. Moreover this situation is closer to the normal application of the driving assistant.

Fig5-12 is an example of result obtained when the throttle control is let to a human driver. The upper part of the figure represents the speed of the controlled vehicle and the driving assistant torque in function of the longitudinal position of the car. It can be seen that the speed of the car decreases as soon as the vehicle is close enough of the obstacle to create an assisting torque on the pedal. The lower part of the figure represent the driving assisting torque and the driver torque on the pedal during the simulation. It can be observed that after the driving assistant torque reached its max level, even if the driver keeps pressing the pedal the car remains stopped.

Fig5-13 shows the distance at which the car was stopped in different scenarios. The cases in blue correspond to a pedal blocked at a certain position and the yellow ones are
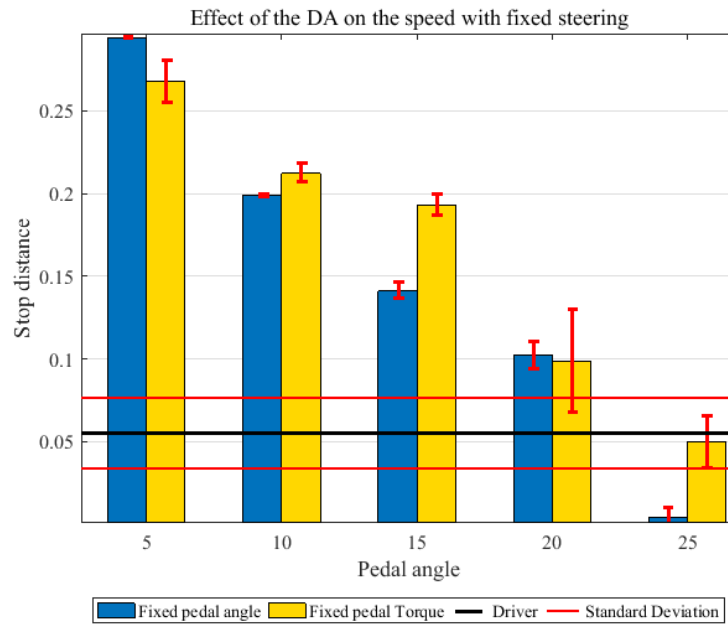
Fig. 5-13: Distance between the controlled car and the obstacle when the first one stop.

obtained with constant torques applied on the pedal. It can be seen that the DA is more efficient in the last situation. The black line correspond to the mean distances reached when the drivers were free to control the speed of the car with the assistance of the support pedal torque. The red lines embodies the standard deviations of those tests. Finally it can be stated that the driving assistant offers a behavior that is conform to the purpose it was designed for, by slowing down the car when it gets to close of the obstacle, even if the throttle assistance only may not be able to prevent collision with extreme speed. However a high speed also implies an increase of the strength of the driving assistance through the fuzzy logic engine so the number of collisions in that situation is furthermore reduced.

5.2.7 Effect of the Steering Assistance on Collision Avoidance

From the previously obtained results, the necessity to analyze the effect of the steering assistance in situation of collision avoidance is obvious. Several experiments were then conducted where the speed of the vehicle was fixed to different values corresponding to
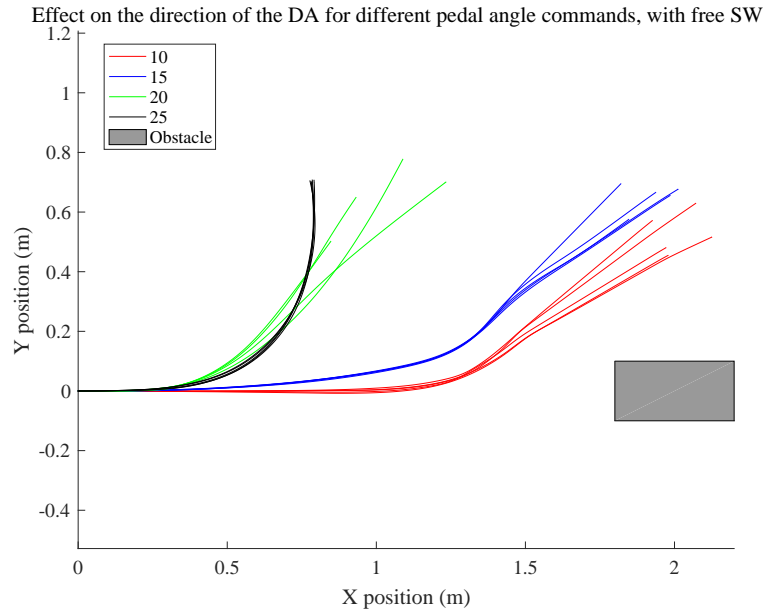
Fig. 5-14: Trajectories followed by the controlled car when letting the DA do the avoidance alone.

different pedal positions. The purpose of those tests was to study separately the effect of the driving assistant on the steering without considering the throttle support. First the driving assistant was let free to control the trajectory of the car, describing a situation where the driver has no influence on the steering. This can happen when K_{hum} is reduced , by instance if the driver was detected as drowsy. Fig5-14 gathers the trajectories followed by the car in this situation. It can be observed that the collisions are avoided in all cases and that the higher the speed the sooner the car turns. However if the speed is too high, the direction of the car can be modified too strongly. This situation could lead to road exits. This is why in real application car potential should be associated with road and line potentials, in order to let the late one perform the road keeping. Indeed the potential of a car is very local, implying that if the controlled car get too far from the obstacle then this one cannot realign the vehicle with the road, conversely to the line potential that are not restrained to a specific location on the road.

Fig5-15 was obtained with a method very similar the previous one, except that the

Effect on the direction of the DA for different pedal angle commands, SW held by a driver
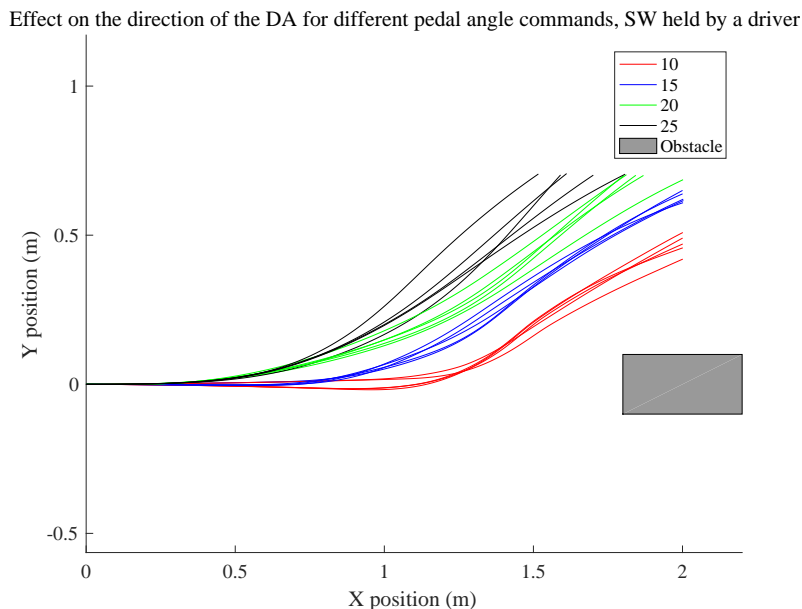
Fig. 5-15: Trajectories followed by the controlled car when both the DA and the driver chose the direction.

driver also had the control of the steering wheel. This corresponds to a more normal situation where the status of the driver is normal and where K_{hum} is equal to 1. It can be observed that this combination produces softer trajectories but that the behavior remains similar. With the driver also in control of the car trajectory, this one is closer to the trajectory that would be followed by a driver without support. Moreover the higher the speed, the sooner the trajectory is modified.

Fig5-16 transcripts the minimum distances to the obstacle in the previous tests. We can see that this distance is increasing with the command speed and that it is smaller when the driver keeps an influence on the steering wheel, indicating a more natural way of preventing the collision. It also indicates that in these conditions the driving assistant is able to efficiently avoid the collision with the car obstacle.
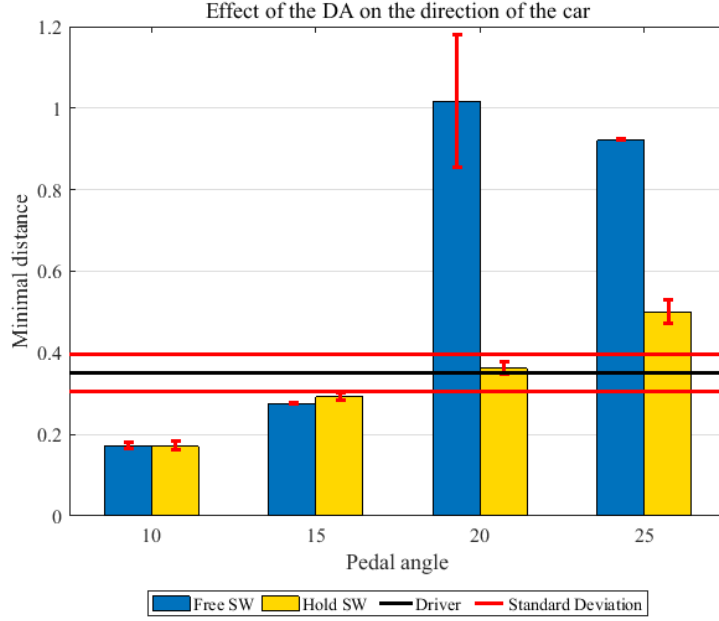
Fig. 5-16: Minimum distance between the obstacle and the vehicle with the steering assistance.

5.2.8 Example of Full Collision Avoidance

Fig.5-17 is an example of result obtained with the complete collision avoidance system and a control shared with the human driver where K_{hum} is equal to 1. The upper part of the figure transcripts the trajectory followed by the car to avoid the obstacle and the different torques created by the driving assistant. It can be observed that the support torque on the steering wheel start to be noticeable at a greater range compared to the pedal one. This is why the trajectory is modified before slowing down the vehicle. In that example the trajectory modification is such that the support torque on the pedal remains close to 0 during the avoidance. That means that if possible, i.e. if there is no danger to start a passing maneuver, the driving assistant tends to provoke a lane changing of the controlled vehicle before slowing down this one. This late situation only appears if car is not able to proceed to a line changing, for example in the case of a one lane road or if the adjacent lane is occupied by an other vehicle.

The lower part of Fig.5-17 represents the different driver torques and and driving assistant torque. Concerning the torques applied on the pedal, as the driving assistant torque
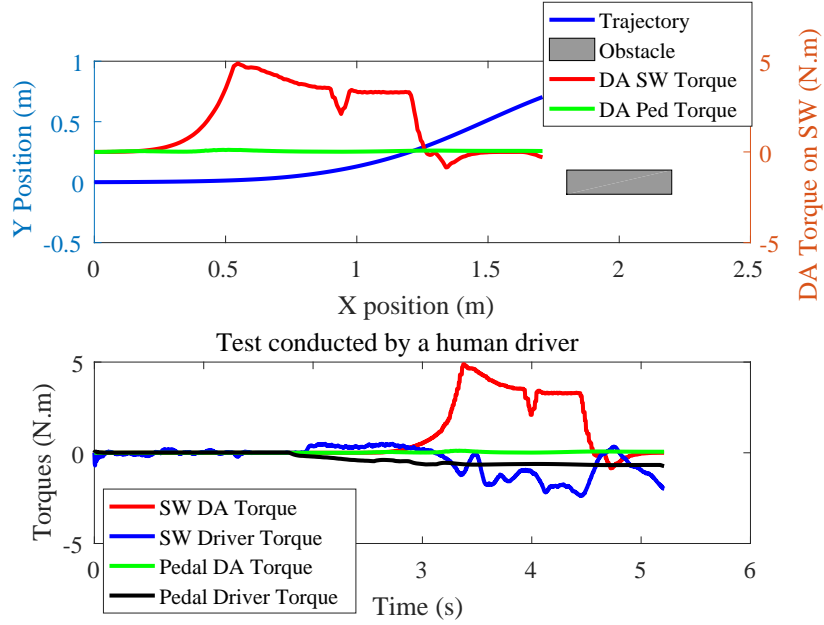
Fig. 5-17: Example of result of the complete collision assistance.

is negligible , only the driver controls the speed of the car. It can also be observed that the torque of the driver on the steering wheel seems to be in opposition with the driving assistant torque but of smaller amplitude, indicating that the human user holds the steering wheel and let the driving assistant guide the steering movement.

5.2.9 Effect of Time Delay on Collision Avoidance

Table 5.2: Measurements of ping mean values from a computer of the laboratory, in Hiyoshi, Yokohama, 24th of July 2017.

Destination	Mean ping value	Destination	Mean ping value
France	178ms	United States	116ms
Australia	108ms	Lab. server	< 1ms
Yokohama	4ms	China	113ms
Ghana	384ms	Brazil	112ms
Poland	264ms		

The next experiments where conducted in order to estimate the impact of the communication time delay in the case of collision avoidance. First, the driver were asked to drive
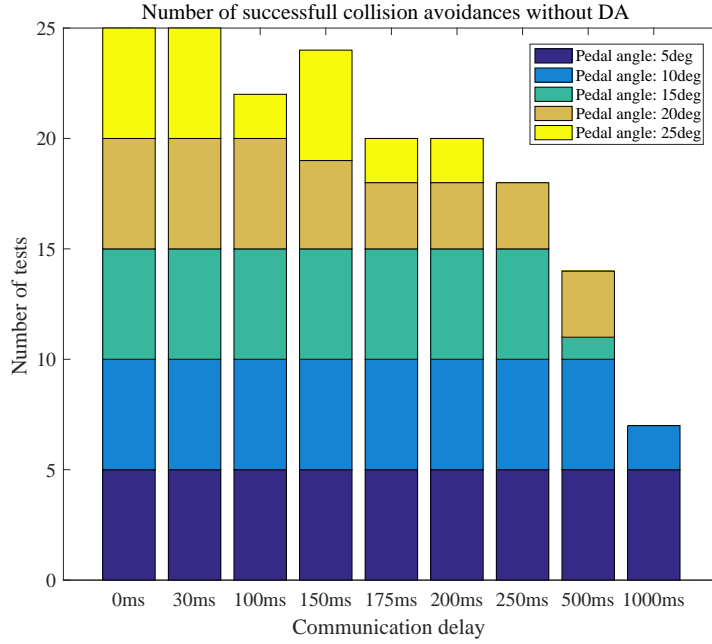
Fig. 5-18: Collision avoided depending of the communication delay, no DA.

the controlled vehicle in order to avoid collision, without driving assistance. Several values of time delay were tested, and for each of these values, the car was set to a speed corresponding to certain values of the pedal angular position. For each couple of value of time delay and speed, 5 tests were conducted. A test was successful if the driver was able to avoid the collision with the obstacle. Fig.5-18 gathers all of the results obtained through those tests by accounting the number of successful avoidances, for each speed and time communication delay. As expected the number of collisions is increasing with the time delay and the speed of the controlled vehicle, at a point where, when the communication time delay become too important it is impossible for the driver to react quickly enough to prevent the accident, unless driving at extremely low speed. In order to estimate the efficiency of the driving assistant to compensate the communication time delay, the same experiments were conducted but with the addition of the driving assistant. The results are shown in Fig.5-19. It can be noted that the driving assistant is able to successfully prevent all collisions even at high speed and very long time delay. From that point of view, the driving assistant is then able to reduce the number of accidents in case of remote
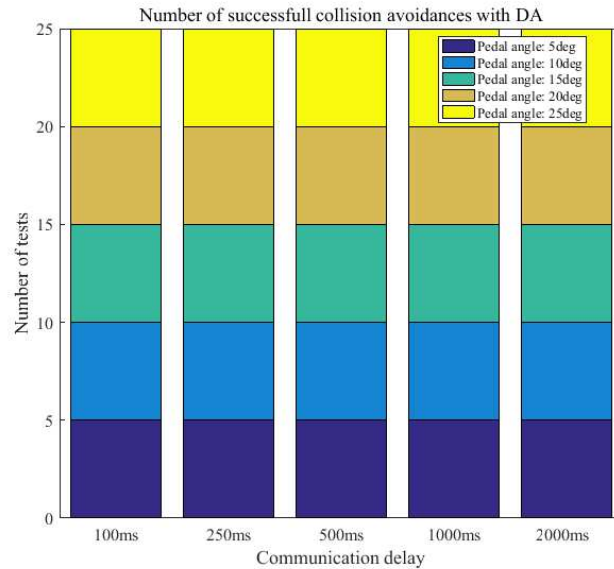
Fig. 5-19: Collision avoided depending of the communication delay, DA.

control.

Fig.5-20 illustrates the different trajectories followed by the controlled vehicle with a communication time delay of 700ms with and without driving assistant. It can be observed that without assistance the trajectories often lead to collision or are dangerously reorienting the car, while being close of the obstacle. With the assistant the trajectories are sufficiently far from the obstacle and are then safer, moreover they are closer in their shapes to what happen without delay.

Finally Fig.5-21 provides an example of the torques applied both on the RoboCar® and on the driving station. The effect of the time is clearly observable. Indeed the driver torque is a reaction of the support torque that is applied on the driving station. First the driver by holding the steering wheel is in opposition with the driving assistant but then cooperate with it. From the RoboCar® point of view, the DA torque is created locally in reaction of the obstacle getting closer and the driver torque is received with a delay corresponding to two times 700ms, corresponding to the time required to send the DA information to the driving station and then from the reaction of the driver to reach the controlled vehicle.

It is interesting to consider the comparison of the tested time delays and typical time
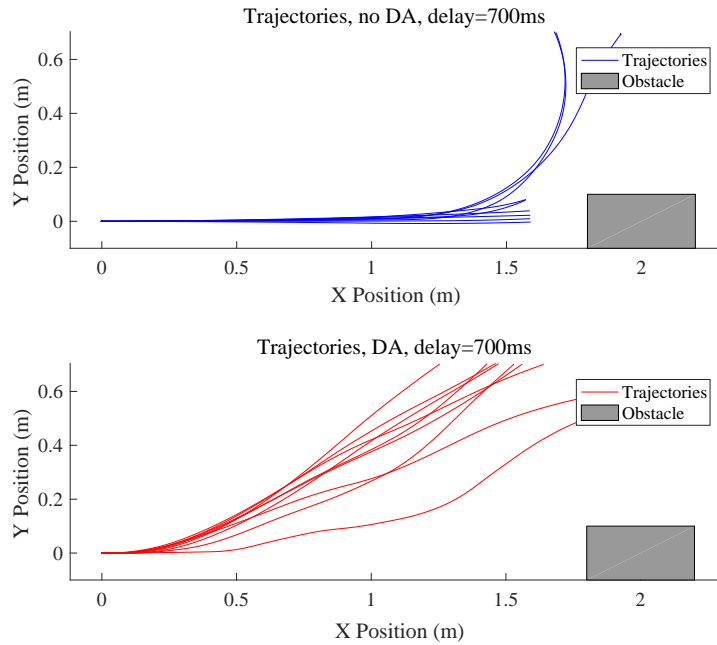
Fig. 5-20: Trajectories followed with a 700ms communication delay.

delays that can be observed in traditional internet communications. In order to estimate that kind of delay, the ping function is probably the most widespread and commonly used utility. This tool measures the round-trip time between a host and a destination. That means that a ping measurement includes twice the communication time delay as defined in this thesis. In this work, the maximum value of the time delay during the tests was 2000 ms which corresponds to a 4000 ms ping value. With that communication time delay, it was possible to efficiently prevents the collisions and no instability was observed. Fig.5-22 represents the average internet speed by country and gives some indication about the correlation between the distance and the expected latency. 10, 50 and 75 ms latency are represented by circle centered around some cities. It can be observed that, of course, the distance between the host and the destination has an impact on the latency, independently of the quality of the network. Fig.5-23 is an instantaneous measurement of the status of the network between cities around the world, indicated by ping values. It can be seen that even for very remote places, ping values are inferior to 450 ms. This statement was tested by conducting several ping measurements from the laboratory to globally dispatched
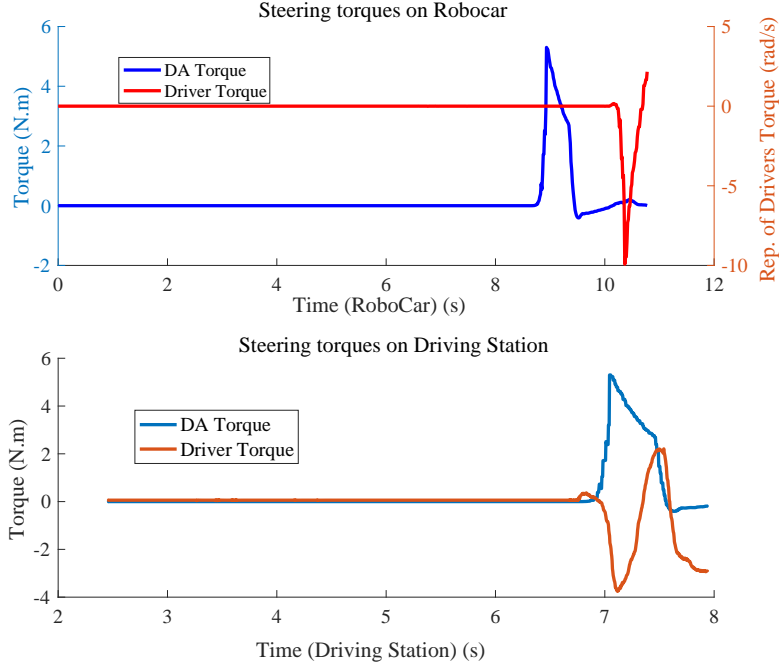
Fig. 5-21: Command torques on the controlled vehicle and driving station with 700ms communication time delay.

servers. The results are summed up in Table 5.2. Even in this scenario the round-trip times were inferior to 400 ms. It can then be stated that the communication time delays tested during collision avoidance scenarios were significantly superior to typical round-trip time values, and that the proposed system could be applicable in remote driving, even from a very remote location. Of course that time delay could be worsen in case of poor network connection, but considering a standard connection for that kind of application, and the fact that the remote control would probably not be applied on a vehicle at the opposite part of the world compared to the driving station, it can be stated that instability caused by the communication time delay is not a problem. Moreover in case of high time delay the value of K_{hum} is reduced, diminishing the appearance of instability.

Thus the efficiency of the proposed active driving assistant to counter the effect and hazards of the communication time delay induced by the remote control application is proved.
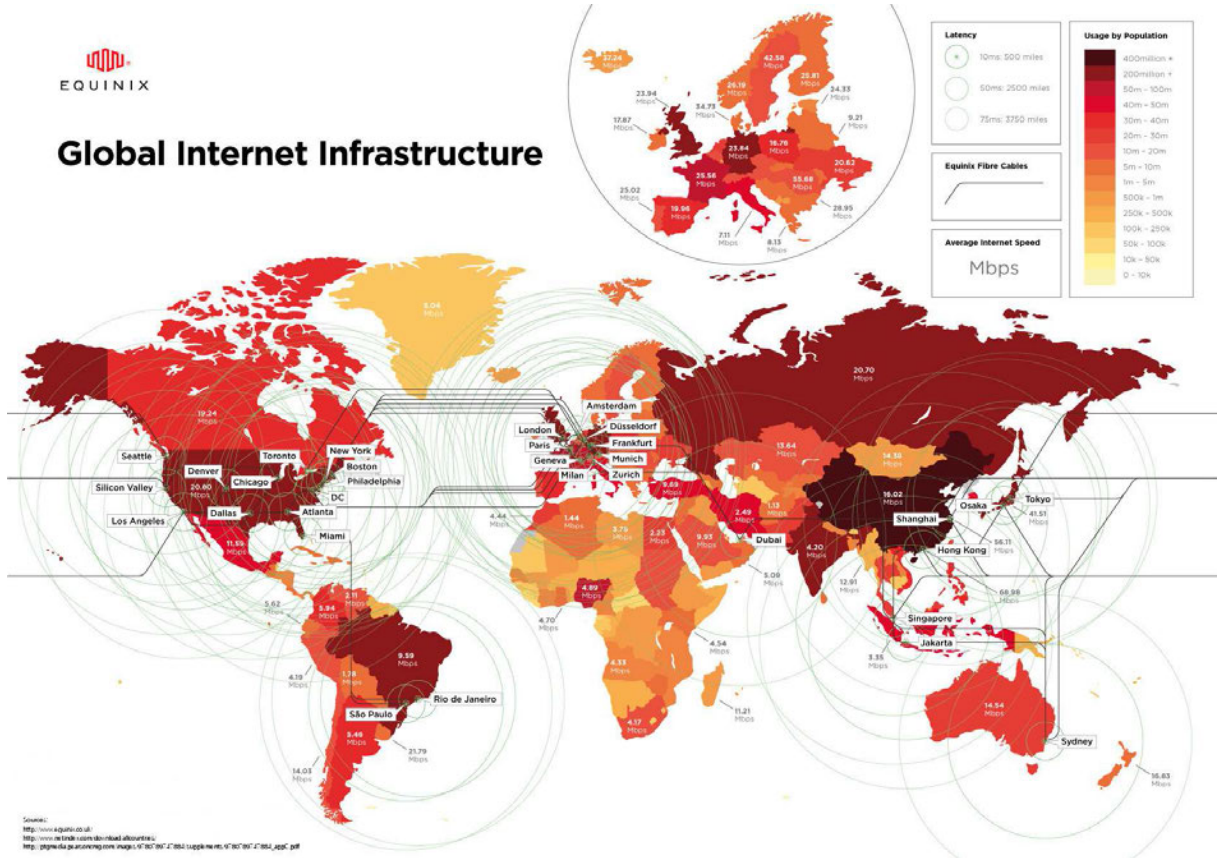
Fig. 5-22: Global Internet architecture according to equinix's analyses[4].

	Barcelona ✖	Paris ✖	Tokyo ✖	Toronto ✖	Washington ✖
Amsterdam ✖	● 44.015ms	● 6.173ms	● 251.679ms	● 105.037ms	● 91.259ms
Auckland ✖	● 433.75ms	● 294.476ms	● 244.048ms	● 203.668ms	● 229.403ms
Berlin ✖	● 54.391ms	● 13.364ms	● 258.453ms	● 105.066ms	● 112.81ms
Copenhagen ✖	● 43.655ms	● 21.447ms	● 274.793ms	● 109.13ms	● 98.488ms
Dallas ✖	● 152.75ms	● 126.875ms	● 146.154ms	● 38.57ms	● 32.081ms
London ✖	● 35.449ms	● 3.924ms	● 236.899ms	● 85.466ms	● 74.17ms
Los Angeles ✖	● 159.388ms	● 131.942ms	● 112.567ms	● 60.315ms	● 63.19ms
Moscow ✖	● 72.622ms	● 53.848ms	● 293.836ms	● 214.471ms	● 144.521ms
New York ✖	● 128.392ms	● 74.689ms	● 171.164ms	● 14.432ms	● 6.558ms
Paris ✖	● 41.776ms	—	● 288.06ms	● 119.504ms	● 81.024ms
Stockholm ✖	● 57.039ms	● 28.113ms	● 292.569ms	● 126.058ms	● 116.414ms
Tokyo ✖	● 279.744ms	● 268.544ms	—	● 176.065ms	● 178.259ms

Fig. 5-23: Example of ping values between different cities, measures taken the 24th july 2017[5].

5.3 Evaluation Criteria

5.3.1 Principle

The driving task is very complicated and involves a great number of reactions of the driver to numerous different situations. Moreover the evolution of a car in its environment is complex. Therefore it is really difficult to construct criteria evaluating the whole driving task from simple values obtained from the sensors of the vehicle. It is also problematic to define what would be the perfect driving behavior, as it is really dependent of the situation and of the car's environment. Moreover it seems that the human appreciation is required to evaluate the skills of a driver, as obtaining a driving license can only be achieved through the evaluation of a human examiner. The consequences of that statement are that it is similarly difficult to estimate the performances of a proposition of driving assistant, and then to compare two of them in order to determine which one is the best. Thus this section aims at proposing an index based on several criteria in order to evaluate and compare driving assistant solutions. The proposed method may not be the only one suitable a evaluate such systems, but can be adapted in function of the desired behavior of the driving assistant. The suggested index is based on the evaluation of three factors.

- The safety.

- The comfortability.

- The operability.

Of course the safety is an extremely important factor in the efficiency of a driving assistant. It can even be defined as the main concern of such systems, and describe the ability of a driving assistant to avoid the collision, road exit or more generally every dangerous situation. The comfortability can be seen as a notion close to the one the comfort notion of the passenger of the controlled vehicle and aims at ensuring that using the driving assistant is not unpleasant for the passengers. Lastly the operability corresponds to the comfort of use by the current driver and is related to the ability of the driving assistant to not restrain the human user but to help him.

Table 5.3: Meaning of index weights.

λ	0	0.5	1
Meaning	Not important	Important	Extremely important

Table 5.4: Chosen weights.

Weight	Chosen value
λ_s	1
λ_c	0.4
λ_o	0.6

5.3.2 Index Construction

The created index called E, is a number contained between 0 and 1, that indicates a better efficiency as it gets closer to 1. It is constructed from a weighted mean of similar values attributed to the three aspects previously presented, the safety, the comfortability and the operability. The efficiency index can be expressed as follows.

$$E = \frac{\lambda_s E_s + \lambda_c E_c + \lambda_o E_o}{\lambda_s + \lambda_c + \lambda_o} \qquad (5.1)$$

Where E_s is the index representing the safety index, E_c the comfortability index and E_o the operability index, and the different λ their respective weights. Those weights are chosen according to Table 5.3.

This way, it is possible to estimate the efficiency of the proposed active driving assistant in function of its desired behavior. It is also possible to compare several architectures of driving supports to measure their efficiency in certain domains. The coefficients chosen in that study are gathered in Table 5.7.

The following subsections will describe of the efficiency indexes representing safety, comfortability and operability are obtained.
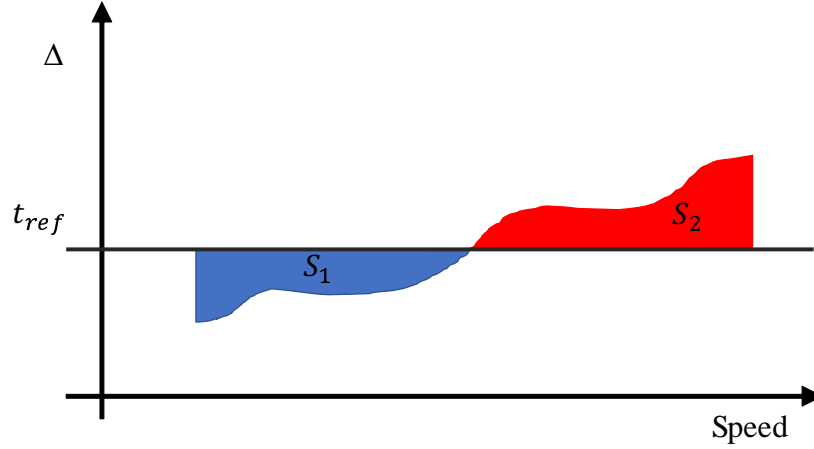
Fig. 5-24: Deltas compared to a referential time, used for criteria definition.

5.3.3 Safety

The main concern of the proposed driving assistant is the safety. Indeed this one was designed in order to reduce the number of casualties on the road. In the presented case the safety is mostly relevant to the ability of the proposed architecture to prevent collisions, road exits or involuntary lane changing. This subsection will describe the criteria used to defined E_s. Those three criteria are represented by numbers between 0 and 1, and are detailed thereafter.

- E_{sc} is defined as the square of the ratio of prevented collisions, undesired lane changing or road exit, depending of the case, in the different tests. Even if this criterion seems trivial, it is central to estimate the safety of the assistant algorithm. It is unfortunately dependent of the number of conducted tests and of the variety of situations covered by those tests. The square component allows to increase the impact of a failure on the criteria. It is possible to write the following relation.

$$E_{sc} = \left(\frac{s}{t}\right)^2 \tag{5.2}$$

Where t is the number of conducted tests and s the number of successful ones.

- The second criterion's purpose is to evaluate the impact of the remote control on the safety of the driving assistant. It compares the ratio of successfully conducted

tests with the remote control and the ratio of successfully conducted test without the remote control. This criterion is dependent of the used communication time delay but enables to observe the evolution of efficiency with the evolution of the time delay.

$$E_{sd} = \frac{s_d t_{nd}}{t_d s_{nd}} \tag{5.3}$$

With t_{nd} the number of tests without delay, t_d the number of tests with delay, s_{nd} the number of successful tests without delay and s_d the number of successful tests with delay.

- The third criteria used to evaluate the safety of the proposed system is based on the minimal distance to the danger during the test. However just taking into account that distance does not consider the speed at which the danger was avoided. This is why a value called Δ is used and can be defined as follows.

$$\Delta = \frac{D}{V} \tag{5.4}$$

With D the minimal distance to the obstacle and V the velocity at which the car goes closer to it. Δ is similar to a time, that would describe the minimum time before collision to the danger. It is then possible to represent the values of Δ in function of the speed and to compare it with a referential time that would describe the expected behavior of the driving assistant. Fig.5-24 shows en example of such representation. Two surfaces can be observed. S_1 corresponds at the surface on which Δ is smaller than that referential time an S_2 to the surface where Δ is bigger than it. It is then possible to define the following criteria.

$$E_{sm} = \frac{1}{2 + K_{sm}S_1} - \frac{1}{2 + K_{sm}S_2} + \frac{1}{2} \tag{5.5}$$

K_{sm} is a gain used to regulate the influence of the difference of surface. E_{sm} is such that it tends to 0 if S_2 is small and S_1 is big and to 1 in the invert situation.

Finally E_s can be expressed by the following equation.

Table 5.5: Chosen weights for E_s.

Weight	Chosen value
λ_{sc}	0.6
λ_{sd}	0.6
λ_{sm}	0.4

$$E_s = \frac{\lambda_{sc}E_{sc} + \lambda_{sd}E_{sd} + \lambda_{sm}E_{sm}}{\lambda_{sc} + \lambda_{sd} + \lambda_{sm}} \tag{5.6}$$

5.3.4 Comfortability

The comfortability, aiming at representing the feeling of the controlled vehicle passengers it should sanction the cinematic behavior of the car that would cause uneasiness. E_c is computed from three criteria.

- A primal source of uneasiness is the brutal modification of the orientation of the car caused by the assistant. This criterion is heavily dependent of the shape of the potentials and their types. Thus the mean maximum variation of the car orientation $\dot{\omega}_{max}$ should be considered. It is then possible to define $E_{c\omega}$ as follows.

$$E_{c\omega} = \frac{1}{1 + \alpha\dfrac{\dot{\omega}_{max}}{V}} \tag{5.7}$$

  Where α is a modulation constant and V the velocity of the car. Indeed $\dot{\omega}$ is dependent of the speed of the car, as demonstrated by the cinematic model, $E_{c\omega}$ describes then the correlation between the speed and the evolution of orientation.

- An other aspect is the ability of the driving assistant to react only when getting close to the obstacle. Indeed it can be disturbing for the passengers if the support reacts to very remote objects. This criterion is based on the use of the Δ variable and a referential time. For this criterion Δ is not computed from the minimal distance but from the inflection distance, the distance to the obstacle at which the trajectory of the car begin to be modified. The equation is defined as follows.

Table 5.6: Chosen weights for E_c.

Weight	Chosen value
$\lambda_{c\omega}$	0.6
λ_{cm}	0.5
λ_{co}	0.4

$$E_{cm} = \frac{1}{2 + K_{cm}S_2} - \frac{1}{2 + K_{cm}S_1} + \frac{1}{2} \tag{5.8}$$

E_{cm} is such that it tends to 0 if S_1 is small and S_2 is big and to 1 in the invert situation.

- The comfort of the passengers of the vehicle is directly affected by oscillations, either of the direction control or of the speed control. A criterion E_{co} is then created from the oscillations of the pedal and steering wheel angle caused by the driving assistant. To construct it, the angular positions of those motors are sent to a low pass filter and the filtered result is subtracted to the angular position. The result indicates the angular variations caused by oscillation. The root mean square value of those oscillations, R, is then computed, and the criterion is computed from the following equation.

$$E_{co} = \frac{1}{1 + \beta R_{mean}} \tag{5.9}$$

mean

Where β is a modulating coefficient.

Finally E_s can be expressed by the following equation.

$$E_c = \frac{\lambda_{c\omega}E_{c\omega} + \lambda_{cm}E_{cm} + \lambda_{co}E_{co}}{\lambda_{c\omega} + \lambda_{cm} + \lambda_{co}} \tag{5.10}$$

5.3.5 Operability

The operability is an index characterizing the comfort of the driver when using the driving assistant and the cooperation between those two. Similarly to the previous coef-

ficients, it is computed from three criteria.

- The first criterion aims at estimating the opposition of the driver to the driving support. This situation is determined by $\tau_{da}\tau_{driver} < 0$. In order to obtain an index evolving between 0 and 1 the following equation is used.

$$E_{oo} = \frac{1}{1 - K_{oo} \int_t \tau_{da}\tau_{driver}dt} \tag{5.11}$$

  The integration is conducted when $\tau_{da}\tau_{driver} < 0$ and K_{oo} is a coefficient to equalize the impact of the different torque value that are very different from the steering wheel and pedal. The criteria describes the opposition between the driver and the support on a a whole simulation concerning a specific object, by instance a collision avoidance or a line crossing prevention.

- The second criterion is based on the evaluation of the cooperation between the driver and the driving assistant a situation that appears when $\tau_{da}\tau_{driver} > 0$. The criterion is then computed as follows.

$$E_{oc} = 1 - \frac{1}{1 + K_{oc} \int_t \tau_{da}\tau_{driver}dt} \tag{5.12}$$

  As previously stated the integration is performed on periods where $\tau_{da}\tau_{driver} > 0$ and K_{oc} is used to equalize the influence of he different kind of torques.

- The last index is obtained from the opinion of the drivers that tested the system. If the value of this index can be doubtful to compute an efficiency by itself, it seems important to evaluate the feeling of drivers external to the project creation to estimate the possible acceptance from the public of the proposed method. The final criterion E_{od} could then be conceived as a grade from 0 to 1.

Finally E_o can be expressed by the following equation.

$$E_o = \frac{\lambda_{oo}E_{oo} + \lambda_{oc}E_{oc} + \lambda_{od}E_{od}}{\lambda_{oo} + \lambda_{oc} + \lambda_{od}} \tag{5.13}$$

Table 5.7: Chosen weights for E_o.

Weight	Chosen value
λ_{oo}	0.6
λ_{oc}	0.5
λ_{od}	0.2
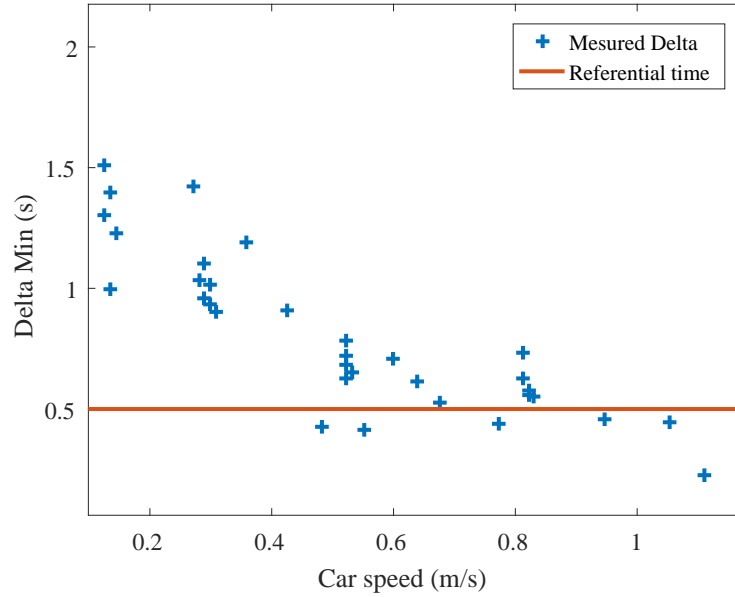
Fig. 5-25: Δ_{min} on collision avoidance depending of the car speed, with $K_{hum} = 1$.

5.3.6 Example

This subsection will describe an example of application of the previously defined indexes to the collision avoidance application. Two situations will be taken into account. The first one correspond to the standard condition of use of the driving assistant and the second one to a case where K_{hum} is set to 0, in order to estimate the efficiency of driving support without intervention of a human driver. However in that last condition the concept of operability is not pertinent as there is no human operator. Moreover, the criterion based on the drivers' opinions, E_{od}, will not be considered as it values lies more in the comparison of two system based on the felt operability.

In all the conducted experiments testing the active driving support on collision avoidance with a complete driving assistance no collisions were observed, whether the human
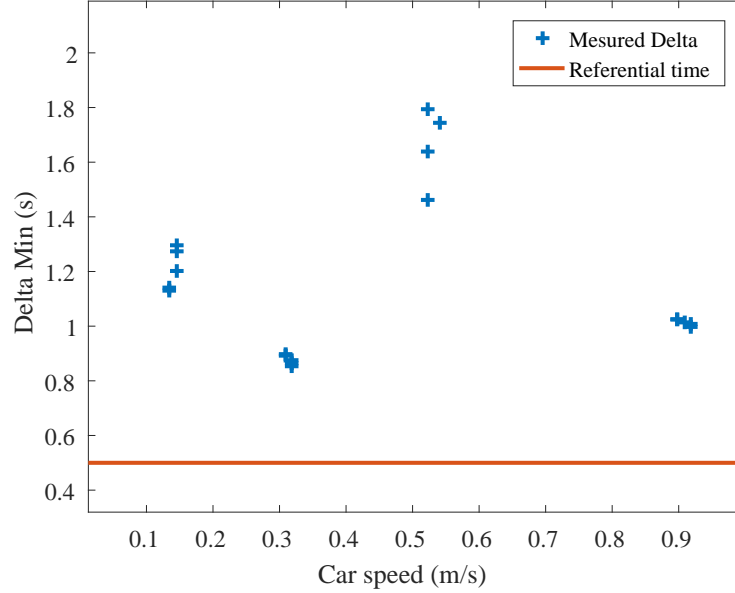
Fig. 5-26: Δ_{min} on collision avoidance depending of the car speed, with $K_{hum} = 0$.

was participating in the piloting or not. So E_{sc} and E_{sd} are equals to 1 both with $K_{hum=0}$ and $K_{hum=1}$.

Fig.5-25 and Fig5-26 represent the obtained Δ during the tests and computed from the minimal distance to the obstacle. It can be observed that when $K_{hum=1}$, Δ is decreasing as the speed of the controlled car is increasing. However the speed of the car does not seems to have the same impact when $K_{hum=0}$. The surfaces required to compute E_{sm} are estimated by taking for each point the difference to the referential time and dividing the final results by the number of tests conducted. Using $K_{sm} = 5$ the obtained results are $E_{sm0} = 0.806$ when $K_{hum} = 0$ and $E_{sm1} = 0.697$ when $K_{hum} = 1$. This result confirms the fact that when the driving support is the only responsible for the control of the car the trajectory of the vehicle tends to go further from the obstacle.

In order to compute $E_{c\omega}$ the different values of $\dfrac{\dot{\omega}_{max}}{V}$ were measured and means values were computed. For $K_{hum} = 0$, the mean value of $\dfrac{\dot{\omega}_{max}}{V}$ was 1.7571 with a standard deviation of 0.4451, and 1.1575 with a 0.3439 std for $K_{hum} = 1$. From the std values compared to the mean values, it is possible to say that $\dfrac{\dot{\omega}_{max}}{V}$ is a consistent index that does not vary with the speed of the car. With $\alpha = 0.25$ the obtained indexes are $E_{c\omega0} = 0.695$
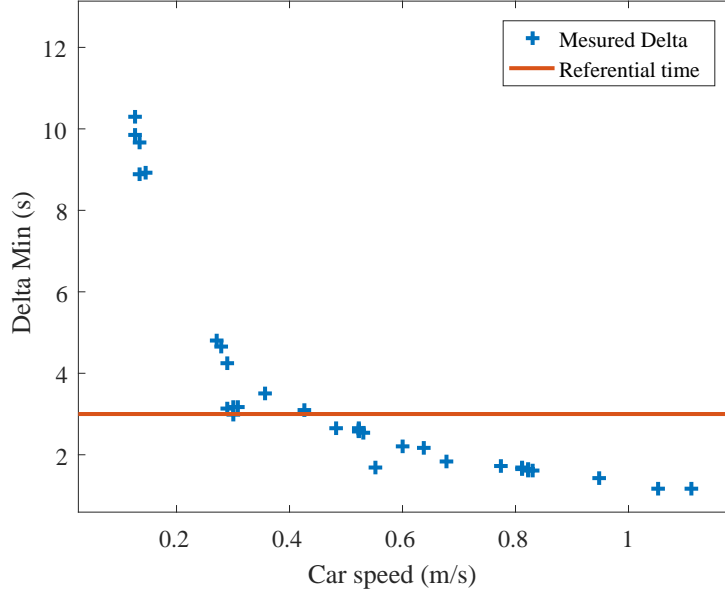
Fig. 5-27: Δ_{inf} on collision avoidance depending of the car speed, with $K_{hum} = 1$.

and $E_{c\omega 1} = 0.776$.

Fig.5-27 and Fig.5-28 represent the Δ computed from the distance from the obstacle at which the vehicle begin to change its trajectory. In both case that distance is decreasing with the increase of the speed. With K_{cm} the results are $E_{cm0} = 0.465$ and $E_{cm1} = 0.623$. It is then possible to conclude that the driving assistant, if let free, tends to over disturb the trajectory of the car compared to a collaborative situation.

Fig.5-29 represents the method used to measure the effect of the oscillations on the steering wheel. Only the steering wheel is considered here, as in collision avoidance the throttle assist is under represented compared to the steering assist. First the angular position is filtered and that result is subtracted form the angular position to obtain the oscillation component. The root mean square value of those oscillations is computed. This value is not dependent of the value of K_{hum}, and its computed mean on all the test is 0.0700 rad with a standard deviation of 0.0319 rad. With $\beta = 1$, E_{co} is equal to 0.588.

Finally, in order to compute E_{oo} and E_{oc} the different integration are computed as well as their means. It is then possible to obtain $E_{oo} = 0.729$ and $E_{oc} = 0.683$.

From all the previously detailed indexes different efficiency were computed end gathered
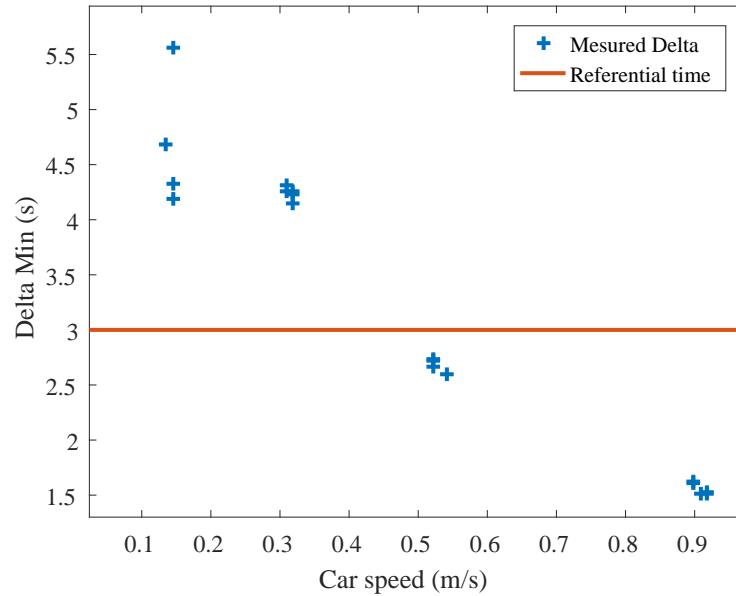
Fig. 5-28: Δ_{inf} on collision avoidance depending of the car speed, with $K_{hum} = 0$.

in Table 5.8. It is possible to observe that the efficiency score of the driving assistant alone concerning the safety is higher that the one obtained by combining driver and support, but this efficiency is obtained through a reduced score on the comfortability for the passengers. The final efficiency score presented here is not relevant by itself, because of the high number of used parameters. However it is more meant to be an example of a tool that could be used for later comparison of different active driving assistant architecture.
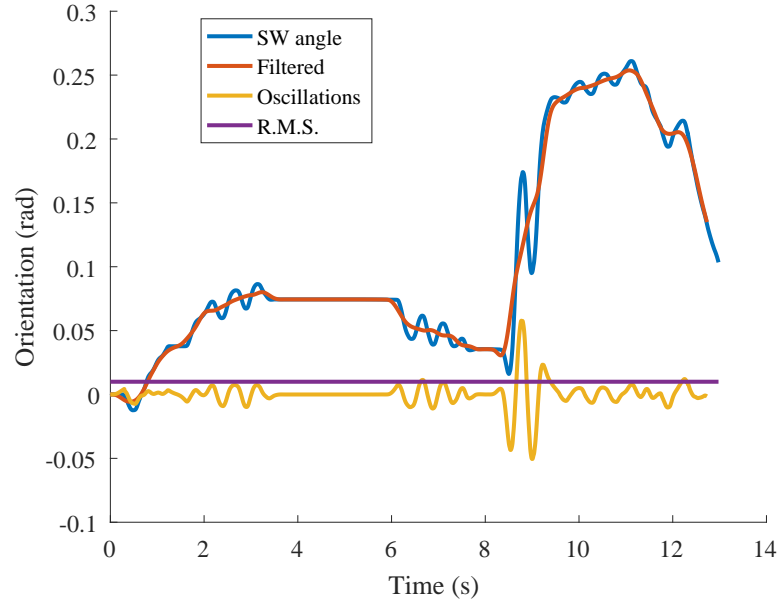
Fig. 5-29: Example of oscillations extraction.

Table 5.8: Obtained values for the efficiency index.

Third rank Indexes	$K_{hum=0}$	$K_{hum=1}$	Second rank Indexes	$K_{hum=0}$	$K_{hum=1}$	Final Index	value
E_{sc}	1						
E_{sd}	1		E_s	0.951	0.924		
E_{sm}	0.806	0.697					
$E_{c\omega}$	0.695	0.776					
E_{cm}	0.465	0.623	E_c	0.590	0.675	E	0.810
E_{co}	0.588						
E_{oo}	X	0.729	E_o	X	0.708		
E_{oc}	X	0.683					

5.4 Summary

This last chapter was the occasion to confront the realized active driving assistant with what was expected of it, and to try to evaluate the achieved performances. The first part of this chapter was dedicated to the analysis of experimental results. The efficiency of the line detection was demonstrated even though a variation of the orientation of the detected line was observed. However that variation was small and can be imputed to differences to perfect models. The driving assistant was also proven to be able to prevent involuntary line crossing that could be provoked by a lack of attention from the driver. The driving assistant was then able to prevent the crossing and realign the car with the line. Moreover the behavior in case of forced line crossing is conform to the expectations, with first a crossing prevention torque and then a realignment torque. Then the interest of a modulation operated through fuzzy logic of the driving support was showed. When a driving intent was detected, the torque required to change lane was reduced and the driving assistant did not disturb the trajectory of the car. The opposite statement can be formulated when a situation is estimated as dangerous. Indeed in that case the torque required to cross a line is extremely high and the driving assistant strongly disturb the crossing. Moreover the collision avoidance's behavior was observed as conform to the expectations. It was able to slow down or make the car turn around the obstacle to prevent the collision. It was observed that the avoidance seemed more efficient when combined with the driver and closer to what would be a natural cruising. It was also stated that at a normal speed, the effect of the steering support was felt before the throttle one. Finally the effect of the time delay on the ability of a driver without driving assistance was monitored. It appeared that a high speed combine with a long time delay drastically reduced the number of successful collision avoidance. However combining remote control and driving support allowed to successfully prevent collisions without consideration of speed and time delay duration. The second part of this chapter was dedicated to the creation of an efficiency index, based on the notion of safety, comfortability and operability. This index can be used to compare several configurations of the proposed driving assistant but also to compare several architectures of driving support. As coefficients are used, it is possible to compare assistants on different configurations to estimate a better suitability of a

proposition on some criteria. By instance, in the presented configuration, the driving assistant applied in the condition of an autonomous vehicle was considered as safer but with a lower level of comfortability compared to a shared control between the driving support and the driver. By choosing the relative importance given to either the safety or comfortabilty aspects, the highest efficiency could be obtained by one or by the other solution.

Chapter 6

Conclusion

This thesis presented a proposition of remote control applied to cruising situation combined with an active driving assistance. The purpose of this proposal is to tackle the problem of road traffic deaths. This problem appears to be the major cause of decease among the 15-29 years old. Most of the traffic incidents are provoked by the behavior of the drivers. Indeed, because of the high number of parameters to take into account while cruising, the driver has to remain extremely focused on his task. This focus become harder to keep as the duration of the driving session tends to get longer. Remote control can be seen as a solution to that consideration in specific applications, such a fret transport, as it is a method that permit to reduce the duration of such sessions. However, remote control, by its very nature, causes a communication time delay between the controlled object and the controller. The environment of a car evolving on a road in a cruising situation is subject to rapid evolution, thus the driver has to be able to react quickly to any potentially hazardous evolution of that environment. In that condition the communication time delay can become dangerous and prevent the driver to react efficiently. This problem is not limited to the application of remote control to a vehicle, as several external factors can slow down the reactions of a human and then cause accidents, even in a standard driving situation, with a human driver inside of the controlled vehicle. These factors can be drowsiness, focus loss or alcohol by instances. The ad-junction of an automation process can be used to solve that reaction delay problem in both of the previously mentioned situations. Such process, here in this thesis an active driving assistant, can react quickly

to dangers in the surrounding of the car by compensating the slow reactions of a human driver and the communication time delay. This active driving support operates through torques applied to steering wheel and pedal which controls are shared with the driver.

Nonetheless, the ability of such assistant to behave correctly is heavily related to its capacity to analyze the surrounding of the controlled vehicle. Therefore this thesis introduced a computer vision based method used to detect potential threats in the environment of the car. This algorithm is based on the use of a stereo camera to extract the location in the car referential of pedestrians, vehicles and road marks. In order to be operated on cruising vehicles, this program is run using GPU computation and a multi-threaded architecture to realize real time computation. However a detection solely based on a camera would not be fully efficient because of its limited field of view, so a hazards information protocol was designed in order to transmit more efficiently data concerning potential dangers.

This thesis also described how the control of the car was performed, both with and without the application of remote control, and how this one is shared between the driving assistant and the human driver. In order to compute the required assisting torques, hazards are modelized by virtual potential fields from which the previously mentioned torques are estimated in two scenarios, the line crossing and the collision avoidance. Those potential were designed to increase the safety of the driving but also to be less restraining as possible to the driver. However in order to improve the efficiency of the proposed driving assistant, a fuzzy logic engine is used to modulate the relative importance, on the trajectory of the vehicle, of the driver and support. The purpose of this engine is to strengthen the support in dangerous situations while letting the driver free to control the car when no hazard is detected. The use of fuzzy logic enable to mimic the human way of estimating a situation in order to reach a more organic reaction of the modulation process that uses variables difficultly compatible with crispy logic and boolean thresholds.

Thereafter, the two systems used to conducts the validation experiments were introduced. To evaluate the efficiency of the proposed method in conditions as close as possible of what a real implementation on a vehicle would be, an electric vehicle was modified to enable the application of the driving support. This car is used in line crossing tests but cannot be used to perform collision avoidance tests as any failure would have lead to

potential injuries of testers and damages on the system. This is why a 1/10th scale car was used to conduct such experiments.

Finally the results of the conducted experiments were analyzed. The proposed driving assistant coupled with the remote control showed the expected behavior. Indeed the line crossing was prevented or encouraged depending of the results of the fuzzy logic engine, was able to modify or slow down the car in function of the situation to prevent the collision. Moreover the effects of an increase on the communication time delay on the ability of a human driver to avoid a collision were studied. The proposed driving support also demonstrated a proper assistant behavior. Indeed it was able to help the driver to prevent dangerous events,as demonstrated in the different experiments where collisions were prevented and involuntary line crossings made impossible, while not disturbing the driving in safe situations. This last point have been enlightened by the very behavior of the assistant. The support torques only appear when the controlled car is close of the danger, avoiding to unnecessarily restraining the human user, and the capacity of the fuzzy logic engine to lower the effect of the assistant, by instance to cross a line in specific situations, has also proven the ability of the proposed system to reduce as mush as possible the constraints applied to the pilot of the vehicle. The efficiency of the driving assistant to compensate for that time delay was also demonstrated. Furthermore evaluation criteria based on the safety, the comfortability and operability of the realized assistance were proposed to facilitate the comparison between future works and the presented system. They were applied to two variations of the proposed method to compare the efficiency of a shared control of the vehicle compared to a more autonomous behavior.

Remarks on Future Works

As explained through this thesis, the ability of the driving assistant to react with a correct and safe behavior to every evolution of the car environment is heavily dependent of its capacity to analyze this one. If the use of a stereo camera enables to detect and locate efficiently objects located in its field of view, it would be interesting to improve the detection capacity of the controlled car. If this could be conducted through an increase of the number of sensors and of their types, the problematic of sensor fusion and how combine

the detections of several sensors to increase the global accuracy should be considered.

Moreover one of the limitation of the presented system is its difficulty to estimate the position of the car in the environment referential because of the small number of sensors measuring the cinematic of the car. More accurate results could be obtained by using inertial measurement units or by adding extra sensors on the wheels to enable the use of a more complex cinematic model.

Finally the present thesis only demonstrated the effect of a driving assistance on a single controlled vehicle. It would also be interesting to consider the interaction of several vehicles using the same assistant to see how the offered support react to each other and what specific consideration should be tackled in a more widespread use of such technology.

Moreover even if the interest of the proposed method was demonstrated in this thesis, its application on commercial vehicles would require the proposed driving assistant to consider a wider range of situations. Its principles, to analyze the environment, to represent the dangers with potential, to offer assisting torques and finally to adapt the level of support to the environment of the controlled vehicle and to the status of the driver thanks to a fuzzy logic engine, can be extended to enclose a better coverage of what could happen in cruising situation. However the environment awareness of the driving assistant is the crucial point to improve in order to reach a satisfying commercial solution. In its current state, the detection is mostly based on artificial vision. The information extracted from that process are similar to what could be estimated by a human driver. If the current driving assistant is able to react quicker and without distraction, it cannot obtained data that would not be accessible to the pilot. However the driver would expect that kind of assistant to offer information that he cannot acquire by himself, especially in more complicated situation, like difficult weather conditions or urban traffic in crowded situations . This need leads to a requirement to increase the detection capacity of the driving assistant by adding other sensors, that could analyze the weather, use GPS information or communicate with other devices in the surrounding of the car. The presented hazard sharing protocol is a first step in that direction but may be inefficient to cover every situation by just including other vehicle and fixed transmitters. It could be interesting to consider the inclusion of a maximum of connected devices to get information about other vehicles, pedestrians, road traffic conditions, and other objects encountered while

driving. This approach is linked to the Internet of Things and could drastically increase the environment awareness of the controlled vehicle, to the price of safety concerns shared by all connected devices. The regulation of the strength of the support conducted by the fuzzy logic engine should also be expanded to consider extra inputs that would contribute to describe more deeply the driving conditions, by instance weather conditions. Of course the number of objects modelized with potential fields should be increased. Finally it is necessary to consider the possible evolution of the driving interface. Indeed, the steering wheel and pedals combination, even if presenting the advantage of decoupling the steering and throttle control, is not adapted to every driver, especially to persons with handicap. Then a multiplication of the control method is to be expected, by instance joysticks with force feedback. Such methods could presents better operability on the throttle control compared to a pedal that does not allow to slow down the vehicle by lifting the pedal with the foot. The proposed active driving assistant could be applied on different driving interfaces. However it would be necessary to change the computation of the support torques to fit the chosen controllers.

References

[1] World Health Organization. (2015) Road traffic injuries: the facts. [Online]. Available: http://www.who.int/violence_injury_prevention/road_safety_status/2015/magnitude_A4_web.pdf?ua=1

[2] ——, *Global status report on road safety 2015*, 2015.

[3] C. I. S. website. (2015) Automated driving: Legislative and regulatory action. Accessed: 2016-03-20. [Online]. Available: http://cyberlaw.stanford.edu/wiki/index.php/Automated_Driving:_Legislative_and_Regulatory_Action

[4] Mozbot. Internet Speed, Usage and Latency by Country. Accessed: 2017-07-27. [Online]. Available: http://www.mozbot.co.uk/internet-speed-usage-latency-country/#!prettyphoto/0/

[5] WonderNetwork. Global Ping Statistics. Accessed: 2017-07-27. [Online]. Available: https://wondernetwork.com/pings/

[6] B. C. Teft, "Acute sleep deprivation and risk of motor vehicle crash involvement," AAA Foundation for Traffic Safety, Tech. Rep., 2016.

[7] Takeoka Jidousha Kougei. Milieu R. Accessed: 2017-05-20. [Online]. Available: http://www.takeoka-m.co.jp/milieuR.html#hyo

[8] ZMP. 1/10 scale RoboCar® 1/10. Accessed: 2017-05-20. [Online]. Available: http://www.zmp.co.jp/products/robocar-110?lang=en

[9] S. Kraus, M. Althoff, B. Heissing, and M. Buss, "Cognition and emotion in autonomous cars," in *Intelligent Vehicles Symposium, 2009 IEEE*, June 2009, pp. 635–640.

[10] A. Belbachir, R. Boutteau, P. Merriaux, J.-M. Blosseville, and X. Savatier, "From autonomous robotics toward autonomous cars," in *Intelligent Vehicles Symposium (IV), 2013 IEEE*, June 2013, pp. 1362–1367.

[11] C. Urmson, C. R. Baker, J. M. Dolan, P. Rybski, B. Salesky, W. R. L. Whittaker, D. Ferguson , and M. Darms, "Autonomous driving in traffic: Boss and the urban

challenge," *AI Magazine*, vol. 30, no. 2, pp. 17–29, June 2009.

[12] D. J. Fagnant and K. Kockelman, "Preparing a nation for autonomous vehicles: opportunities, barriers and policy recommendations," *Transportation Research Part A: Policy and Practice*, vol. 77, pp. 167 – 181, 2015.

[13] Y. Jing, L. Zhang, I. Arce, and A. Farajidavar, "Androrc: An android remote control car unit for search missions," in *IEEE Long Island Systems, Applications and Technology (LISAT) Conference 2014*, May 2014, pp. 1–5.

[14] M. Guimaraes and J. Lindberg, "Remote controlled vehicle for inspection of vertical concrete structures," in *Proceedings of the 2014 3rd International Conference on Applied Robotics for the Power Industry*, Oct 2014, pp. 1–6.

[15] M. Sasayama and T. Murakami, "Compliant velocity based force coordinate transformation control for gait rehabilitation," in *2014 IEEE 13th International Workshop on Advanced Motion Control (AMC)*, March 2014, pp. 254–259.

[16] K. Kiguchi, "A study on emg-based human motion prediction for power assist exoskeletons," in *2007 International Symposium on Computational Intelligence in Robotics and Automation*, June 2007, pp. 190–195.

[17] C. E. Carr and D. J. Newman, "Exoskeleton energetics: Implications for planetary extravehicular activity," in *2017 IEEE Aerospace Conference*, March 2017, pp. 1–14.

[18] N. Mir-Nasiri and H. S. Jo, "Autonomous low limb exoskeleton to suppress the body weight," in *2017 3rd International Conference on Control, Automation and Robotics (ICCAR)*, April 2017, pp. 47–51.

[19] H. Inose, S. Mohri, Y. Yamada, T. Nakamura, K. Yokoyama, and I. Kikutani, "Development of a lightweight power-assist suit using pneumatic artificial muscles and balloon-amplification mechanism," in *2016 14th International Conference on Control, Automation, Robotics and Vision (ICARCV)*, Nov 2016, pp. 1–6.

[20] T. Fong, C. Thorpe, and C. Baur, "Advanced interfaces for vehicle teleoperation: Collaborative control, sensor fusion displays, and remote driving tools," *Autonomous Robots*, vol. 11, no. 1, pp. 77–85, 2001.

[21] J. L. B. Abesamis, A. M. F. Mediodia, C. J. M. Akol, R. P. M. Quesea, and E. Sybingco, "A remote-controlled land and water traversing vehicle for flood search operation," in *2014 International Conference on Humanoid, Nanotechnology, Information Technology, Communication and Control, Environment and Management (HNICEM)*, Nov 2014, pp. 1–6.

[22] S. Zhou, Y. Jiang, J. Xi, J. Gong, G. Xiong, and H. Chen, "A novel lane detection

based on geometrical model and gabor filter," in *2010 IEEE Intelligent Vehicles Symposium*, June 2010, pp. 59–64.

[23] A. F. Hurtado, J. A. Gómez, V. M. Peñeñory, I. M. Cabezas, and F. E. García, "Proposal of a computer vision system to detect and track vehicles in real time using an embedded platform enabled with a graphical processing unit," in *2015 International Conference on Mechatronics, Electronics and Automotive Engineering (ICMEAE)*, Nov 2015, pp. 76–80.

[24] G. Li, P. Ren, X. Lyu, and H. Zhang, "Real-time top-view people counting based on a kinect and nvidia jetson tk1 integrated platform," in *2016 IEEE 16th International Conference on Data Mining Workshops (ICDMW)*, Dec 2016, pp. 468–473.

[25] Y. Ukidave, D. Kaeli, U. Gupta, and K. Keville., "Performance of the nvidia jetson tk1 in hpc," in *2015 IEEE International Conference on Cluster Computing*, Sept 2015, pp. 533–534.

[26] I. S. Yoo and S. W. Seo, "Accurate object distance estimation based on frequency-domain analysis with a stereo camera," *IET Intelligent Transport Systems*, vol. 11, no. 4, pp. 248–254, 2017.

[27] M. S. H. Achmad, W. S. Findari, N. Q. Ann, D. Pebrianti, and M. R. Daud, "Stereo camera - based 3d object reconstruction utilizing semi-global matching algorithm," in *2016 2nd International Conference on Science and Technology-Computer (ICST)*, Oct 2016, pp. 194–199.

[28] K. Hisatomi, M. Kano, K. Ikeya, M. Katayama, T. Mishina, Y. Iwadate, and K. Aizawa, "Depth estimation using an infrared dot projector and an infrared color stereo camera," *IEEE Transactions on Circuits and Systems for Video Technology*, vol. PP, no. 99, pp. 1–1, 2016.

[29] C.-Y. Chen, S.-Y. Chien, Y.-W. Huang, T.-C. Chen, T.-C. Wang, and L.-G. Chen, "Analysis and architecture design of variable block-size motion estimation for h.264/avc," *IEEE Transactions on Circuits and Systems I: Regular Papers*, vol. 53, no. 3, pp. 578–593, March 2006.

[30] J.-C. Tuan, T.-S. Chang, and C.-W. Jen, "On the data reuse and memory bandwidth analysis for full-search block-matching vlsi architecture," *IEEE Transactions on Circuits and Systems for Video Technology*, vol. 12, no. 1, pp. 61–72, Jan 2002.

[31] S. Zhu and K.-K. Ma, "A new diamond search algorithm for fast block-matching motion estimation," *Image Processing, IEEE Transactions on*, vol. 9, no. 2, pp. 287–290, Feb 2000.

[32] G. de Haan, P. W. A. C. Biezen, H. Huijgen, and O. A. Ojo, "True-motion estimation with 3-d recursive search block matching," *IEEE Transactions on Circuits and Systems for Video Technology*, vol. 3, no. 5, pp. 368–379, 388, Oct 1993.

[33] J. Hafner, H. S. Sawhney, W. Equitz, M. Flickner, and W. Niblack, "Efficient color histogram indexing for quadratic form distance functions," *IEEE Transactions on Pattern Analysis and Machine Intelligence*, vol. 17, no. 7, pp. 729–736, Jul 1995.

[34] P. Viola and M. Jones, "Rapid object detection using a boosted cascade of simple features," in *Computer Vision and Pattern Recognition, 2001. CVPR 2001. Proceedings of the 2001 IEEE Computer Society Conference on*, vol. 1, 2001, pp. I–511–I–518 vol.1.

[35] M. T. Pham and T. J. Cham, "Fast training and selection of haar features using statistics in boosting-based face detection," in *2007 IEEE 11th International Conference on Computer Vision*, Oct 2007, pp. 1–7.

[36] Y. Pang, X. Li, Y. Yuan, D. Tao, and J. Pan, "Fast haar transform based feature extraction for face representation and recognition," *IEEE Transactions on Information Forensics and Security*, vol. 4, no. 3, pp. 441–450, Sept 2009.

[37] R. Lienhart and J. Maydt, "An extended set of haar-like features for rapid object detection," in *Proceedings. International Conference on Image Processing*, vol. 1, 2002, pp. I–900–I–903 vol.1.

[38] N. Dalal and B. Triggs, "Histograms of oriented gradients for human detection," in *Computer Vision and Pattern Recognition, 2005. CVPR 2005. IEEE Computer Society Conference on*, vol. 1, June 2005, pp. 886–893 vol. 1.

[39] Q. Zhu, M.-C. Yeh, K.-T. Cheng, and S. Avidan, "Fast human detection using a cascade of histograms of oriented gradients," in *2006 IEEE Computer Society Conference on Computer Vision and Pattern Recognition (CVPR'06)*, vol. 2, 2006, pp. 1491–1498.

[40] J. Zhang, K. Huang, Y. Yu, and T. Tan, "Boosted local structured hog-lbp for object localization," in *CVPR 2011*, June 2011, pp. 1393–1400.

[41] Y. He, H. Wang, and B. Zhang, "Color-based road detection in urban traffic scenes," *IEEE Transactions on Intelligent Transportation Systems*, vol. 5, no. 4, pp. 309–318, Dec 2004.

[42] S. Zhou, Y. Jiang, J. Xi, J. Gong, G. Xiong, and H. Chen, "A novel lane detection based on geometrical model and gabor filter," in *2010 IEEE Intelligent Vehicles Symposium*, June 2010, pp. 59–64.

[43] J. Canny, "A computational approach to edge detection," *IEEE Transactions on Pattern Analysis and Machine Intelligence*, vol. PAMI-8, no. 6, pp. 679–698, Nov 1986.

[44] J. Matas, C. Galambos, and J. Kittler, "Robust detection of lines using the progressive probabilistic hough transform," *Computer Vision and Image Understanding*, vol. 78, no. 1, pp. 119 – 137, 2000.

[45] D. C. W. Pao, H. F. Li, and R. Jayakumar, "Shapes recognition using the straight line hough transform: theory and generalization," *IEEE Transactions on Pattern Analysis and Machine Intelligence*, vol. 14, no. 11, pp. 1076–1089, Nov 1992.

[46] N. Guil, J. Villalba, and E. L. Zapata, "A fast hough transform for segment detection," *IEEE Transactions on Image Processing*, vol. 4, no. 11, pp. 1541–1548, Nov 1995.

[47] V. Kamat and S. Ganesan, "An efficient implementation of the hough transform for detecting vehicle license plates using dsp's," in *Proceedings Real-Time Technology and Applications Symposium*, May 1995, pp. 58–59.

[48] S. W. Keckler, W. J. Dally, B. Khailany, M. Garland, and D. Glasco, "Gpus and the future of parallel computing," *IEEE Micro*, vol. 31, no. 5, pp. 7–17, Sept 2011.

[49] J. Nickolls and W. J. Dally, "The gpu computing era," *IEEE Micro*, vol. 30, no. 2, pp. 56–69, March 2010.

[50] J. D. Owens, M. Houston, D. Luebke, S. Green, J. E. Stone, and J. C. Phillips, "Gpu computing," *Proceedings of the IEEE*, vol. 96, no. 5, pp. 879–899, May 2008.

[51] J. Yoon and C. D. Crane, "Ladar based obstacle detection in an urban environment and its application in the darpa urban challenge," in *2008 International Conference on Control, Automation and Systems*, Oct 2008, pp. 581–585.

[52] W. S. Wijesoma, K. R. S. Kodagoda, and A. P. Balasuriya, "Road-boundary detection and tracking using ladar sensing," *IEEE Transactions on Robotics and Automation*, vol. 20, no. 3, pp. 456–464, June 2004.

[53] C.-C. Wang, C. Thorpe, and A. Suppe, "Ladar-based detection and tracking of moving objects from a ground vehicle at high speeds," in *IEEE IV2003 Intelligent Vehicles Symposium. Proceedings (Cat. No.03TH8683)*, June 2003, pp. 416–421.

[54] R. Volpe and P. Khosla, "Manipulator control with superquadric artificial potential functions: theory and experiments," *IEEE Transactions on Systems, Man, and Cybernetics*, vol. 20, no. 6, pp. 1423–1436, Nov 1990.

[55] E. J. Rossetter, "A potential field framework for active vehicle lanekeeping assis-

tance," Ph.D. dissertation, Stanford University, 2003.

[56] O. Khatib, "Real-time obstacle avoidance for manipulators and mobile robots," in *Proceedings. 1985 IEEE International Conference on Robotics and Automation*, vol. 2, Mar 1985, pp. 500–505.

[57] D. N. Nia, H. S. Tang, B. Karasfi, O. R. E. Motlagh, and A. C. Kit, "Virtual force field algorithm for a behaviour-based autonomous robot in unknown environments," *Proceedings of the Institution of Mechanical Engineers, Part I: Journal of Systems and Control Engineering*, vol. 225, no. 1, pp. 51–62, 2011.

[58] M. T. Wolf and J. W. Burdick, "Artificial potential functions for highway driving with collision avoidance," in *2008 IEEE International Conference on Robotics and Automation*, May 2008, pp. 3731–3736.

[59] K. Ohnishi, "Robust motion control by disturbance observer," *Journal of the Robotics Society of Japan*, vol. 11, no. 4, pp. 486–493, 1993.

[60] T. Murakami, F. Yu, and K. Ohnishi, "Torque sensorless control in multidegree-of-freedom manipulator," *Industrial Electronics, IEEE Transactions on*, vol. 40, no. 2, pp. 259–265, Apr 1993.

[61] B. Rouzier and T. Murakami, "Principle for the validation of a driving support using a computer vision-based driver modelization on a simulator," *International Journal of Advanced Robotic Systems*, vol. 12, no. 7, p. 105, 2015. [Online]. Available: http://dx.doi.org/10.5772/60831

[62] L. Zadeh, "Fuzzy sets," *Information and Control*, vol. 8, no. 3, pp. 338 – 353, 1965.

[63] G. Feng, "A survey on analysis and design of model-based fuzzy control systems," *IEEE Transactions on Fuzzy Systems*, vol. 14, no. 5, pp. 676–697, Oct 2006.

[64] A. Pandey, R. K. Sonkar, K. K. Pandey, and D. R. Parhi, "Path planning navigation of mobile robot with obstacles avoidance using fuzzy logic controller," in *2014 IEEE 8th International Conference on Intelligent Systems and Control (ISCO)*, Jan 2014, pp. 39–41.

[65] E. Vans, G. Vachkov, and A. Sharma, "Vision based autonomous path tracking of a mobile robot using fuzzy logic," in *Asia-Pacific World Congress on Computer Science and Engineering*, Nov 2014, pp. 1–8.

[66] B. M. Novakovic, M. Crnekovic, and C. Oluic, "An analytic fuzzy logic control of robots," in *Emerging Technologies and Factory Automation Proceedings, 1997. ETFA '97., 1997 6th International Conference on*, Sep 1997, pp. 403–408.

[67] S. Ghaffari and M. R. Homaeinezhad, "Intelligent path following of articulated eight-

wheeled mobile robot with nonholonomic constraints," in *2016 4th International Conference on Robotics and Mechatronics (ICROM)*, Oct 2016, pp. 173–178.

[68] GStreamer. Gstreamer open source multimedia framework. Accessed: 2017-06-12. [Online]. Available: https://gstreamer.freedesktop.org/

[69] PS4 Developper Wiki. Playstation 4 camera. [Online]. Available: http://www.psdevwiki.com/ps4/PlayStation_4_Camera

[70] usb.org. Universal serial bus 3.0 connectors and cable assemblies compliance document. Accessed: 2017-06-12. [Online]. Available: http://www.usb.org/developers/docs/devclass_docs/CabConn_3_0_Compliance_Document_v1.02_2011-10-04.pdf

[71] GitHub. Ps4 camera tools. [Online]. Available: https://github.com/ps4eye/ps4eye

[72] elinux.org. Jetson tk1. [Online]. Available: http://elinux.org/Jetson_TK1

[73] ——. Jetson tx1. [Online]. Available: http://elinux.org/Jetson_TX1

[74] J. Rada-Vilela. The fuzzylite libraries for fuzzy logic control. Accessed: 2017-05-25. [Online]. Available: http://www.fuzzylite.com/

AppendixA

PlayStation® 4 Camera

In order to perform the analysis of its environment, the system is equipped with a Stereo Camera. This type of device us based on the use of two cameras to estimate the positions of objects in the stereo system referential. The selected device is a PlaySation 4 Camera, see Fig.A-1. This Stereo Camera uses two 1-megapixel image sensors CMOS OV9713[69]. Those sensors are defined by a f/2.0 aperture and a field of view of 85°. The PlayStation® 4 Camera is compatible with standard video format like RAW16 and RAW8 or YUV422 and YUV8 and can furnish a 12 bits tonal graduation. Table.A.1 summarizes the different resolutions and frame-rates offered by this stereo camera system. The indicated resolutions are the ones returned by each of the OV9713 sensors.

The main backlash of the PlayStation® 4 Camera is the fact that it was designed to be used only on PlayStation® 4 systems. Then, the AUX connector used by that camera is not compatible with computers. However the AUX connection is based on the USB 3.0[70] norm and can then be modified to be adapted on a USB 3.0 connector. The Fig.A-2 represents the section of a USB 3.0 cable. That kind of cable include two power lines and three pairs of data lines. The UTP signal pair is inherited from the USB 2.0 norm, while the SDP pairs are specific to the 3.0 norm. The AUX norm used by the PlayStation® 4 Camera also use the SDP signal pairs but not the UTP one. By sectioning the cable of the camera it is possible to replace its AUX connector by a USB 3.0 connector. The camera can then be connected to any computer equipped with a compatible port.

However to be used on other Operating Systems than the one of PlayStation® 4, the use of a configuration tool is required. This one is available on the ps4eye GitHub[71], and enable the use of the PlayStation® 4 Camera on Linux and OSX environments.

Fig. A-1: PlayStation® 4 Camera.

Table A.1: PlayStation® 4 Camera Modes.

| Resolution	Frame Rate
1280x800	7.5, 15, 30 or 60fps
640x400	7.5, 15, 30, 60 or 120fps
320x200	7.5, 15, 30, 60, 120 or 240fps
160x100	7.5, 15, 30, 60, 120 or 240fps
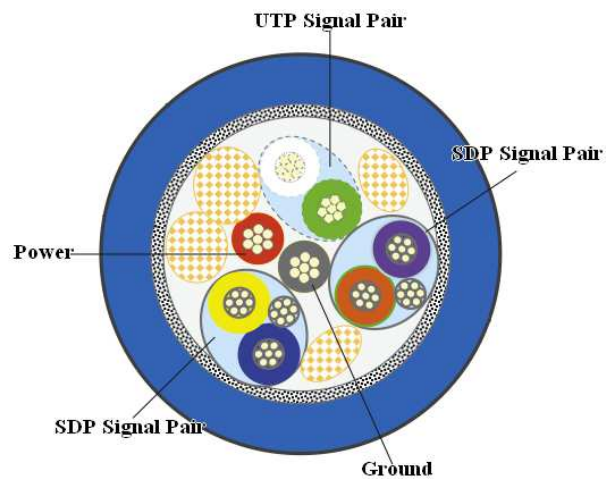
Fig. A-2: USB3.0 cable section.

AppendixB

Jetson Development Kits

In order to conduct the computer vision processes on the different constructed systems, dedicated hardware was chosen. As artificial vision is very consumptive in term of computation resources but can generally see its speed increased by the use of parallel computing, the use of Graphic Processing Units was one method to ensure that the computation required to conduct the work described in this thesis could be conducted in real time condition. Moreover in order to be easily combined with the previously mentioned systems, the device chosen to performed the computer vision algorithm should also be portable. Indeed a reduced size is much more easier to integrate in vehicles, and a reduced energy consumption is also required to maintain a satisfying duration/size ratio of the batteries included in the mobile robots.

For all the previously enumerated reasons, the hardware chosen to conduct the artificial vision program is Jetson boards, produced by NVidia. Two different versions of this board were used, the Jetson TK1[72] and the Jetson TX1[73].

Those boards are mobile processor with the same features and architecture as desktop GPU but with low power consumption. They are able to use the same CUDA® code that could be run on desktop GPUs. Those kits are running a Linux environment. Their main differences are their specifications.

The Jetson TK1, the first to be released in 2014, possesses the following features.
- GPU: NVIDIA Kepler™ "GK20a" GPU with 192 SM3.2 CUDA® cores (upto 326 GFLOPS).
- CPU: NVIDIA "4-Plus-1" 2.32GHz ARM® quad-core Cortex-A15 CPU (32 bits) with Cortex-A15 battery-saving shadow-core.
- DRAM: 2GB DDR3L.
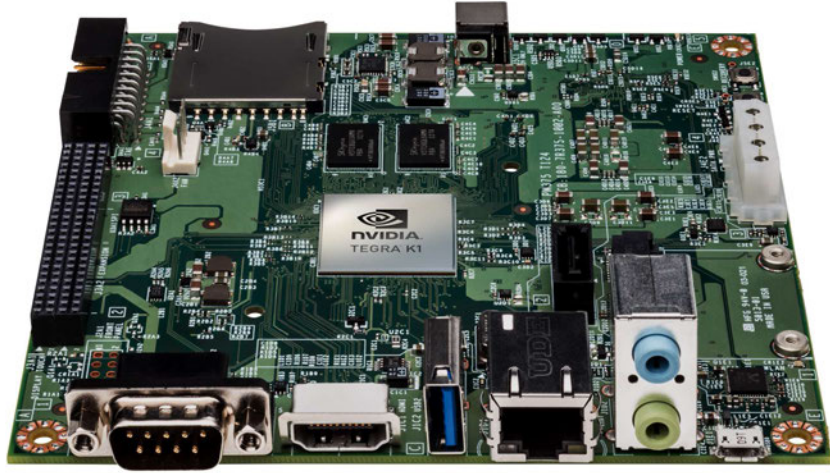
Fig. B-1: Jetson TK1 Development Kit.

Fig. B-2: Jetson TX1 Development Kit.

- Storage: 16GB eMMC.
- Ethernet port.
- USB 3.0 port.
- Energy consumption: 1 to 5 Watts.

The Jetson TX1, released in 2016, is characterized as follows.
- GPU: NVIDIA 256-core Maxwell$^{\text{TM}}$ GPU (1 TFLOPS)

- CPU: quad-core ARM® Cortex-A57 (64 bits)

- DRAM: 4GB LPDDR4.

- Storage: 16GB eMMC.

- Ethernet port.

- 802.11ac WiFi card.

- USB 3.0 port.

- Energy consumption: 10 Watts.

The Jetson development kits are compatible with the use of a PlayStation® 4 Camera.

AppendixC

Fuzzy Logic Engine

This annex will be focused on giving the details of the realized Fuzzy Logic Engine. This one was created using FuzzyLite®[74], a tool allowing to graphically design a Fuzzy Logic Engine and to export the result in several computing languages. Fig.C-1, Fig.C-2 and Fig.C-3 list the different variables used in the Fuzzy Logic Engine that regulate the control sharing offered by the driving assistant. The different values are not specified as this engine is used on systems of different scale.

The used rules are the following.

- if CarSpeed is Parking then Kda is Weak
- if CarSpeed is Normal then Kda is Normal
- if CarSpeed is Excessive or CommunicationDelay is Long then Kda is High
- if (BlinkMeanDuration is Drowsy or BlinkMeanDuration is MicroSleep) and YawMeanDuration is Drowsy and GazeMovementAmplitude is FixedGaze then Kda is High
- if CarSpeed is Parking then Krd is Weak
- if MirrorTime is Checked then Krd is Weak
- if MirrorTime is NotChecked then Krd is Normal
- if CarSpeed is Excessive then Krd is High
- if VehicleDistanceClosest is Close and VehicleDistanceEvolution is Negative then Kve is High
- if VehicleDistanceClosest is Close and VehicleDistanceEvolution is Null then Kve is Normal
- if VehicleDistanceClosest is Close and VehicleDistanceEvolution is Positive then Kve is Normal
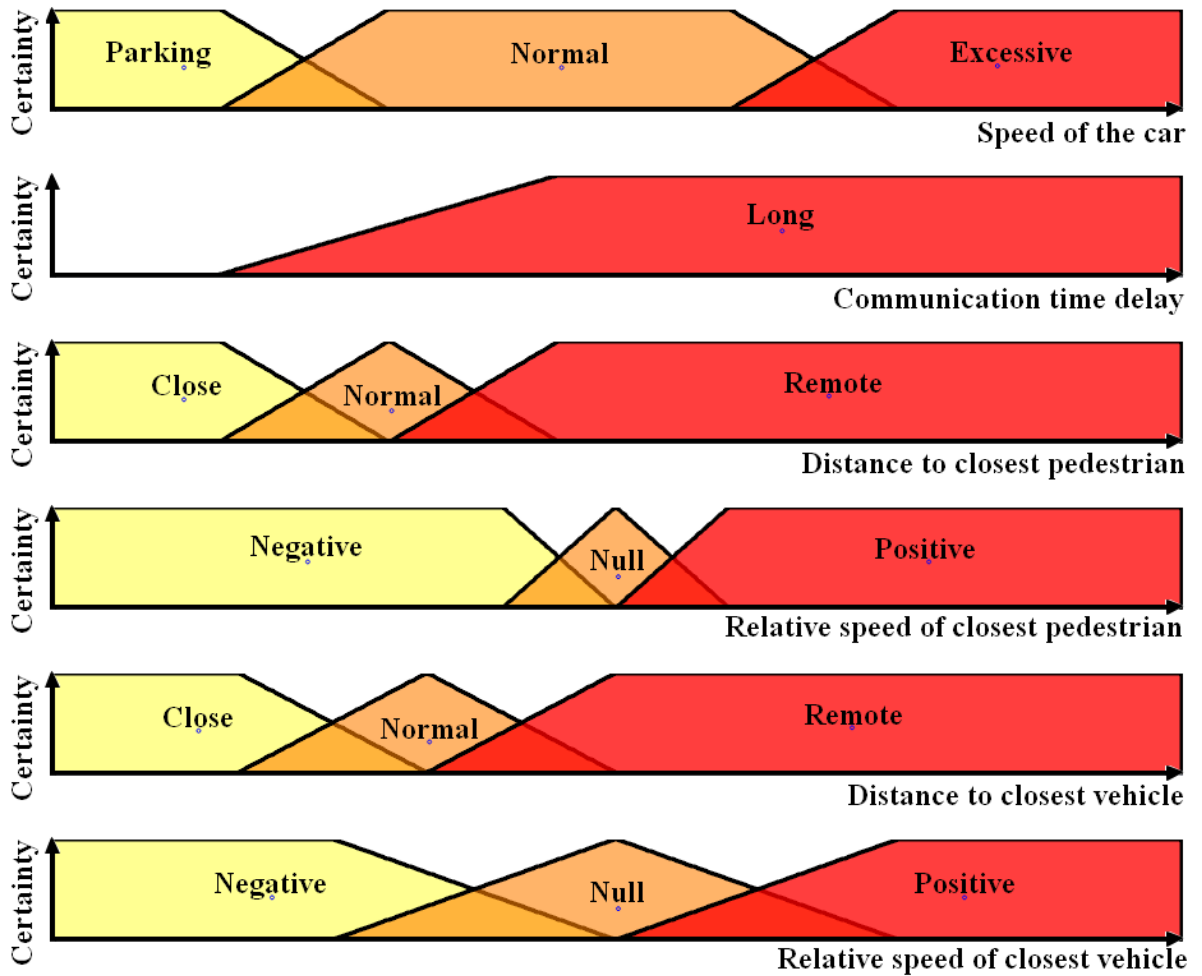
Fig. C-1: Fuzzyfied input variables.

- if VehicleDistanceClosest is Medium and VehicleDistanceEvolution is Negative then Kve is Normal
- if VehicleDistanceClosest is Medium and VehicleDistanceEvolution is Null then Kve is Normal
- if VehicleDistanceClosest is Medium and VehicleDistanceEvolution is Positive then Kve is Weak
- if VehicleDistanceClosest is Remote and VehicleDistanceEvolution is Negative then Kve is Normal
- if VehicleDistanceClosest is Remote and VehicleDistanceEvolution is Null then Kve is Weak
- if VehicleDistanceClosest is Remote and VehicleDistanceEvolution is Positive then
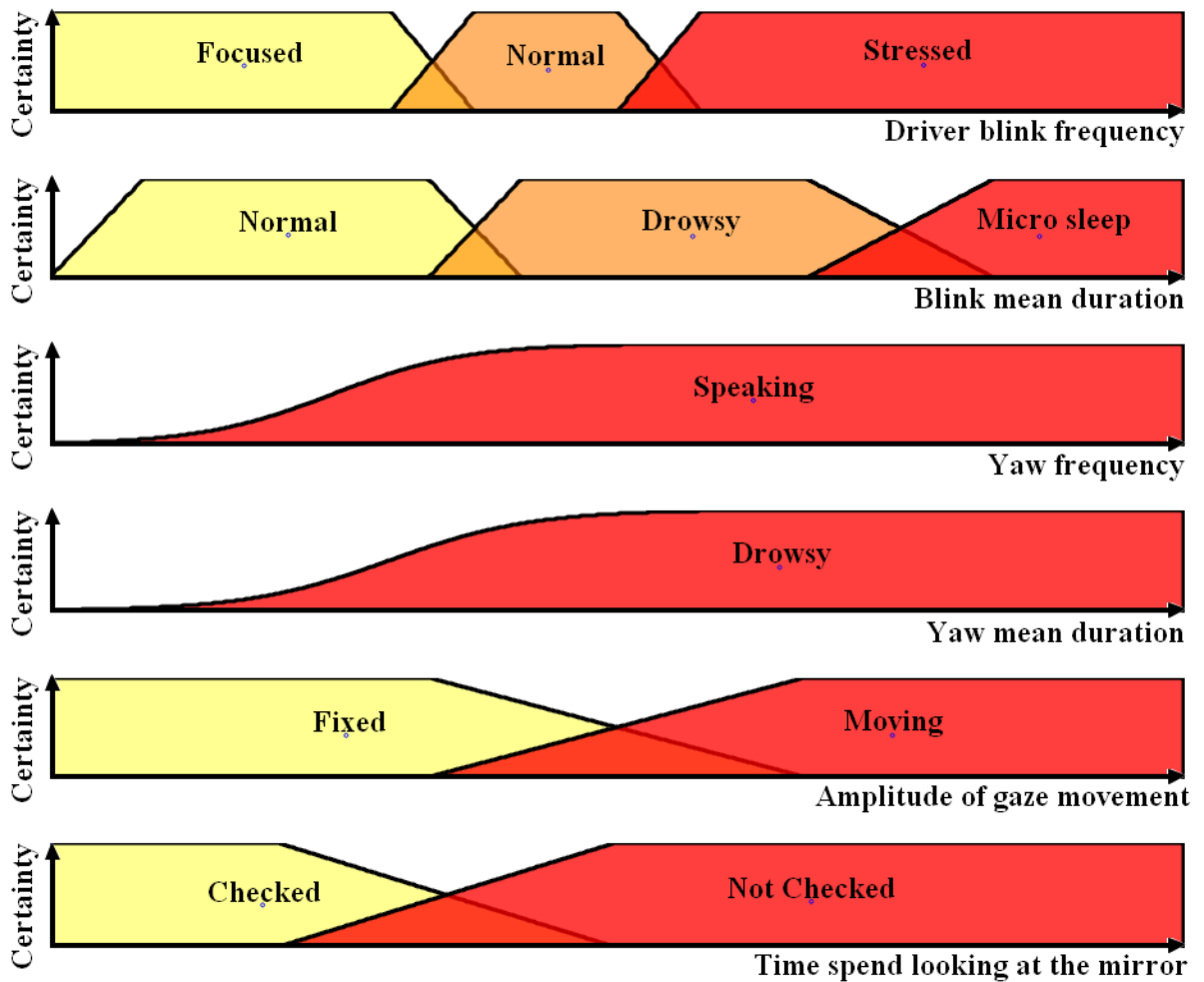
Fig. C-2: Fuzzyfied input variables.

Kve is Weak

- if PedestrianDistanceClosest is Close and PedestrianDistanceEvolution is Negative then Kped is High

- if PedestrianDistanceClosest is Close and PedestrianDistanceEvolution is Null then Kped is High

- if PedestrianDistanceClosest is Close and PedestrianDistanceEvolution is Positive then Kped is Normal

- if PedestrianDistanceClosest is Medium and PedestrianDistanceEvolution is Negative then Kped is High

- if PedestrianDistanceClosest is Medium and PedestrianDistanceEvolution is Null then Kped is Normal
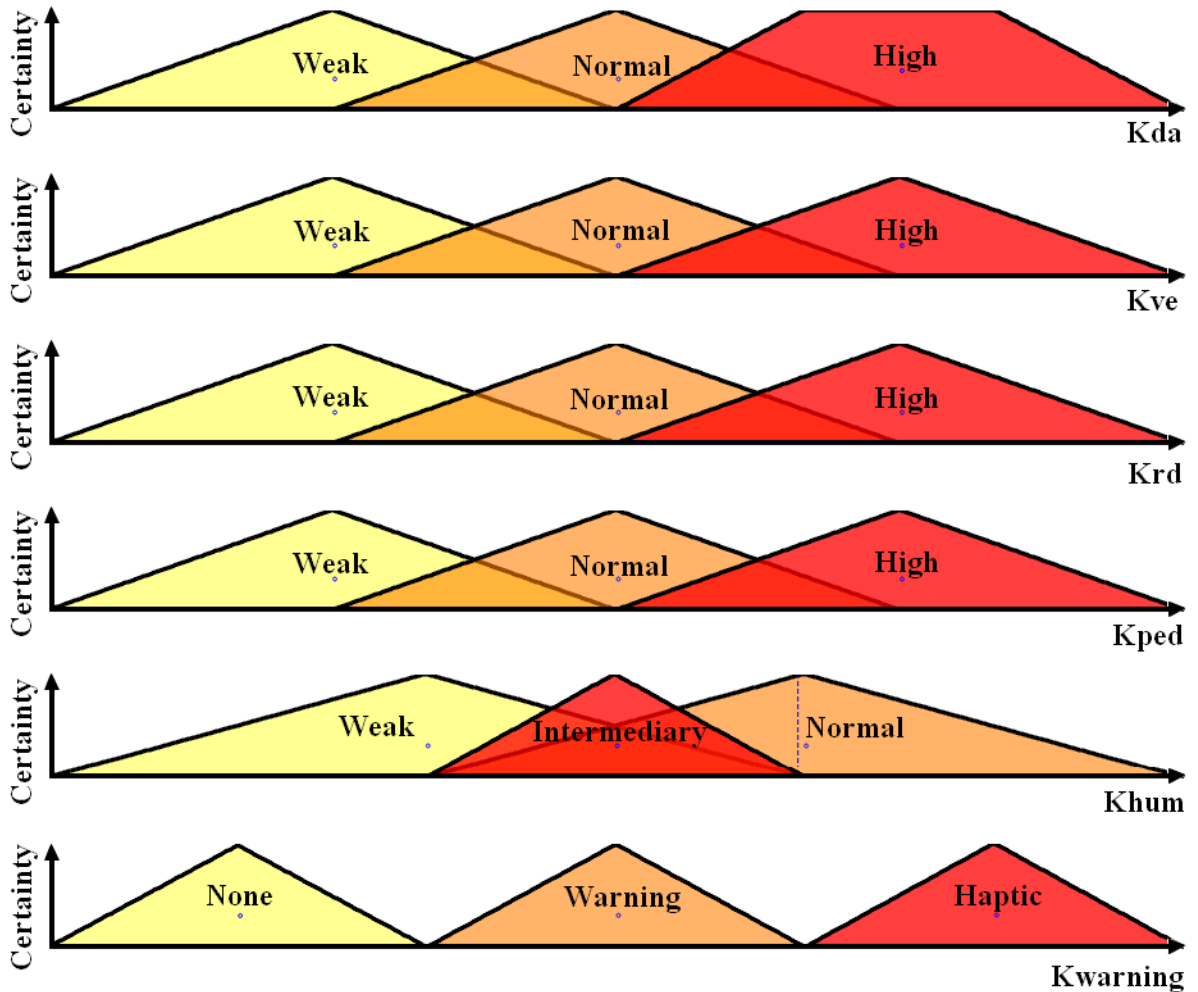
Fig. C-3: Fuzzyfied output variables.

- if PedestrianDistanceClosest is Medium and PedestrianDistanceEvolution is Positive then Kped is Weak
- if PedestrianDistanceClosest is Remote and PedestrianDistanceEvolution is Negative then Kped is Normal
- if PedestrianDistanceClosest is Remote and PedestrianDistanceEvolution is Null then Kped is Weak
- if PedestrianDistanceClosest is Remote and PedestrianDistanceEvolution is Positive then Kped is Weak
- if BlinkMeanDuration is MicroSleep or YawMeanDuration is Drowsy then Kwarning is Haptic

- if BlinkFrequency is Stress or BlinkMeanDuration is Drowsy or YawFrequency is Speaking or GazeMovementAmplitude is FixedGaze or CarSpeed is Excessive then Kwarning is Warning

- if GazeMovementAmplitude is MovingGaze and BlinkMeanDuration is Normal and (BlinkFrequency is Focused or BlinkFrequency is Normal) and (CarSpeed is Parking or CarSpeed is Normal) then Kwarning is None

- if GazeMovementAmplitude is MovingGaze and BlinkMeanDuration is Normal and (BlinkFrequency is Focused or BlinkFrequency is Normal) then Khum is Normal

- if BlinkMeanDuration is Drowsy or BlinkFrequency is Stress or GazeMovementAmplitude is FixedGaze then Khum is Intermediary

- if BlinkMeanDuration is MicroSleep or YawMeanDuration is Drowsy then Khum is Weak

List of achievements

Journal Papers

(1) B. Rouzier and T. Murakami, "Principle for the Validation of a Driving Support using a Computer Vision-Based Driver Modelization on a Simulator", *International Journal of Advanced Robotic Systems*, 12:105, 2015.

(2) B. Rouzier and T. Murakami, "Line Crossing Assistance Based on Situation Modulated Potentials Using Stereo Camera Detection", *IEEJ Transactions on Industry Applications*, (accepted).

International Conferences Papers

(1) B. Rouzier and T. Murakami, " Gaze detection based driver modelization in an electric vehicle using virtual force field and Steer by Wire system," *2014 IEEE 13th International Workshop on Advanced Motion Control (AMC)*, Yokohama, 2014, pp. 350-355.

(2) B. Rouzier and T. Murakami, "Hazard detection and cognition for an active driving assistance," *2016 IEEE 14th International Workshop on Advanced Motion Control (AMC)*, Auckland, 2016, pp. 340-345.

Exhibition

(1) B. Rouzier and T. Murakami, "Time delay compensation using a driving assistant in a remotely controlled vehicle", *17th Annual Keio Science and Technology Exhibition (KEIO TECHNO-MALL 2016)*, Tokyo International Forum, December 2017.

Honors and Awards

(1) Fujiwara Scholarship 2014-Present